EMIGRANT GAP ANTICLINE PROSPECT
Natrona County, Wyoming

PROSPECT SUMMARY

Michael L. Pinnell, Geologist, WPG #1090

Our primary prospect objective is an anticline containing Tensleep Sandstone. The Tensleep is a Permo-Penn age, primarily aeolian (dunal)-marginal marine sandstone with ultimate recoverable reserves in the central Rocky Mountain province of several billion barrels of oil. Our Tensleep objective is a shallow (2,500 feet drill depth), porous (in excess of 20% porosity in places), permeable (over 2,000 millidarcies, locally, and probably fractured), thick (223 feet of pay greater than 10% porosity in a nearby well) sandstone with most likely recoverable reserves of six to twelve million barrels of oil.

We have had our eye on this prospect, with future plans to lease and drill, but were forced to act when Donald S. Stone published his recent AAPG paper "Morphology of the Casper Mountain uplift and related, subsidiary structures, central Wyoming: Implications for Laramide kinematics, dynamics, and crustal inheritance." One of his structure maps and two cross-sections exactly identified our prospect anticline. Our hand was called, so to speak. We were very fortunate to be able to lease the entire potentially productive area with lease expirations in 2013.

Our geologic studies have identified a possible "Old", pre-Laramide anticline in the environs of our prospect. Oil migrated from Phosphoria Formation phosphatic shales 140 to 200 million years ago and remained in Tensleep Sandstones of "Old" anticlines or "Old" stratigraphic traps until the onset of major folding and faulting of Laramide age (30 to 40 million years ago). A "Young" Laramide anticline, forming some distance from an oil accumulation in an "Old" anticline, has little chance of containing commercial Tensleep oil today. On the other hand, a "Young" Laramide anticline forming at the same location as an "Old", already oil filled anticline has an excellent chance to produce abundant commercial oil. Voila'! Emigrant Gap Anticline prospect.

When we compare the Wind River Basin Winkleman Dome oil field and its adjacent, more prominent, Tensleep barren, 2,000 feet structurally higher Sage Creek Anticline with the Casper Arch Emigrant Gap prospect and its adjacent, more prominent, Tensleep barren, 1,000 feet structurally higher Emigrant Gap main anticline, we note several striking similarities: geometry, depth, structural offset, size, and surface geologic formations. Winkleman Dome has produced 55 million barrels of oil from Tensleep Sandstone.

Areas of complex geology, like the Casper Mountain-Casper Arch region, can contain excellent oil reserves. South Casper Creek is a Tensleep oil field at a drill depth of 2,500 feet, and was discovered in 1919. It is located 14 miles northwest of our prospect. It has an area of closure a little larger than our structure, and has produced 17 million barrels of oil; it is still producing 137,000 barrels of oil per year. Part of South Glenrock Oil field, a stratigraphic trap located several townships east of our prospect, is partially beneath an overthrust of the Laramie Range and has essentially the same overthrust-like structural geometry we expect on the south end of our prospect closure.

Emigrant Gap Anticline Prospect, Bibliography

Allen, A., and C. Tenney, 1986, Fremont Canyon Tensleep surface section, Section 9, T23N, R83W, Copyright

Barlow, James A., Hammond, and Haun, Geologists Inc., 1977, Structural Geology of the West Half of the Wind River Basin, Copyright by The Petroleum Ownership Map Company, POMCO

Ciftcil, Bozkurt, A. Aviantaral, D. Kerr, and N. F. Hurley, 2001, Outcrop Based 3-D Modeling of the Tensleep Sandstone at Alkali Creek, Bighorn Basin, Wyoming, AAPG Bulletin, V. 85, No. 13

Curry, W. H., and W. H. Curry, III, 1972, South Glenrock oil field, Wyoming: prediscovery thinking and post-discovery description, in Stratigraphic oil and gas fields--classification, exploration methods, and case histories, AAPG Mem. 16, 421 p.

Gries, Robbie, 1983, Oil and Gas Prospecting Beneath Precambrian of Foreland Thrust Plates in the Rocky Mountains, AAPG Bulletin, V. 67, No. 1, PP. 1-28

Hurley, N. F., A. Aviantaral and D. Kerr, 2001, Structural and Stratigraphic Compartments Determined from Horizontal Drilling in an Eolian Reservoir, Tensleep Sandstone, Wyoming, AAPG Bulletin, V. 85, No. 13. (Supplement)

Lawson, Don E., and Jordan R. Smith, 1966, Pennsylvanian and Permian Influence on Tensleep Oil Accumulation, Big Horn Basin, Wyoming, AAPG Bulletin, V. 50, No. 10, PP. 2197-2220

Montgomery, Scott L., 1996, South Casper Creek Field: South Casper Creek Field: A Study in Reservoir Heterogeneity, AAPG Bulletin, V. 80, No. 8, PP. 1161-1176

Stone, Donald S., 2002, Morphology of the Casper Mountain Uplift and Related, Subsidiary Structures, Central Wyoming: Implications for Laramide Kinematics, Dynamics, and Crustal Inheritance, AAPG Bulletin, V. 86, No. 8, PP. l1417-1440

Unknown, Maps of various oil fields in Wyoming, from the Wyoming Oil and Gas Conservation Commission website, http://www.wogcc.state.wy.us/, downloaded in October, 2003

EMIGRANT GAP ANTICLINE
Natrona County, Wyoming

Illustration Descriptions
Michael L. Pinnell, Geologist, WPG #1090

FIGURE 1: Location Map. The Casper Arch is a structural high dividing the Powder River basin on the east and the Wind River basin on the west. The Casper Arch is a northwest trending, somewhat lower structural extension of the more pronounced Laramie Range. The prospect area exhibits structural influences of both the Arch and the Range. The prospect is only a few miles west of the town of Casper, Wyoming and is along State Highway 220 which connects Casper with Rawlins and Lander.

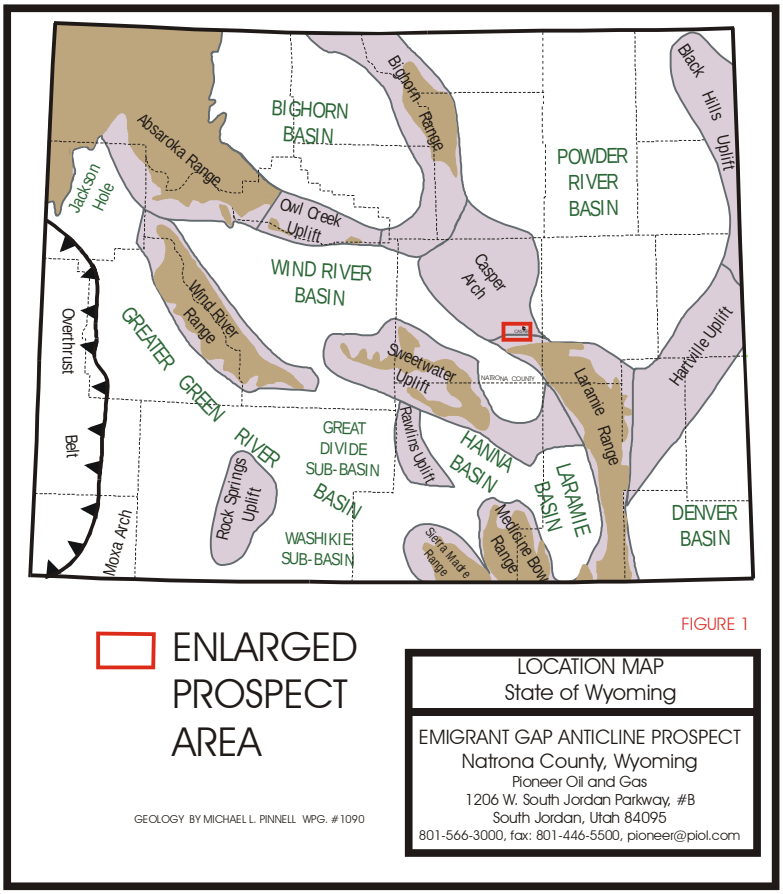

FIGURE 2: Stratigraphic Column. Cody Shale is the predominant lithology exposed around the prospect area. Because the prospect structure is a tightly folded and uplifted anticline, most formations between the Cody Shale and older Jurassic shales have been eroded and are exposed in an almost perfect presentation for geologic study along the core of the anticline. Virtually every geologic field trip of eastern Wyoming stops at the road cut just east of our drill site to study the Muddy Sandstone, Mowry

Shale (which contains fish fossils consisting of mostly fish scales with an occasional skeleton), and Cloverly Formation (Dakota equivalent and Lakota conglomerate).

The Tensleep Sandstone, our primary drill objective, is an almost perfect reservoir rock. It can be over 300 feet thick consisting mostly of ancient sand dunes. Along anticlinal crests it is commonly fractured, enhancing permeability (see Appendix 1, a photograph of a nearby anticline with Tensleep at its core). Tensleep Sandstone is also exposed along Casper Mountain Road, seven miles south-east of the prospect.

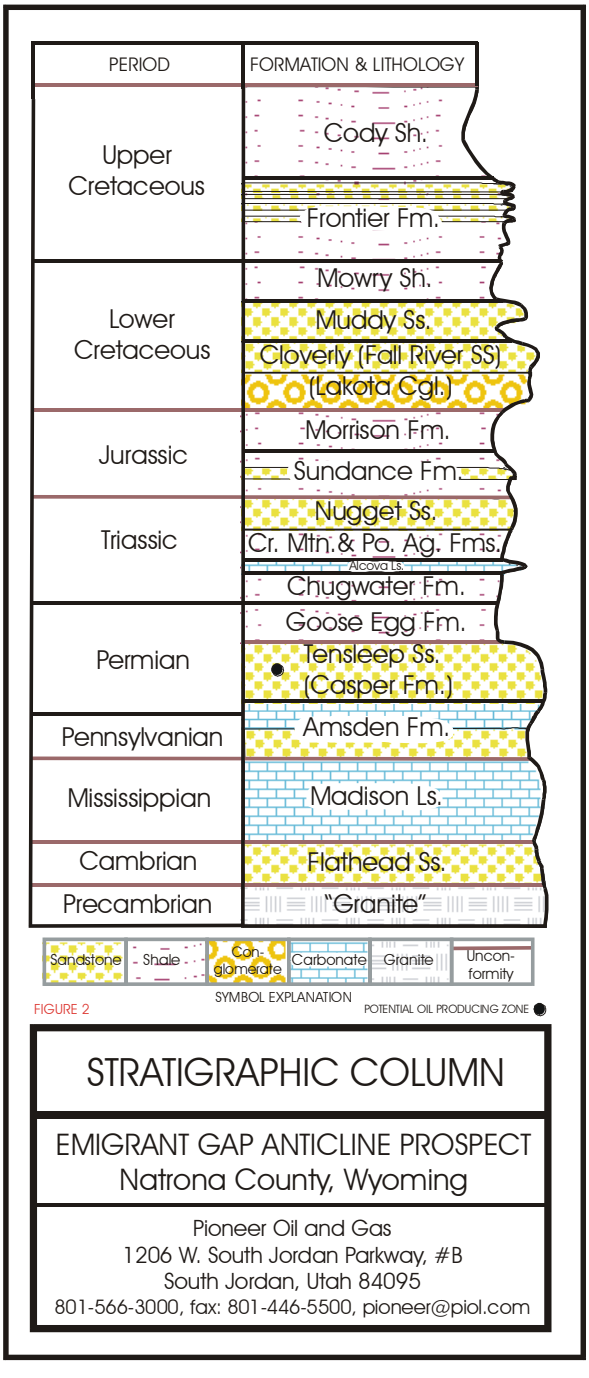

FIGURE 3: Land Map. We feel very fortunate to have a prospect wherein we own all the potentially productive leasehold. If we have a discovery, we do not have to worry about farm-ins, drilling options, unitizations for water floods, or corner shooters. Most leases are federal, issued by the Bureau of Land Management. Several small leases are fee simple on the westernmost portion of the lease block. Leases expire in 2013. A detailed land description is attached to the prospect terms.

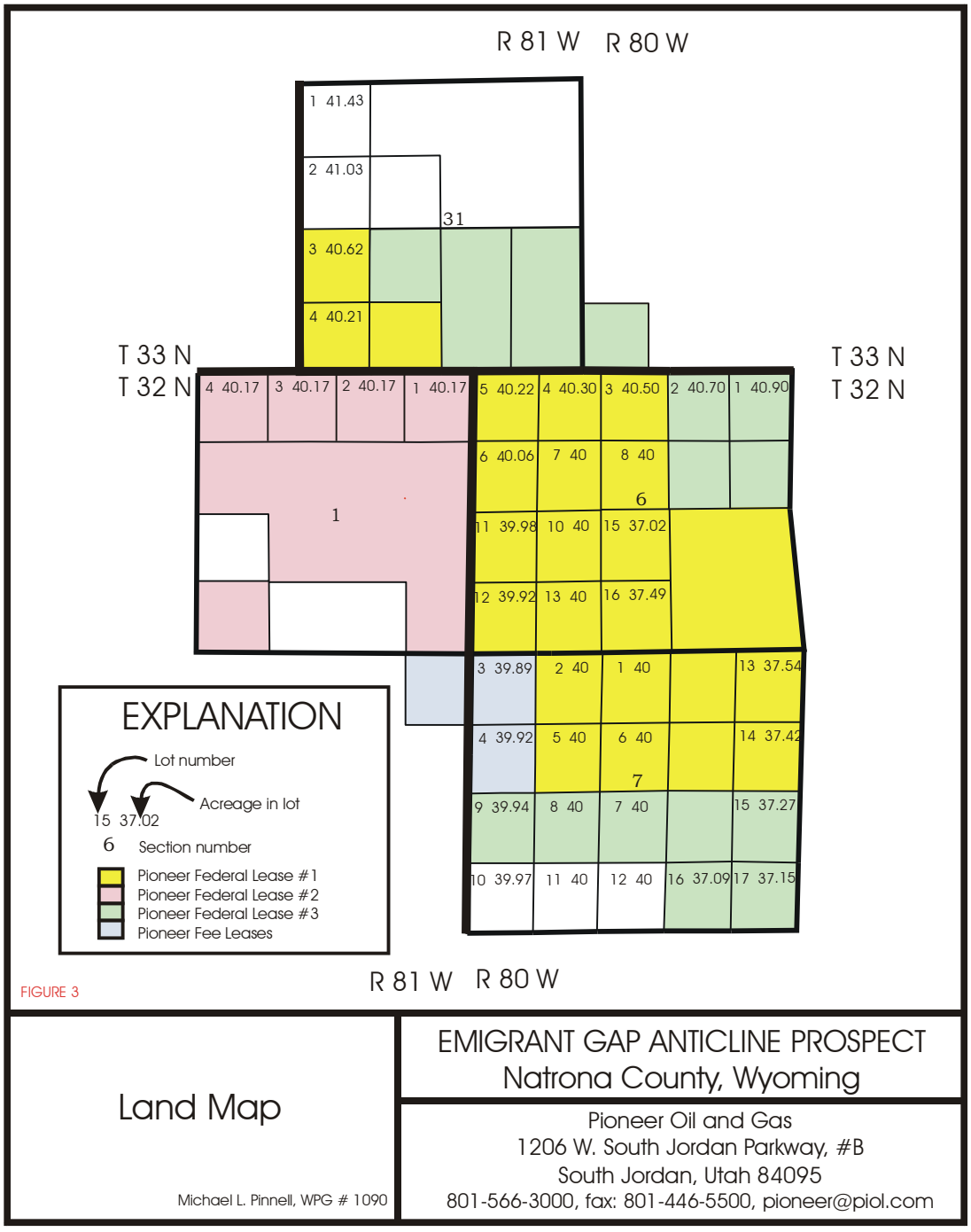

FIGURE 4: Geologic Map. A first glance at the geologic map does not tell the entire subsurface geologic story. The Emigrant Gap Anticline is the most obvious map feature being a large, northwest trending, tightly folded anticline. It extends to the northwest at least 30 miles. Casper Mountain, to the south, displays an east-west up-thrusted fault block. The southern portion of the prospect structure (see red outline) appears to be, but is not part of, this faulted block. The complex geology of Casper Mountain is deceptively hiding part of a potentially significant oil field.

This map was published by Beck, et al, in 1985 before a re-survey of the township and section lines, so the exact location of the mapped units may not precisely fit more recently generated topographic maps of the area. The highway is a good guide for locating our proposed well. Furthermore, the geologic concepts as to the nature and cause of the faulting and the resulting prospect structure were generated much more recently. Were it not so, our prospect anticline would have been drilled long ago.

Casper Mountain, complicating the geologic map, was caused by Laramide age tectonics: compressional folding and thrusting which probably occurred during the Eocene around 30 to 40 million years ago. Casper Mountain has been faulted up and over the Casper Arch generally, and over the prospect area more specifically, at a fairly flat angle of about 45 degrees. No wells have been drilled through the Casper Mountain block in the immediate area of our prospect. If you were to drill a well just south of the first Casper Mountain thrust, just south of Highway 220, and on the southern portion of the prospect, you would go quickly through the overthrust block and back into the subthrust, prospect block. Stone's cross section B-B' in his Figure 5, page 1422 of his AAPG paper shows this relationship quite close to our proposed location. The farther south you would drill into the Casper Mountain block, the deeper the prospect block would be encountered until eventually the Casper Mountain Thrust would rest directly on the Tensleep Sandstone of our prospect thus defining the southern extent of our productive area. Several townships east of the prospect is an example of a commercial oil discovery below a similar relationship where oil production was established underneath overthrusted Precambrian granite in the South Glenrock field in T32N, R75W, Section 6. The well, drilled by True Oil Co., was completed for 70 BOPD from Skull Creek Formation (approximately equivalent to Muddy Sandstone) in a broad, fairly flat stratigraphic trap. Gries described this relationship and published a cross section and location map we have redrawn (see Appendix 7).

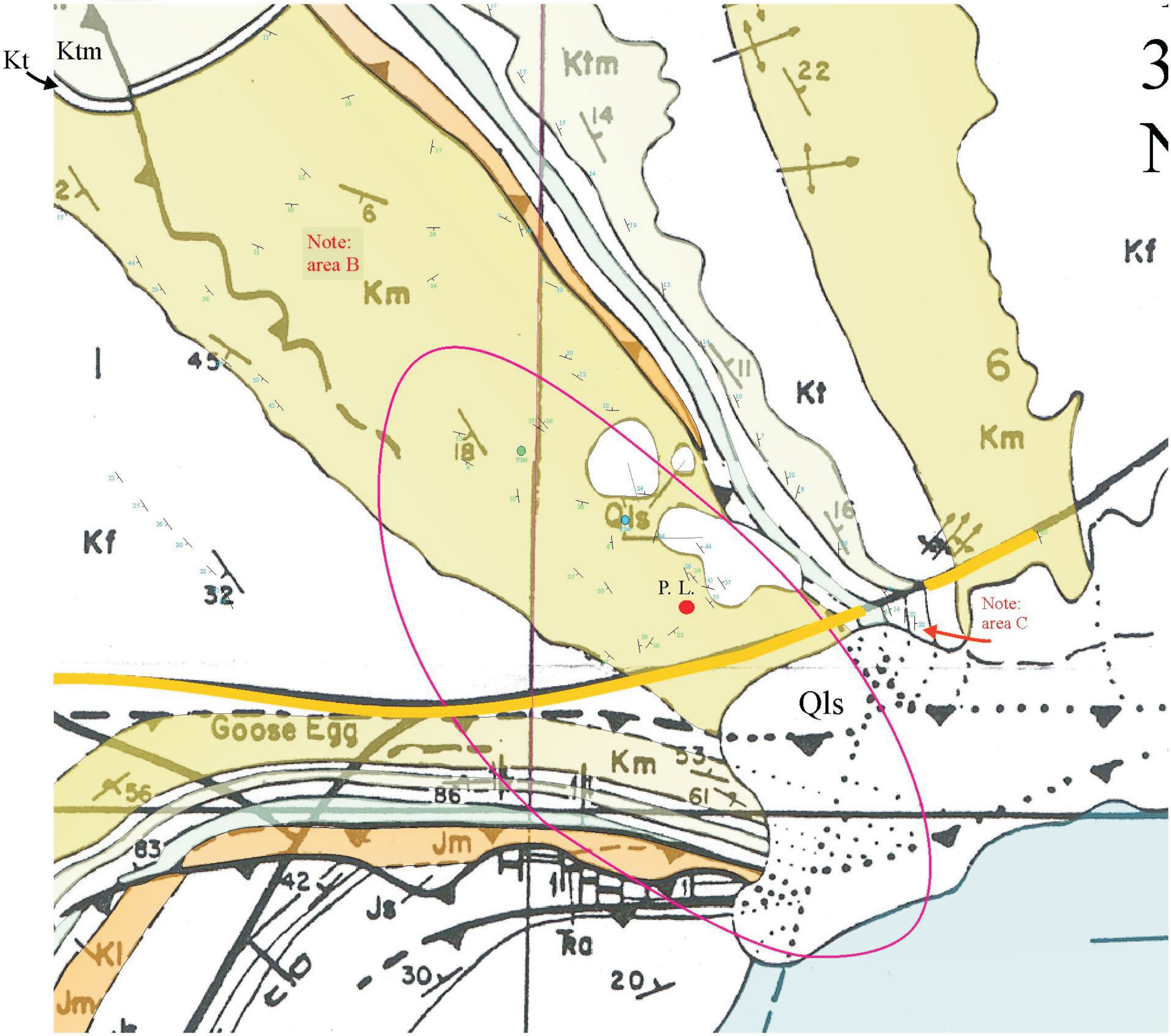

FIGURE 5

DETAILED GEOLOGIC MAP
(With Strikes and Dips by Mike Pinnell)
After W. C. Beck and A. E. Burford, 1985,
Stress analysis of the Casper Mountain-Emigrant Gap Anticline Juncture, Natrona County, Wyoming in Wyoming Geol. Assoc. Guidebook, p. 59-65

25 Strike and dip taken in March, 2003
15 Strike and dip taken in July, 2003
Prospect structure contour: Tensleep @ 3,000 ft.

Michael L. Pinnell, WPG # 1090

EMIGRANT GAP ANTICLINE PROSPECT
Natrona County, Wyoming

Pioneer Oil and Gas
1206 W. South Jordan Parkway, #B
South Jordan, Utah 84095
801-566-3000, fax: 801-446-5500, pioneer@piol.com

FIGURE 5: (Located in a separate folder). Detailed Geologic Map. In an effort to coordinate the relationship of the new geologic concepts of our prospect with the old geologic map, our geologist, Mike Pinnell, spent several days taking strike and dip measurements with a Brunton compass between the Platte River and Casper Mountain, locating himself with a GPS device. As one might expect, there was not a perfect match between the site location by the GPS device and the newly surveyed (since the geologic map was made) topographic maps. Pinnell concluded that the GPS device consistently located data points about 100 feet farther east than their actual location. This conclusion was based on an "In the field" coordination of the hand held GPS device with a portable computer containing a digital version of the topographic map plus GPS notation. In an attempt to tie the old and new data together, he then extracted all the strike and dip data points from the topographic map, drew red lines for the location of section lines and an orange line for the location of Highway 220 all from the topographic base, and did a best fit of this data set to the geologic map of Beck. The result is displayed as Figure 5. Pinnell's work overprints Beck's in a surprisingly consistent pattern. Different colors of dip amounts (squint, they are quite small) are for significantly different dates of data acquisition. Pinnell attempted to dig holes into the Mowry Shale interval in an effort to obtain dip data pertinent to the proposed location. These efforts failed. Strike/dips were often on fracture surfaces, deformed shale partings or small glide plains from shale heaving during expansion from hydration. These values are not plotted.

In the upper left portion of the illustration, at noted area "A", the small white strip of Kt (Thermopolis Shale) between Ktm (Muddy Sandstone) and Km (Mowry Shale) is an important location on the map. The dips at this juncture, being quite steep to the southeast, are anomalous to the crest of the entire extent of the Emigrant Gap Anticline (review Figure 4). They are steep indicating, at depth, either a fault or some other significant change in the deeper geology. This is where Stone elected to locate the division between the northern and southern structural closures he mapped on his Mississippian Madison structure map (which we include, in a re-drawn, easier to see format in Figure 8). We concur with his placement of the division at this location. Whether by faulting or folding, our prospect has its northern boundary near this anomaly.

Progressing further southeast, note how the once fairly consistent southwest dips begin to show significant disarray starting at noted area "B". There are, in fact several dip reversals as well as structurally flat, non measurable dip locations between "B" and Highway 220 indicating not only a possible northeast to southwest surface expression of structural reversal consistent with, but not required for, our prospect, but a deep anomaly below the somewhat convoluted shale outcrops. Surface geology is not needed to confirm our deeper structural closure because our prospect anomaly is hidden below faulted Cretaceous and Jurassic shales in a manner similar to the larger northern crest of the Emigrant Gap Anticline as mapped and drawn from surface geology, well control and seismic data by Stone (refer to Figures 9 and 10).

South closure seems to begin at noted area "C" in the southeastern portion of the map where the directions of dip definitely change from northeasterly to easterly with a slight southerly component. A close examination of the map indicates how Beck interprets the continuation of Muddy and other beds as they wrap around the southern end of the anticline under the area covered by Quaternary landslide (Qls) indicating even

more southerly dip. Again, due to the nature of our prospect, south closure need not be displayed in the surface geology to trap hydrocarbons at the Tensleep horizon, but this is somewhat reassuring, nonetheless.

FIGURE 6: Tensleep Structure Map. This is the most detailed structure map we have created for our prospect. It was constructed by using Stone's Cross-Sections (in his AAPG article, Figure 5-A and B) and Stone's Mississippian Madison structure map (his Figure 4-B). We have conservatively interpreted the crest of the anticline at our prospect to be 1,000 feet lower than the crest of the main Emigrant Gap anticline located four miles northwest (see our Figure 7). It is important to point out that Stone interpreted the prospect anticline and the Emigrant Gap anticline to be at the same structural position at the Mississippian horizon, both cresting at an elevation of +3,500 feet (see our Figure 8, a duplication of a portion of Stone's Figure 4-B). At the Tensleep horizon the entire fault block is significantly wider than on Stone's Mississippian map because the nature of the prospect creating faulting makes the block wider when positioned higher up the stratigraphic column. In other words, a structure map of the Precambrian granite would be narrowest, while a structure map of the Tensleep would be the broadest. See our Cross Section 1-2 (Figure 10).

We interpret approximately 500 feet of structural closure at the Tensleep horizon. Many Tensleep producing fields have less closure including, nearby, the slightly larger Casper Creek field which has 400 feet of closure and a 350 foot oil column (and 17 million barrels of produced oil) and Big Horn Basin's Bonanza field which has 110 feet of closure and a 210 foot oil column with 42 million barrels of 36 degree API oil at 2,900 feet and is four times as large as our prospect (Lawson, et al, pp.2206-2208).

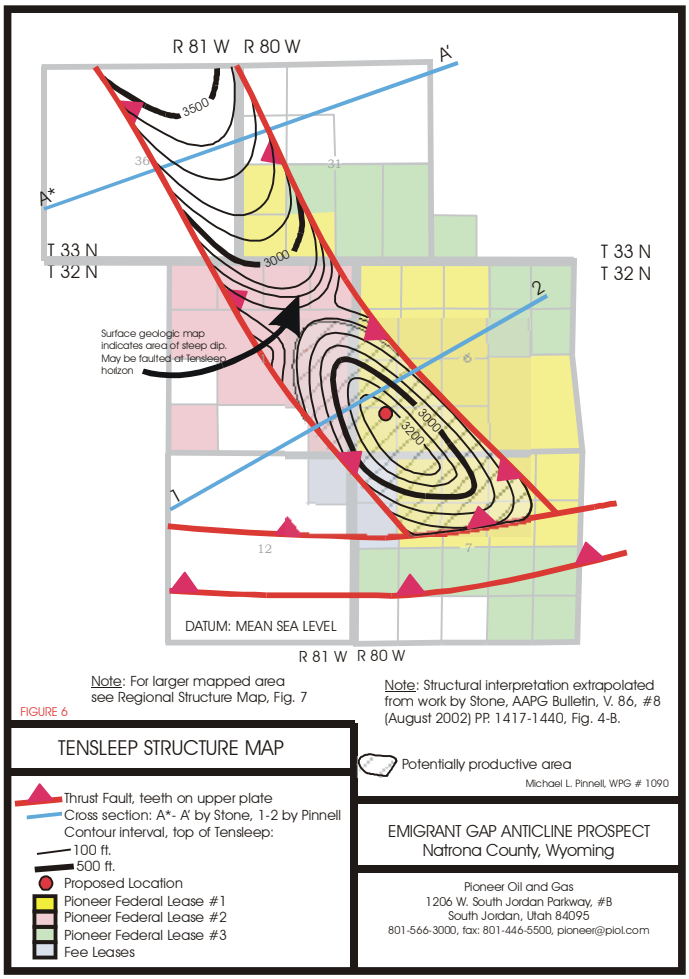

FIGURE 7: Regional Structure Map, Tensleep Sandstone. A regional structure map of the Tensleep Sandstone gives the reader the opportunity to view how our interpretation of regional structure differs from Stone's. There are very few differences. Compare our Figures 7 (our regional Tensleep structure map) and 8 (Stone's regional Mississippian structure map, redrawn at the same scale). In order to add detail to our interpretation we have estimated the top of Tensleep Sandstone in shallower Cloverly (Dakota) wells by adding the Cloverly to Tensleep isopach (from our Figure 11) to the Cloverly top to extract several more control points.

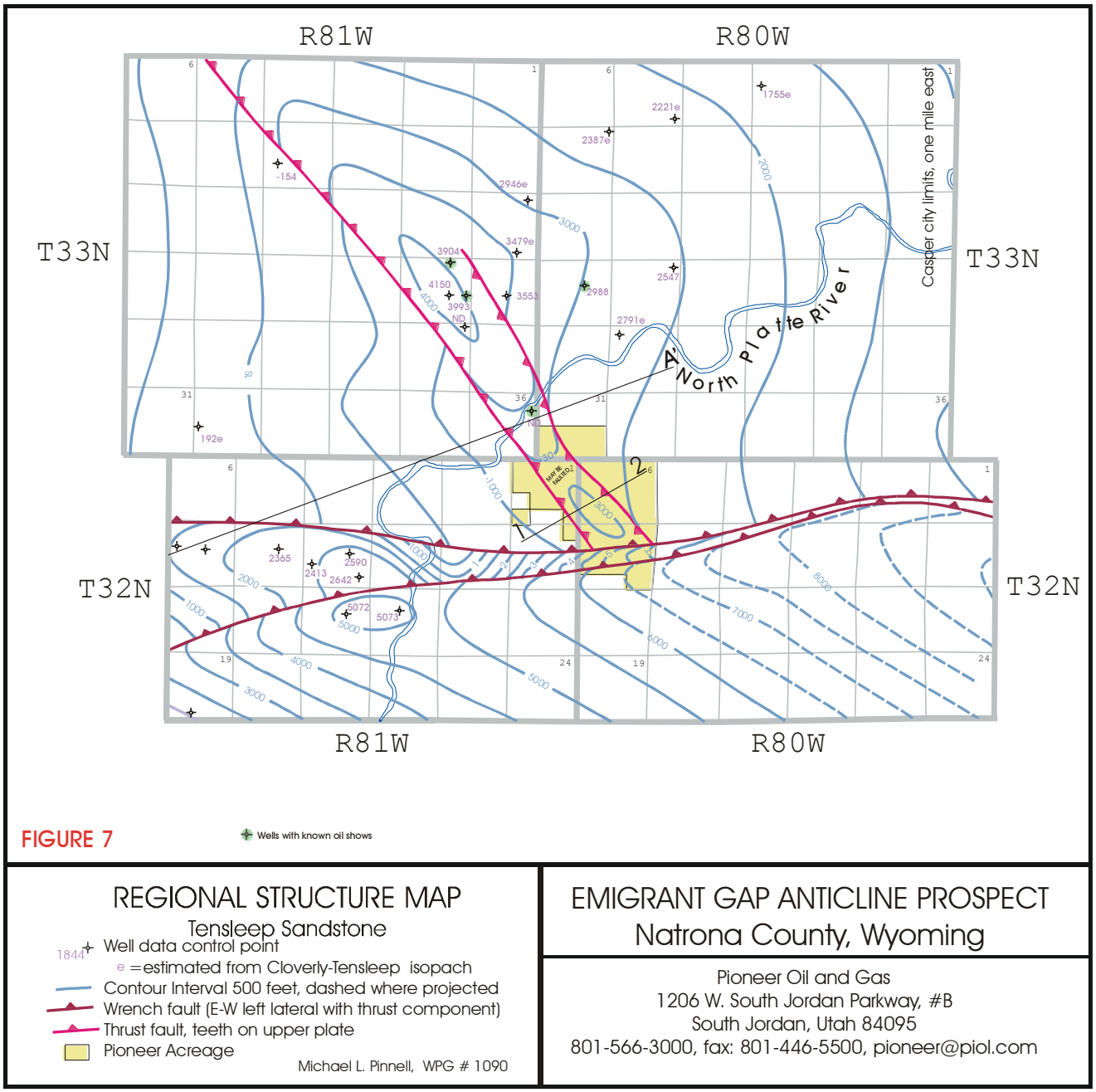

FIGURE 8: Donald S. Stone's Fig. 4-B, Enlarged Structure Map of Mississippian Madison Limestone (slightly modified). This is the most important map drawn by Stone for the definition of our prospect structure. We had been studying this area for several years with plans to lease and drill. When Stone published his AAPG paper containing this map in 2002, the future was now, so to speak, and we had to act quickly to acquire leases before another geologist recognized this undrilled anticlinal structure. We have redrawn the map around the area of the prospect because Stone's complete map covers a much larger area and by zooming in to get a closer look, detail is lost and contour lines become fuzzy.

The northwest trending prospect fault block is narrower at the Mississippian horizon because of the nature of prospect creating faulting. This fault block would be narrowest in a structure map of Precambrian granite and is widest in the Tensleep map. (See the explanation for Figure 7, and review Figures 6-10).

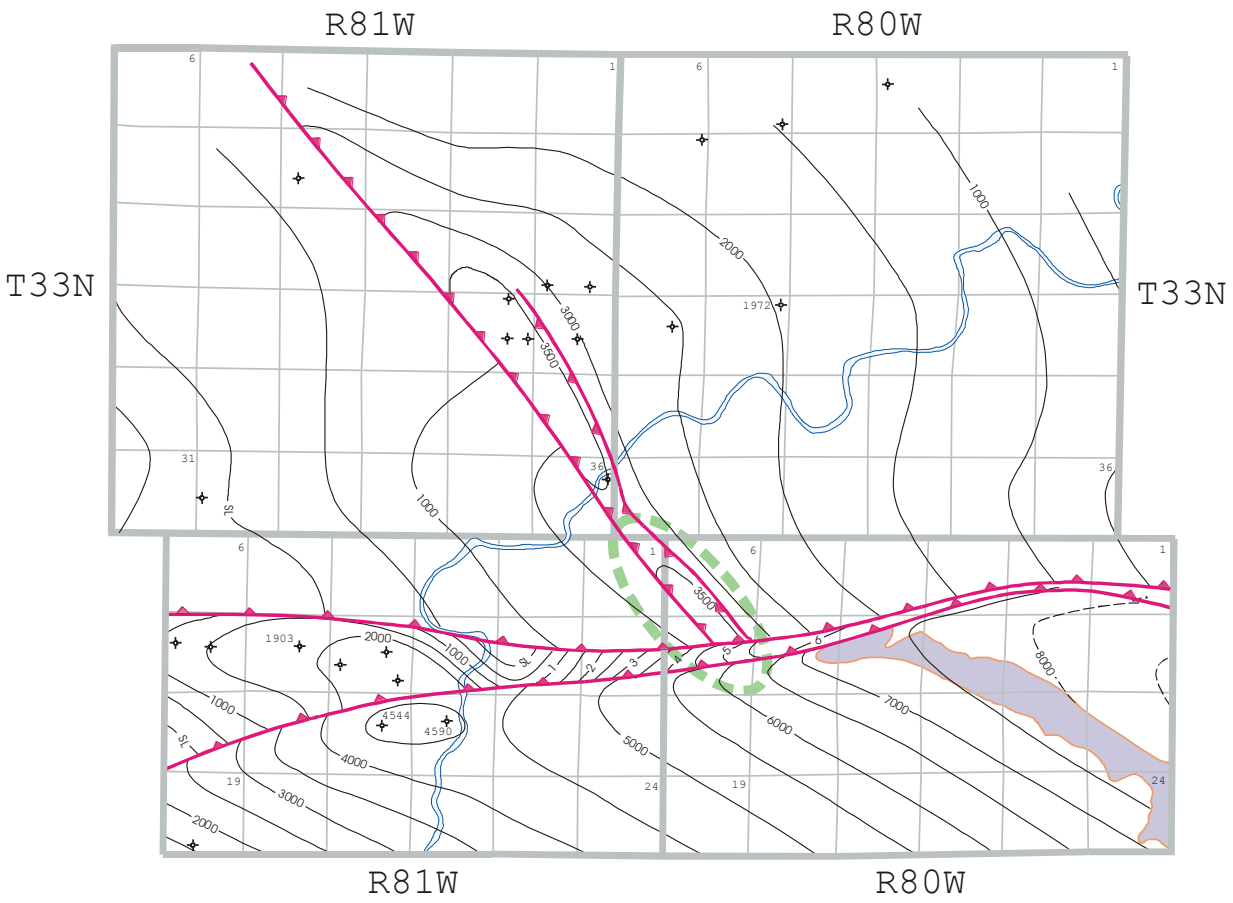

Note: We have redrawn Stone's map here so the reader can better see Stone's detail in the area of our prospect. Because our primary objective Tensleep Sandstone is above Stone's Mississippian horizon, the area of prospect structural closure is greater (see Figs. 6-10). Map source: AAPG Billetin, v. 86, #8,(August 2002), Fig. 4B.

FIGURE 8

Mike Pinnell, WPG #1090

Donald S. Stone's Fig. 4-B, Enlarged

Structure Map of
Mississippian Madison Limestone
(Slightly Modified)

4590 + Well data control point
Contour Interval 500 feet, dashed where projected
Thrust fault. Teeth on upper plate
Mississippian Outcrop
Prospect area

EMIGRANT GAP ANTICLINE PROSPECT
Natrona County, Wyoming

Pioneer Oil and Gas
1206 W. South Jordan Parkway, #B
South Jordan, Utah 84095
801-566-3000, fax: 801-446-5500, pioneer@piol.com

FIGURE 9: Cross Section A-A*-A' by Stone, 2002, Fig. 5-A, Page 1422. So there is no confusion as to Stone's interpretation of his important Cross Section A-A', we have exactly duplicated it. We have added formation colors on top of his stratigraphic horizons to provide the eye an easier visualization. In addition, we have added the Tensleep horizon at a position 450 feet above the Mississippian Madison (Mm) marker. The same colors are used on our Cross Section 1-2. We have added A* to Stone's Cross Section because the entire illustration would be too wide to display; the A* indicates the southwestern extent we display on this drawing and on the maps used in this report. Note the width of Precambrian granite in the prospect fault block. It is narrow. The Mississippian Madison is wider, and Tensleep is widest. With this in mind, the reader can visualize why our prospect structure block at the Tensleep horizon is wider than that shown by Stone in his Mississippian structure map.

Stone's structural interpretation of the Emigrant Gap Anticline is based on well control, surface geology, seismic data, and his superior knowledge and understanding of tectonics of this part of Wyoming accumulated from 40 years of study and hundreds of publications. We are grateful for his publication. It is important to note here that Stone has no financial interest in this prospect. When he drew his maps and cross sections, he did so without any intent to sell a project with this study, as far as we know.

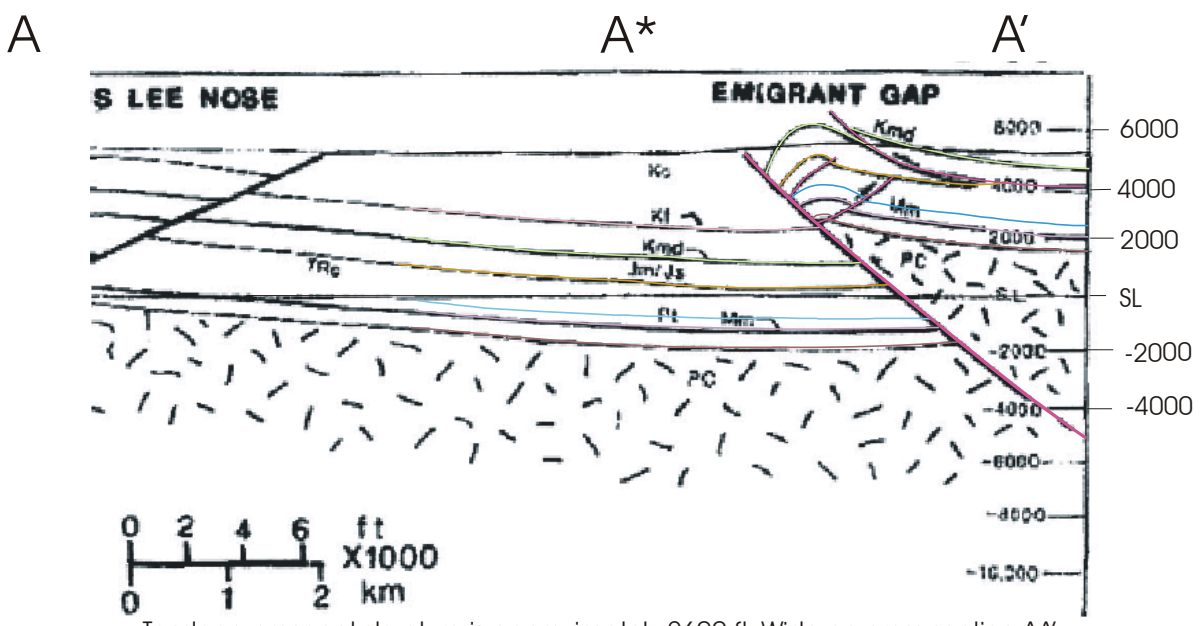

FIGURE 9 Tensleep prospect structure is approximately 2600 ft. Wide on cross section AA'. Tensleep horizon (blue) has been added in stratigraphic position for clarity.

Note: colors are added so the reader can better compare to Pinnell's Cross Section 1-2. Location of this cross section is on Stone figures 4&5, and on Pinnell's Tensleep Structure map.

Cross Section A-A*-A' by Stone, 2002, Fig. 5-A, page 1422

FIGURE 10: Cross Section 1-2. By using Stone's Cross Section A-A', Beck's geologic map (Figure 4), and our recent strike and dip measurements, any geologist can approximately create this illustration. It looks much like Stone's work and it should because it is only just over a mile south of it. Fault location and orientation as well as stratigraphic position of the various formations has already been determined by Stone's work based on well control, surface geology and seismic data interpretation. Our cross section, however, is approximately 1,000 feet lower than Stone's at the Madison and Tensleep horizons (see Stone's Mississippian Madison structure map, duplicated in this report as our Figure 8). Even though we could place it structurally higher than our present interpretation, we prefer this display because: 1. It seems to fit better geologically, and 2. We prefer to err on the conservative side of geologic interpretation.

The maxim potential oil fill up of the prospect would place an oil-water contact approximately 500 feet below the top of the Tensleep. We further calculate the area of maximum oil production from the structure map (Figure 6) to be approximately 485 acres. There are several ways potential reserves may be calculated:

EMIGRANT GAP PROSPECT

ESTIMATED RECOVERABLE OIL RESERVES

AREA OF CLOSURE, ACRES	AREA OF PRODUCTION, ACRES	THICKNESS OF PAY	RECOVERY FACTOR (BO/AF)	TOTAL OIL RECOVERABLE
485	485	250	200	24,250,000
485	485	175	200	16,975,000
485	344	250	200	18,187,500
485	344	175	200	12,731,250
350	263	150	200	7,875,000
350	263	100	100	2,625,000

Most likely reserves for the prospect are between six and twelve million barrels of recoverable oil.

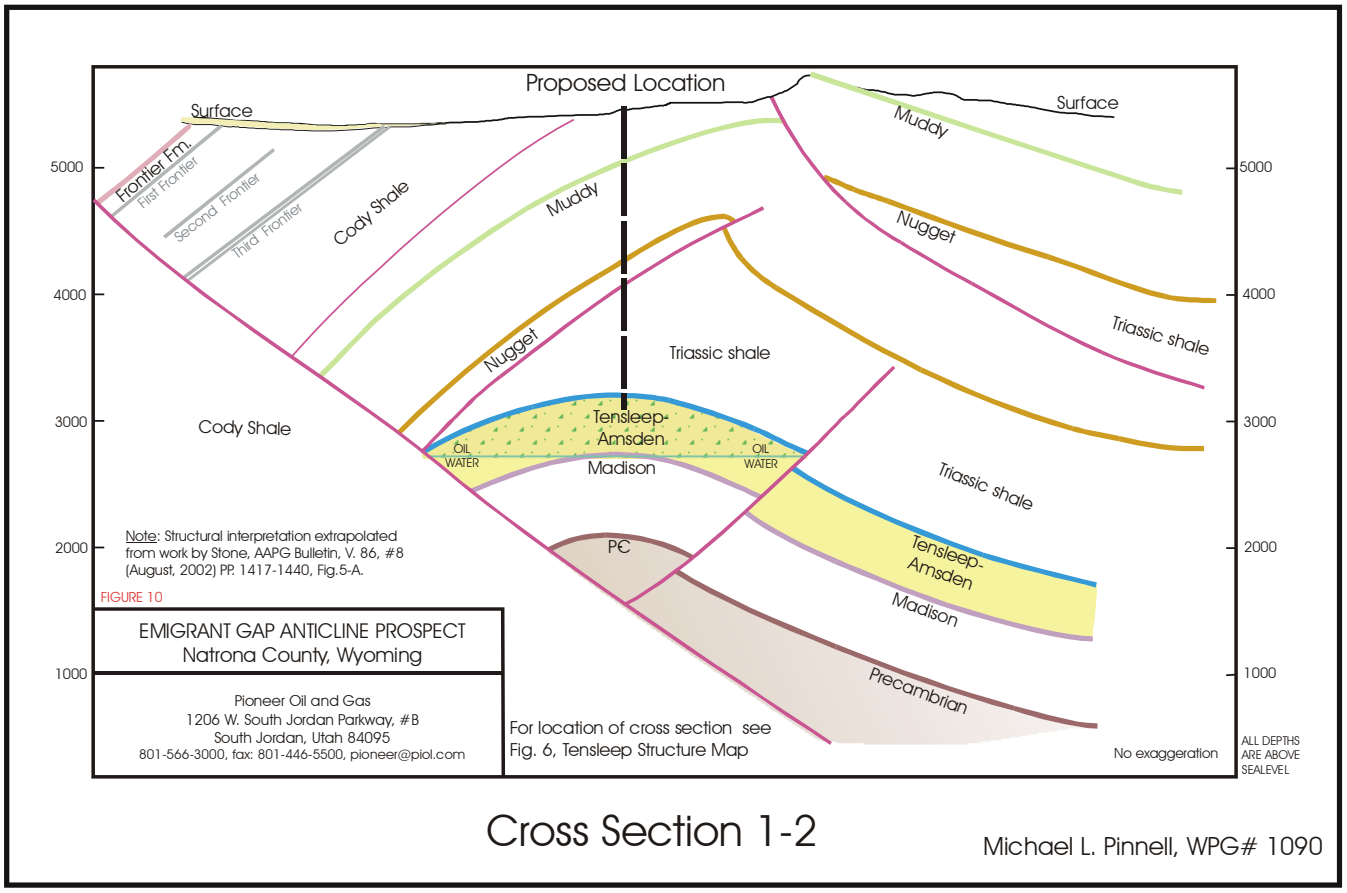

FIGURE 11: (Located in a separate folder). Isopach Map, Cloverly (Dakota) Formation to Tensleep Sandstone. Why will oil be trapped in the prospect closure when it was not trapped in the structurally higher crestal closure of the main Emigrant Gap Anticline (which did have good shows of oil)? This map will help answer the question. (Also review Figure 12 where Little Winkleman Dome field is structurally lower without fault separation from the adjacent, much larger but barren anticline. And read Lawson's paper noted in the bibliography).

Oil in Tensleep Sandstone is almost always generated from Permian age Phosphoria Formation phosphatic shales. In the past, geologists assumed that oil must have been generated from only a few miles away and then migrated into Tensleep sandstones after Laramide age faulting and folding which consummated 30 to 40 million years ago in this area, with the faulting and folding we see at our prospect. The experts of oil migration theory, one of whom is Mr. Donald Stone, no longer accept this. The new concept is that prior to the Laramide Orogeny, perhaps during the Jurassic or early Cretaceous (200 to140 million years ago) oil began cooking from Phosphoria Formation phosphatic shales where they were deeply buried at or near the "Geologic hingeline" in the western part of what is now the state of Wyoming. This migration occurred prior to Sevier age thrusting in the hingeline. This oil moved into the porous Tensleep sandstones

located immediately below the Phosphoria Formation and continued to move up dip sturcturally, or generally speaking, to the east. During this geologic time, a structure map of Wyoming would have appeared almost unstructured, displaying a very gradual, regional western dip component (in other words, nearly flat, but a little higher on the east). There were very few faults and the anticlines present exhibited low relief, and were much mort subtle than the striking but much later Laramide structures we see today. Oil migrated through Tensleep Sandstone with residual pockets occurring at these old, low relief, anticlinal structures. Then, 100+ million years later, the Laramide Orogeny kicked in, faulting and folding in zones of basement weakness. These more prominent anticlines created the more pronounced hydrocarbon traps we drill today. If one of these old, pre-Laramide, low relief, oil filled anticlines were at the same location where a Laramide anticline formed 100+ million years later, a wonderful oil field would have been created like nearby South Casper Creek, or Lost Soldier, or one of the many other examples of fields which produce large volumes of oil from Tensleep Sandstone. On the other hand, if a Laramide structure formed where there was no previously oil filled older structure, no commercial oil would be in the Tensleep, but oil may be in shallower formations due to other geologic factors like nearby Bates Creek, Schrader Flats, or Iron Creek anticlines (see Appendix 9 and 10). And, if a large Laramide structure formed with the old, pre-Laramide structure on its flank, then the larger structure may contain no oil while the smaller one may contain large volumes of oil like *Little* Winkleman Dome Field which has produced 55,000,000 barrels of oil, from Tensleep, adjacent to the much larger, but non-Tensleep productive, Sage Creek Anticline (see Figure 12), or our *little* prospect structure adjacent to the much larger Emigrant Gap Anticline. Note: Please do not confuse the non-productive Sage Creek Anticline adjacent to Little Winkleman Dome Field with an oil productive anticline by the same name in the Big Horn Basin.

This isopach map demonstrates thickness variability of the interval from Tensleep Sandstone to Cloverly (Dakota equivalent). Where it is thick, a swale or syncline was present during that specific interval of geologic time. Synclines, as structural lows, accumulate greater sediment thickness. When oil migrated through Tensleep sandstones during the major oil migration phase, no oil would have stopped in a syncline. On the contrary, where this interval was thin, less sediment was deposited where an anticline was present. Most of the area of the map is represented by gradual, regional changes in thickness and demonstrates neither anticlinal nor synclinal proclivities. Because oil may have migrated sometime during the deposition of this interval, an anticlinal structure (shown by an isopach thin) represents a locale of probable early oil accumulation. The trick is to find one of these oil accumulation sites with a younger Laramide anticline superimposed on top of it. You have surmised correctly that our prospect fits these criteria. There is a gradual, regional thickening of the isopach interval from the northeast to the southwest. Note, however, the marked, counter regional thinning in the wells just north of our prospect and at the Casper Creek field area. We believe this thinning clearly demonstrates two of these older, anticlinal structures described above.

It is possible that the Casper Mountain Wrench Fault Zone created an offset of this old structure. The other portion would be somewhere southeast of the prospect and on the opposite side of the Casper Mountain fault zone. Using geologically biased contouring and with absolutely no well or surface control, we are able to force fit the other, southern portion of this feature to be west of the site of the of the Casper Mountain

anticline centered at Section 7, T32N R79W. We acknowledge this to be a BIG stretch since in Stone's paper he broached the subject and could justify only up to 2800 feet of left-lateral offset with limited data, while, if we are correct, the offset may be as much as a mile. Such reasoning points to the possibility, though remote, that the now breached Casper Mountain Anticline may have been near a large, ancient, pre-Casper Mountain uplift oil field prior to being exposed by erosion. There is economic significance here: We believe other similar prospects of large Tensleep oil accumulations exist, yet undiscovered, elsewhere in this region and in the Rocky Mountain area in general. Using similar geologic techniques, we believe we may be able to find them. We also know most other geologists we talk to at geologic conventions and prospect fairs are not using similar exploration criteria; otherwise our prospect would have already been drilled.

Some faulting exists in the wells used for this study. We have attempted a correction of the faulted interval near our prospect. We made note of it where such faulting exists, uncorrected, elsewhere (see the legend of Figure 11 for clarification).

FIGURE 12: Comparison of Emigrant Gap-Prospect Anticline to Sage Creek-Winkleman Dome Anticline. The similarities between Emigrant Gap Prospect- Emigrant Gap main anticline and Winkleman Dome-Sage Creek Anticline are striking. They have similar geometries, depths, structural offsets, sizes and surface geologic expressions. It is interesting to note their greatest differences: one is that Winkleman Dome is 2,000 feet structurally lower than the much larger Sage Creek Anticline, while we map our Prospect anticline to be 1,000 feet structurally lower than the much larger Emigrant Gap main structure. Another difference is that *Little* Winkleman Dome has produced 55 million barrels of oil from Tensleep Sandstones, while our prospect has not yet been drilled.

A note of clarification: The original name of the Winkleman Dome Field was given to be "Little Winkleman Dome" when discovered in 1917, possibly because the adjacent, oil barren Sage Creek Anticline was so big. We like the term "Little" when referring to Winkleman Dome because this small structure has produced a total of 94,253,968 barrels of oil.

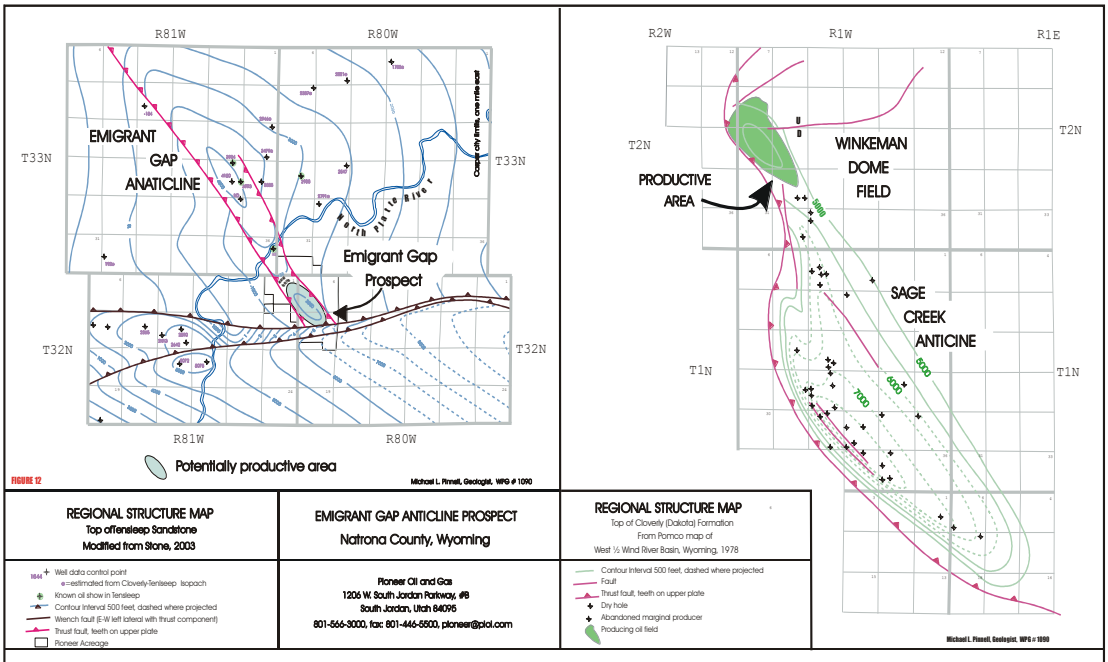

COMPARISON OF EMIGRANT GAP ANTICLINE PROSPECT TO SAGE CREEK-WINKLEMAN DOME ANTICLINE

E. G. ANTICLINE	E. G. PROSPECT	CATEGORY	SAGE CREEK ANTICLINE	WINKLEMAN DOME FIELD
Tensleep Fm.	Tensleep Fm.	PRIMARY OBJECTIVE	Tensleep Fm.	Tensleep Fm.
1,700 ft.	2,300 ft.	DRILL DEPTH TO TENSLEEP	1,100 ft.	2,900 ft.
Oil shows only	Undrilled	TENSLEEP PRODUCTION	Oil shows only	55,000,000 B.O.
None	Undrilled	TOTAL PRODUCTION, ALL ZONES	32,000 B.O.	92,503,495 B.O.
12 miles		LENGTH OF TOTAL ANTICLINAL CLOSURE	12 miles	
	1.2 miles	LENGTH OF "SMALL" ANTICLINAL CLOSURE		1.5 miles
5,000 ft		MAXIMUM STRUCTURAL DISPLACEMENT	5,000 ft.	
	1,000 ft. Low	ANTICLINAL CREST DIFFERENCE FROM LARGER STR.		2,000 ft. Low
Jurassic	Cody, Frontier	Formation at surface	Triassic	Frontier

APPENDIX 1: Emigrant Gap Anticline Prospect Photos. The photo of Emigrant Gap Prospect proposed location was taken from Highway 220. Our proposed location is easy to access, and fairly flat. There are also several easy access locations on the south side of the highway. However, part of the prospect is under Highway 220 and will probably require some horizontal development drilling. Fortunately, great strides have been made in horizontal drilling over the last few years. Furthermore, Tensleep Sandstone has recently been described as an excellent candidate for the horizontal drill bit in several papers (Appendix 17 and 18).

Alcova Anticline, photographed here at the Tensleep horizon, is about the same size closure as our prospect anticline in cross section. This is a fabulous exposure allowing examination of the ancient sand dunes including cross stratifications ranging from 5 to 30 degrees dip with sand grains being blown from the northwest to the southeast. Fractures of various angles, but with a strong vertical component, are present at the apex of the structure and will be present at our prospect. These fractures will significantly enhance permeability at our prospect allowing oil to be produced more rapidly and more efficiently. This outcrop is a must visit for geologists or anyone who wants to better understand the nature of Tensleep Sandstone in Laramide anticlines. It

may be visited either from the water or on foot. The water is a much easier means to visit the outcrop, so take a boat, not a hike.

Proposed location: ne/sw/sw, Section 6, T32N, R80W, Natrona County, Wy.

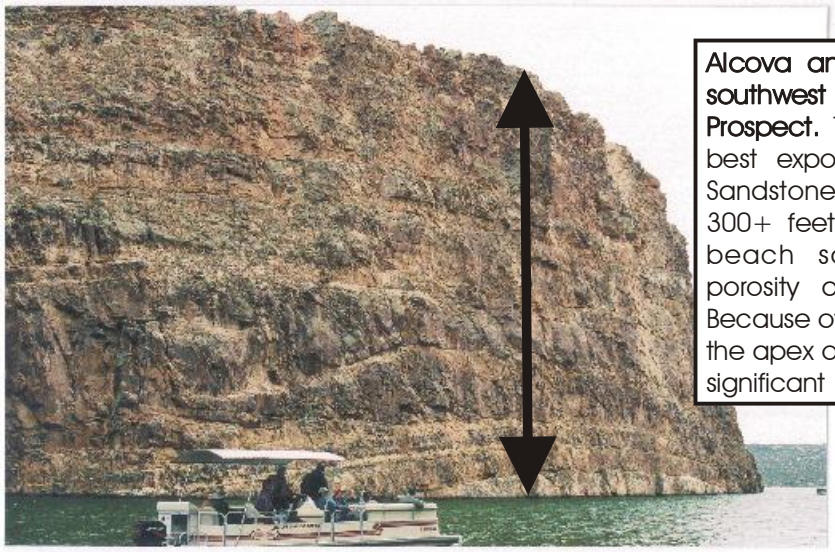

Alcova anticline, 24 miles southwest of Emigrant Gap Prospect. This area has the best exposure of Tensleep Sandstone in the region: 300+ feet thick, dune and beach sands; excellent porosity and permeability. Because of anticlinal folding, the apex of the anticline has significant vertical fractures.

APPENDIX 1

Emigrant Gap Anticline Prospect Photos; Pioneer Oil & Gas

APPENDIX 2: (In pocket of brochure). Fremont Canyon Tensleep surface section, Section 9, T23N, R83W, by Allen and Tenney, 1986. This measured section of Tensleep Sandstone is one of the best-exposed Tensleep outcrops in the Rocky Mountain area. It is located five miles southwest of Alcova Anticline mentioned above.

APPENDIX 3: Porosity (Sonic) Log, Tensleep Sandstone. This well was drilled in 1965 and is located 2.5 miles north of our prospect. Porosity is greater than 10% in 223 feet of sandstone and would be net pay thickness in our prospect if this were the well log from our prospect well. A nine foot core cut in the uppermost part of the Tensleep Sandstone encountered sand with porosity over 20% (where the log indicated 17-18%), up to 2100 millidarcies of permeability and over 8% of pore space filled with oil.

Considering the very high porosity and permeability, it is surprising any oil at all was left in the core. See Appendix 4 for the best available core description.

SONIC LOG-GAMMA RAY

Amerada Petroleum Corporation

Amerada #1 U. S. A. Gap Tract #1

C SW NE Section 19, T33N, R80W

Natrona County, Wyoming

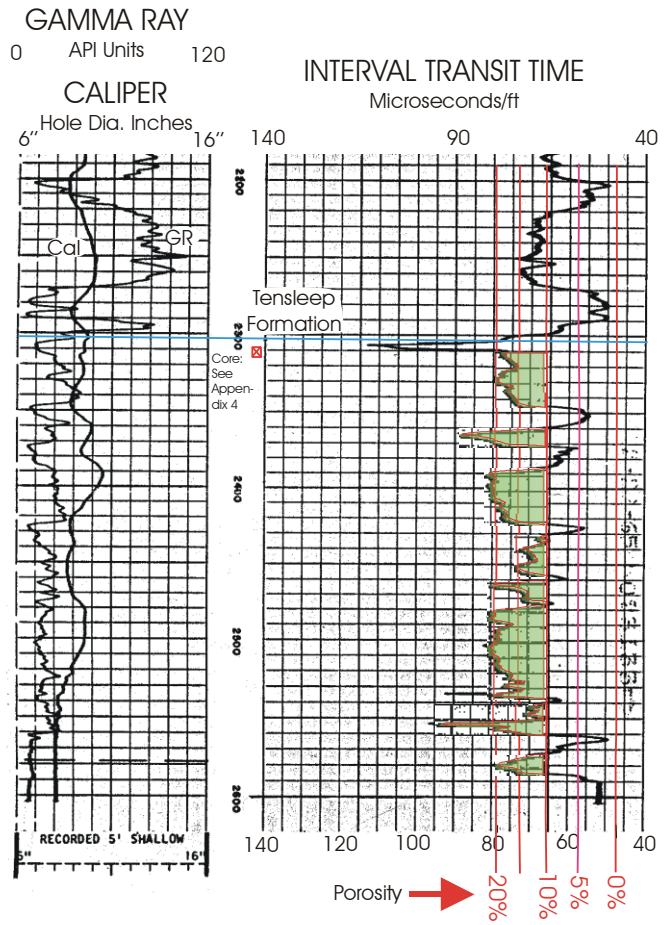

Porosity > 10% is highlighted in green

Porosity > 10% = 223 feet

APPENDIX 3

Porosity Log
Tensleep Sandstone

EMIGRANT GAP ANTICLINE PROSPECT

Natrona County, Wyoming

Pioneer Oil and Gas

1206 W. South Jordan Parkway, #B

South Jordan, Utah 84095

801-566-3000, fax: 801-446-5500, pioneer@piol.com

APPENDIX 4: Oil Shows, Tensleep Sandstone, in Wells Adjacent to Emigrant Gap Prospect. Most Tensleep penetrations near our prospect were drilled over forty years ago. Detailed sample descriptions are hard to find for these old wells. There are a few. Those with oil shows are listed. The most important one is the Amerada Petroleum well in Section 19, T33N, R80W. This well cut a core near the top of the Tensleep Sandstone and measured 8.9% oil saturation in sandstone with 22% porosity and 2183 millidarcies of permeability. There must have originally been higher oil saturation in this core since the porosity and permeability are so high. Similar age Minnelusa sandstones in the Powder River Basin sometime have lower oil saturations in cores from highly porous and permeable, 100% oil saturated zones. See Tensleep Structure map, Figures 7 & 12, for location of wells with shows. Based on the oil shows so near our prospect, oil certainly has accumulated near here in the past, a good indication that a large accumulation may be close…Within 2.5 miles?

OIL SHOWS, TENSLEEP SANDSTONE
in wells adjacent to
Emigrant Gap Prospect

Amerada Petroleum Corp. #1 UAS GAP SW/NE Section 19, T33N, R80W
Located 2.5 miles north of our prospect.
Tensleep @ 2303
Shows: Core #1.

DEPTH, FEET	EFFECTIVE POROSITY PERCENT	HORIZONTAL PERMEABILITY, MILLICARCIES	% PORE SPACE RESIDUAL OIL	% PORE SPACE TOTAL WATER
2307-08	22.0	2183	8.6	90.9
2309-10	21.2	1220	8.9	66.1
2311-12	18.2	856	3.5	86.7
2314-15	13.3	109	TRACE	88.6

Lysite Ventures #23-1 Govt., NE/NW/NE Section 23, T33N, R81W.
Located 2.5 miles northwest of our prospect.
Tensleep @ 1956'.
At base of log submitted to state of Wyoming: DST 2020-2051: rec 330 ' mud-cut water with dark brown live oil ??? cut, sli shows, live brn oil in last 179'.
No sample description available.

Aztec Oil & Gas Company #1 Government-Roush, NE/NW/SE Section 23, T33N, R81W
Located 2 miles northwest of our prospect.
Tensleep @ 1810'
Shows. 1960-1965: Sandstone, clear quartz grains, medium to coarse grained, angular to sub-rounded, porous and friable, few pieces with brown oil stain, weak fluorescence and good cut.
1965-1980: Sandstone, as above, brown oil stain more common, fair fluorescence and good cut. Sample had faint petroleum odor. Lost circulation while drilling at 1983.
1985-2000: Sandstone, white to light gray, medium to fine grained, slightly calcareous, no visible porosity, soft, fair cut from pieces which are speckled with black asphalt-looking speck.
2000-2005: Sandstone, white, dolomitic, as above, yellow fluorescence with no cut.

APPENDIX 4

APPENDIX 5: Dakota structure map of Winkleman Dome and Sage Creek Anticline after Pomco Map, W/2 Wind River Basin. This is the original version of the map we have duplicated in Figure 12 so the reader can examine the original structure map and the prospect map at the same scale and in the same format.

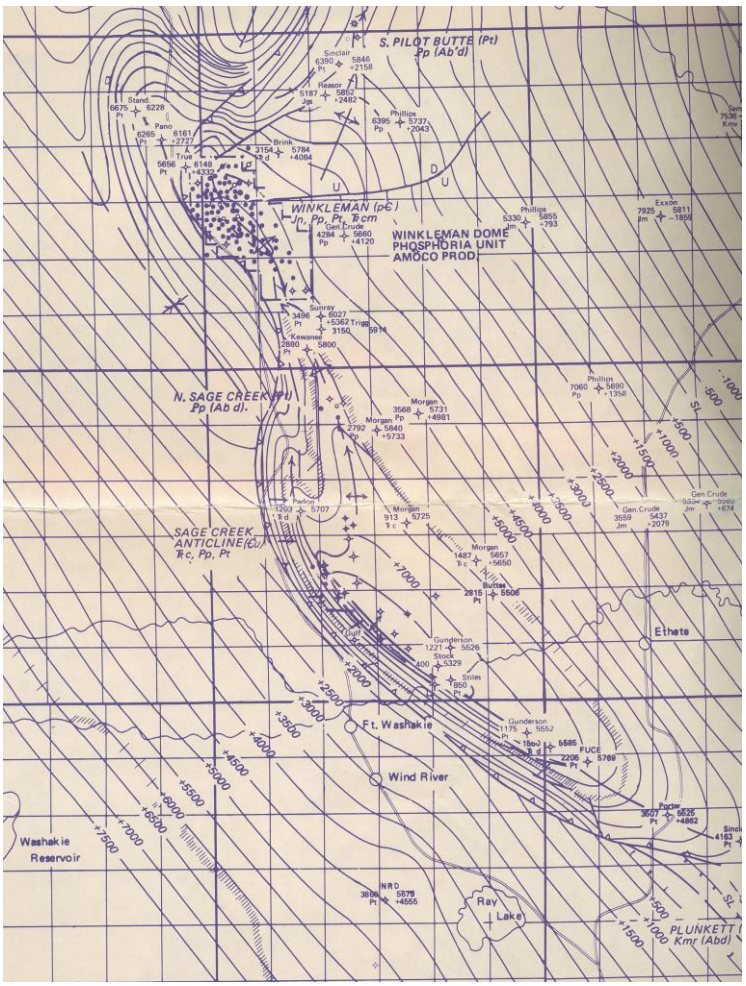

DAKOTA STRUCTURE MAP
WINKLEMAN DOME AND SAGE CREEK ANTICLINE
After Pomco Map, W ½ Wind River Basin

APPENDIX 6: Topographic Map. The topographic map of the prospect area demonstrates ease of access to the drill site as well as other possible locations. Highway 220 will be a problem for development wells, but not an insurmountable one. Several

studies have been recently conducted exploring the benefits of horizontal development wells in the porous, permeable Tensleep Sandstone (see Appendix 17 & 18).

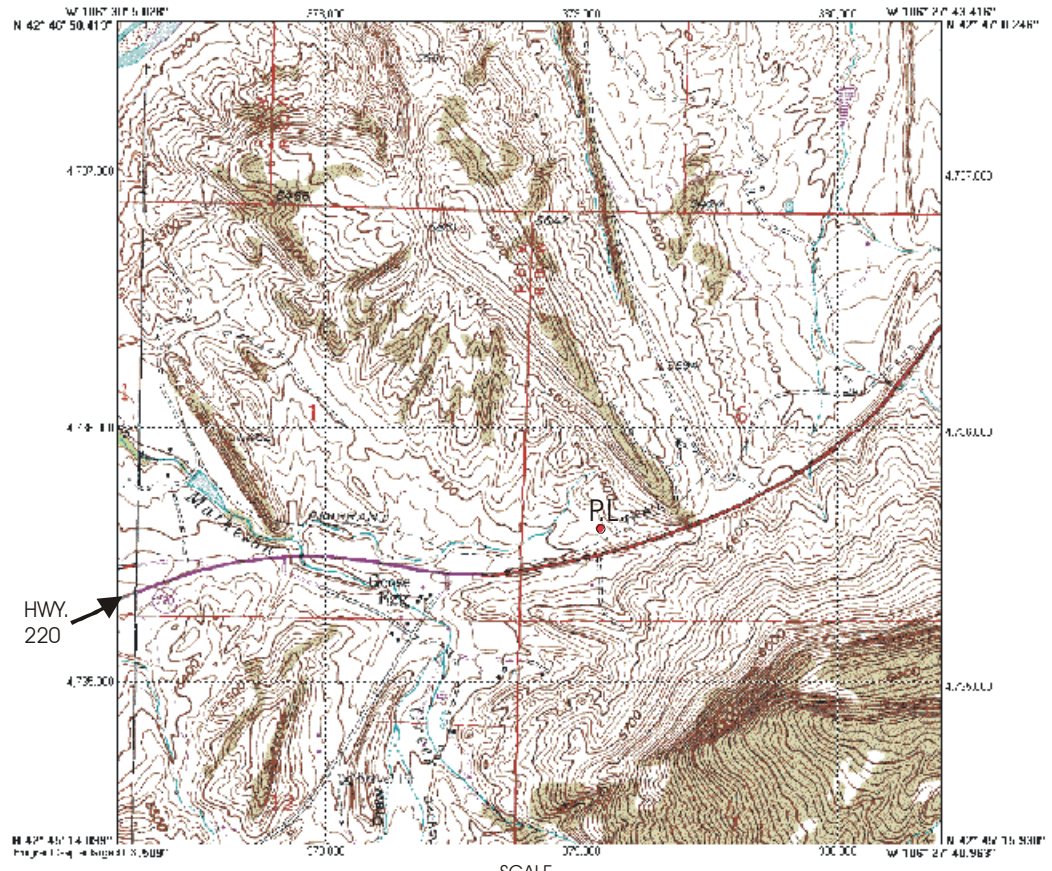

APPENDIX 6

TOPOGRAPHIC MAP

EMIGRANT GAP ANTICLINE PROSPECT
Natrona County, Wyoming

Pioneer Oil and Gas
1206 W. South Jordan Parkway, #B
South Jordan, Utah 84095
801-566-3000, fax: 801-446-5500, pioneer@piol.com

APPENDIX 7: Laramie Range overthrust geology similar to Casper Mountain at Emigrant Gap Prospect. The geometry of the Laramie Range Thrust, as shown here in Gries' drawing, will be the same as the geometry of the Casper Mountain Thrust at our prospect. The fault dips at a fairly flat 45 degrees to the south. Is it possible for an oil field to be partially hidden under an overthrust fault block? Yes indeed!

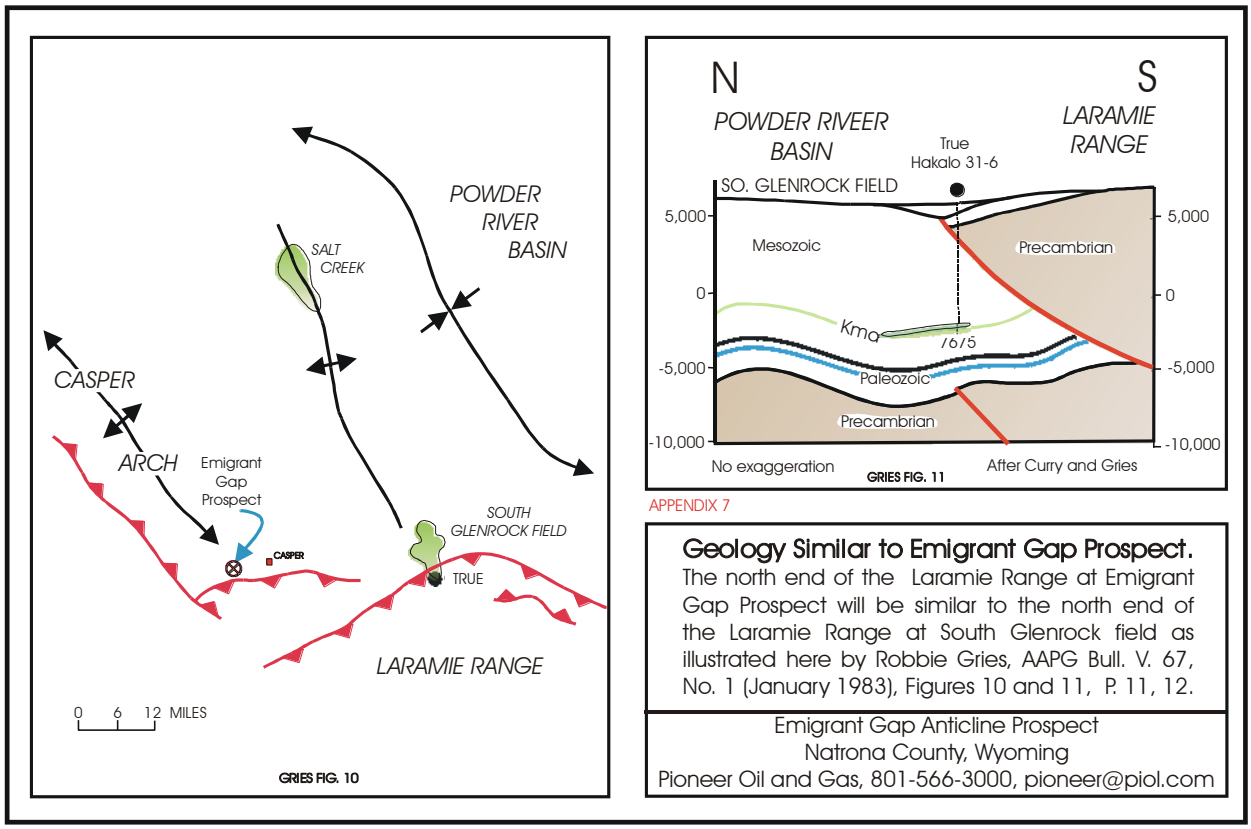

APPENDIX 7

Geology Similar to Emigrant Gap Prospect.
The north end of the Laramie Range at Emigrant Gap Prospect will be similar to the north end of the Laramie Range at South Glenrock field as illustrated here by Robbie Gries, AAPG Bull. V. 67, No. 1 (January 1983), Figures 10 and 11, P. 11, 12.

Emigrant Gap Anticline Prospect
Natrona County, Wyoming
Pioneer Oil and Gas, 801-566-3000, pioneer@piol.com

APPENDIX 8: Emigrant Gap Prospect, estimated recoverable reserves. Tensleep oil reserves in anticlines have great variability. Some great fields have 110 feet of closure, 210 foot oil column (Lawson and Smith) and tens of millions of barrels of recoverable oil reserves. Other structures exceed 1,000 feet of closure and have only minor shows. What's a geologist to do? Make isopach maps of prospect areas in an attempt to determine when the structure first formed. If the anticline has closure now and exhibits a good probability of having had pre-Laramide, anticlinal closure, it has a good chance of being a great oil field (see explanations above in Figures 11 and 12).

Assuming our prospect has only 350 acres of closure, less than the 485 acres of closure we have mapped, and that it will be filled only to 75% of capacity (net productive area of 263 acres) and have a very conservative 150 feet of pay (a nearby log demonstrates 223 feet of pay, see Figure Appendix 3), potential recoverable reserves are

a very respectable 7,875,000 barrels of oil. Several other possible scenarios represent a broad spectrum for consideration and contemplation.

EMIGRANT GAP PROSPECT

ESTIMATED RECOVERABLE OIL RESERVES

AREA OF CLOSURE, ACRES	AREA OF PRODUCTION, ACRES	THICKNESS OF PAY	RECOVERY FACTOR (BO/AF)	TOTAL OIL RECOVERABLE
485	485	250	200	24,250,000
485	485	175	200	16,975,000
485	344	250	200	18,187,500
485	344	175	200	12,731,250
350	263	150	200	7,875,000
350	263	100	100	2,625,000

APPENDIX 8

APPENDIX 9: Adjacent Production, Emigrant Gap Prospect. Eight fields are located within a few miles of our prospect with production from many different horizons. The big winner, though, is Tensleep Sandstone because it is highly porous and permeable and can have a very thick pay zone. In a nearby well (see Appendix 3), the Tensleep has 223 feet of porosity greater than 10% in a 300 foot section, or, in other words, 74% of the entire Tensleep horizon's 300+ feet of sandstone is pay zone. Our fairly small 485 possible acres of closure would have the same reserve potential as a structure with 20 feet of potential pay and 5400 acres of a structural closure. This explains why the Tensleep has been such a popular drill objective. Further evidence of the strength of the Tensleep as a world-class producer is South Casper Creek Field. The primary producing south closure has a productive area approximately the same size as our prospect closure. This little anomaly has yielded 64% of all the oil produced in the eight fields near our

prospect. Lakota, and Sundance are secondary objectives for our proposed well. We anticipate Tensleep oil gravity to be somewhere in the API range of 18 to 25 degrees.

ADJACENT PRODUCTION, EMIGRANT GAP ANTICLINE PROSPECT

Field Name	Disc. Date	Drill Depth to Tensleep	Formation	Oil Produced 2002, BBLS	Oil Gravity	Water Produced 2002, BBLS	Field: Cum. Oil All Zones, 2002	Field: Cum. Oil All Zones, Lifetime
Bates Creek	1954		Frontier-4	397	36	60		
		3,850					397	70,910
Casper Creek South	1919	2,500	Tensleep	137,554	20	13,016,981		
							137,554	17,067,997
Government Bridge	1956		Cody	21,810	40	1,093		
			Muddy	1,146	40	60		
			Steel	0	40	0		
		NDE					22,956	1,975,404
Iron Creek	1917		Frontier	12	ND	225		
			Lakota	300	ND	15,600		
			Muddy	1,542	ND	30,800		
			Muddy-La.		ND	94,850		
		3,900					141,475	297,220
Oil Mountain	1945	2,550	Tensleep	8,347	15	88,442		
							8,347	208,697
Poison Spider	1917		Cody	0	41	33		
			Crow Mtn.	18,826	20	207,110		
			Muddy	363	22	0		
			Sundance	15,988	22	221,349		
		2,140	Tensleep	1,245	14	121,650		
							36,442	4,337,634
Schrader Flats	1961		Muddy	0				
			Sundance	911	37	8,800		
		4,485					911	2,057,343
Tipps	1963		Cody	412	40	0		
			Lakota	2,072	40	90		
		6,536					2,484	351,924
Total Oil							350,566	26,367,129

EMIGRANT GAP ANTICLINE PROSPECT
Natrona County, Wyoming
Primary Objective: Tensleep Sandstone
Drill Depth to top of Tensleep: 2500 feet

Pioneer Oil and Gas
1206 W. So. Jordan Parkway, Unit B
South Jordan, UT 84095
801-566-3000 pioneer@piol.com

APPENDIX 9

APPENDIX 10-19

APPENDIX 10-16: Page 28 and following, also available from the Wyoming Oil and Gas Commission website of field maps of seven oil fields near our prospect. We have also included a detailed report of Casper Creek, South Field from a recent AAPG publication.

10. Bates Creek field

11. Casper Creek South field

11a. South Casper Creek Field: A Study in Reservoir Heterogeneity, Scott L. Montgomery, AAPG Bulletin, V. 80, No. 8 (August 1996), PP. 1161-1176

12. Government Bridge and Tipps fields

13. Iron Creek field
14. Oil Mountain field
15. Poison Spider field
16. Schrader Flats field

APPENDIX 17-18: Horizontal Tensleep drilling articles (abstracts) from AAPG's database

17. Outcrop based 3-D modeling of the Tensleep Sandstone at Alkalai Creek, Bighorn Basin, Wyoming, Bozkurt N. Ciftci, et al, AAPG Bulletin, V. 85 (2001), No. 13 (Supplement)

18. Structural and Stratigraphic Compartments Determined from Horizontal Drilling in an Aeolian Reservoir, Tensleep Sandstone, Wyoming, Neil F. Hurley, et al, AAPG Bulletin, V. 85, No. 13. (Supplement).

APPENDIX 19: Morphology of the Casper Mountain uplift and related, subsidiary structures, central Wyoming: Implications for Laramide kinematics, dynamics, and crustal inheritance, by Donald S. Stone, AAPG Bulletin, V. 86, No. 8 (August 2002) PP l1417-1440

APP. 10

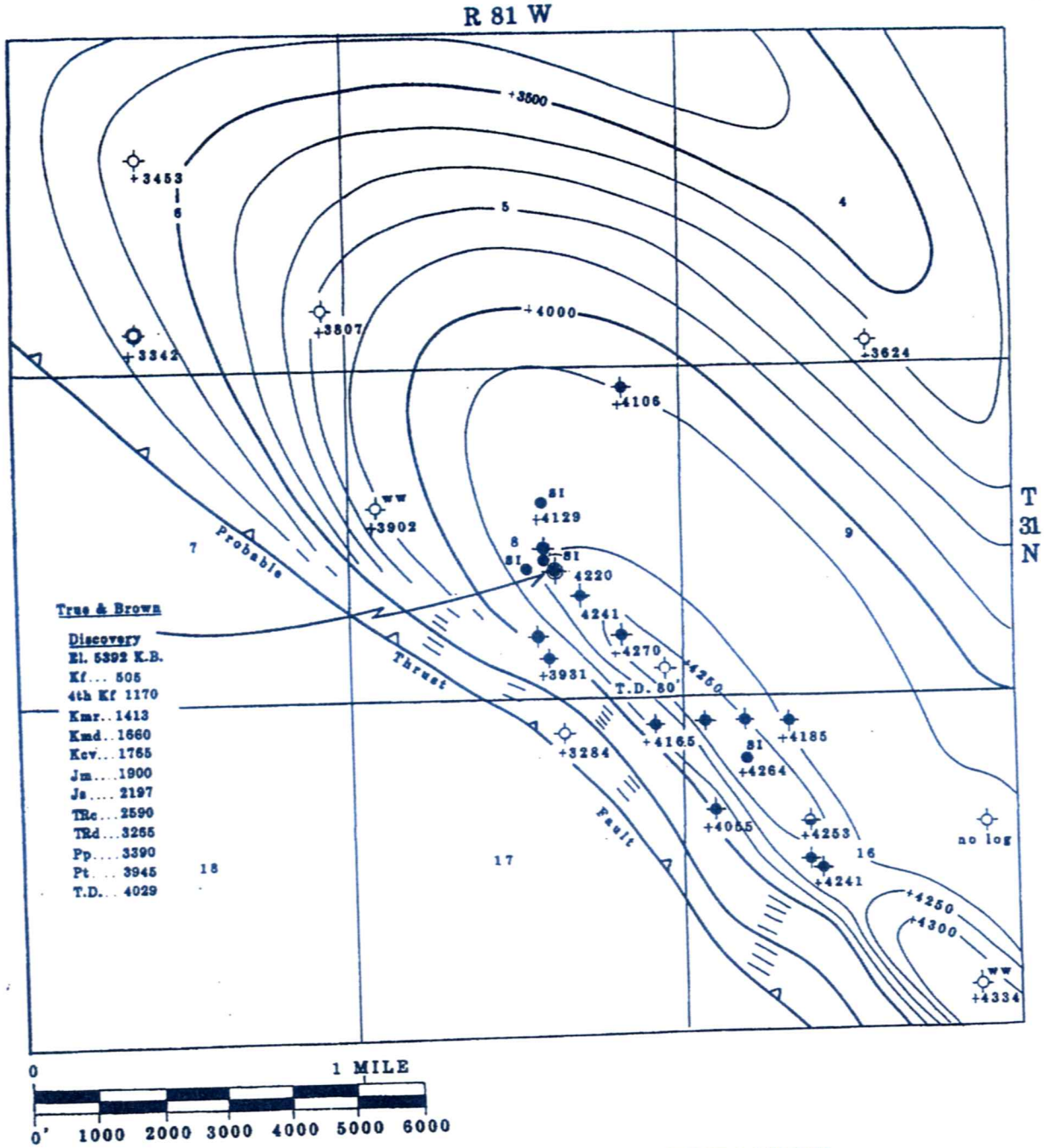

NW SE 8-31N-81W

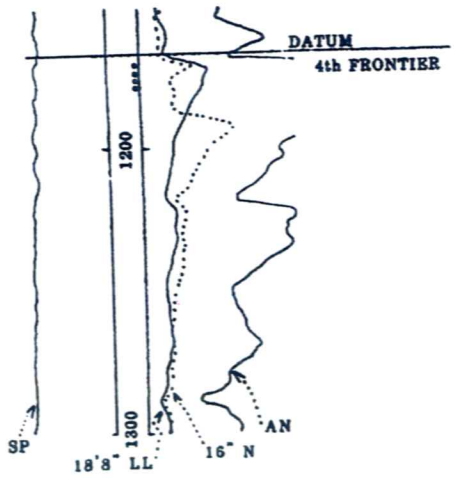

LEGEND

- OIL WELL 4th FRONTIER
- PLUGGED & ABANDONED
- SI OIL WELL. SHUT IN
- DRY HOLE
- SHO OIL
- WW WATER WELL
- DEEP TEST

W.G.A.

BATES CREEK

NATRONA COUNTY, WYOMING
DATUM – 4TH FRONTIER
CONTOUR INTERVAL 100'

APP. 11

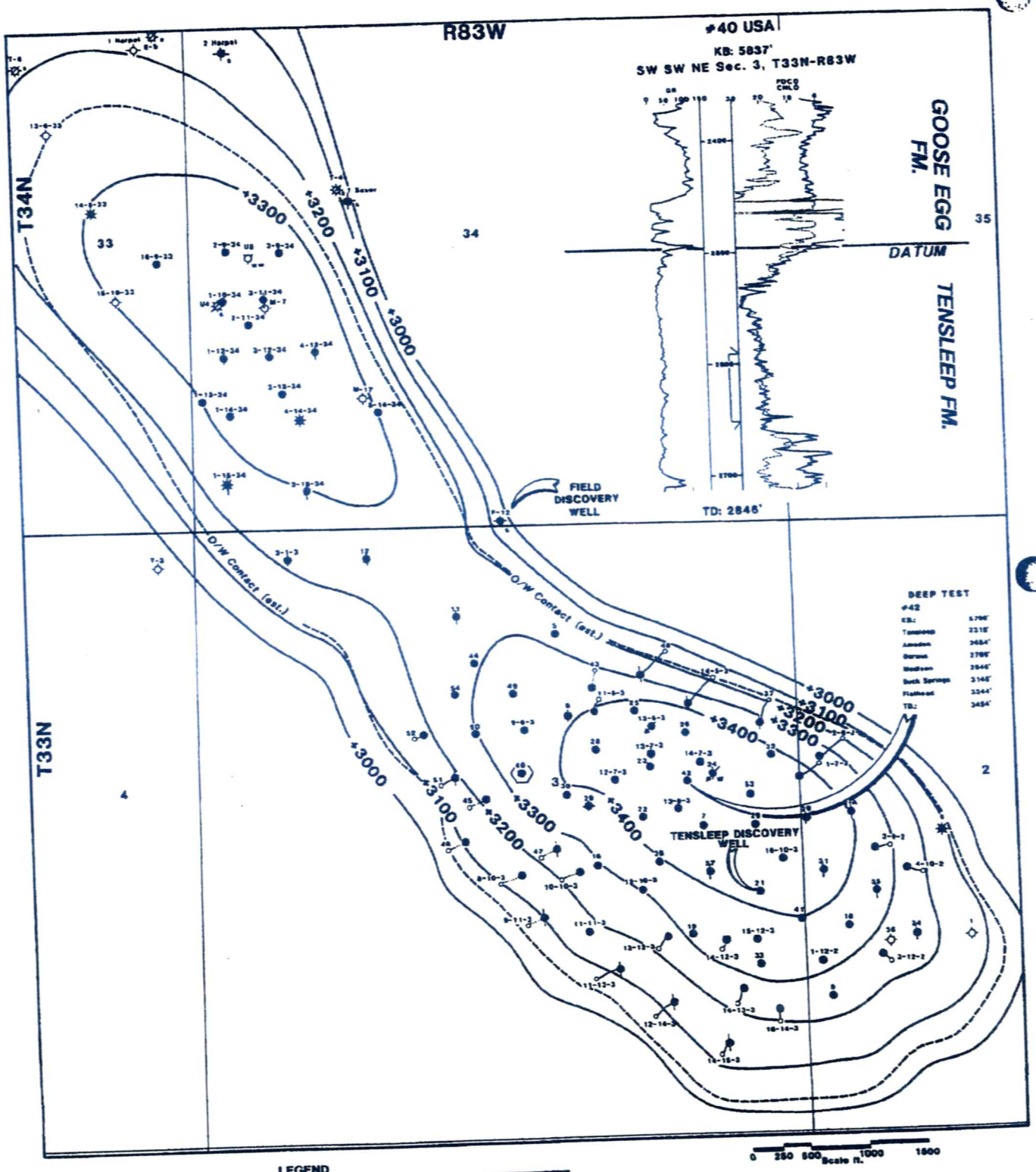

LEGEND

- OIL WELL
- OIL & GAS WELL
- DRY HOLE
- ABANDONED OIL WELL
- ABANDONED GAS WELL
- SHUT IN OIL WELL
- INJECTION WELL
- SURFACE LOCATION
- TYPE LOG
- BRINE DISPOSAL WELL
- WATER WELL
- SUNDANCE

W.G.A.

CASPER CREEK SOUTH

NATRONA COUNTY, WYOMING
DATUM – TENSLEEP
CONTOUR INTERVAL – 100'

App. 11a

E & P Notes

South Casper Creek Field: A Study in Reservoir Heterogeneity

Scott L. Montgomery[1]

ABSTRACT

The Tensleep Sandstone, an eolian and marine deposit, has produced low-gravity oil at South Casper Creek field (Natrona County, Wyoming) since the 1920s. Until recently, the reservoir was considered a relatively homogeneous sandstone body and was modeled as such for secondary recovery operations initiated during the late 1970s and early 1980s. Poor secondary recovery performance led to extensive reevaluation of the reservoir. Characterization studies by the field operator, Union Oil of California (UNOCAL), and through the Reservoir Characterization Project at the Colorado School of Mines produced an entirely revised picture of the Tensleep interval. Significant stratigraphic, diagenetic, and structural heterogeneities were identified, mapped, and correlated against productivity patterns under pilot steamflood programs. The results of this integrated geologic and geophysical effort are significant and have implications for secondary recovery operations elsewhere in the Tensleep and its regional correlatives.

INTRODUCTION

The Pennsylvanian Tensleep Sandstone, an important reservoir in much of central and southern Wyoming, produces low-gravity (12–25° API) oil from fields located in the Big Horn, Wind River, and Green River basins, as well as along the Sweetwater uplift and Casper arch. In combination with its regional correlatives, the Minnelusa Formation and Weber Sandstone, the Tensleep contains ultimate recoverable reserves of several billion barrels. Discovery and early development of Tensleep reservoirs occurred in the 1920s and 1930s. Poor recovery efficiency in these reservoirs is related to the viscous nature of the oil and, in many cases, to complex reservoir heterogeneities. Waterflood and steamflood operations initiated during the last several decades have had mixed or poor results that, until recently, proved difficult to explain and commonly precluded further development or exploration.

Early reservoir modeling characterized the Tensleep as a homogeneous sandstone body. Subsequent studies showed this to be oversimplified (Pedry, 1975; Morgan et al., 1978; Mankiewicz and Steidtmann, 1979). More extensive sampling of the reservoir indicated the existence of multiple nonreservoir layers, typified by low-permeability dolomite cement. On the basis of related data from several field areas, the Tensleep has been divided in each case into a series of individual flow units of varying fluid conductivity, separated by permeability barriers (Morgan et al., 1978; Stevenson and Mullen, 1991). Continued analysis of production results, however, indicated further complexities involving vertical and lateral heterogeneities relating to stratigraphy, diagenetic patterns, and structure.

To determine the nature of these heterogeneities, and to provide conclusions relevant to Tensleep production generally, as well as other reservoirs of similar origin and character, a multiyear interdisciplinary study integrating geologic,

[1]Petroleum Consultant, 1511 18th Avenue East, Seattle, Washington 98112.

Grateful acknowledgment is hereby made to the following individuals who helped make this report possible: Dave List, GeoQuest Inc.; Tom Davis and Bob Benson, Colorado School of Mines.

Send reprint requests to AAPG Publications Manager, P.O. Box 979, Tulsa, Oklahoma 74101-0979.

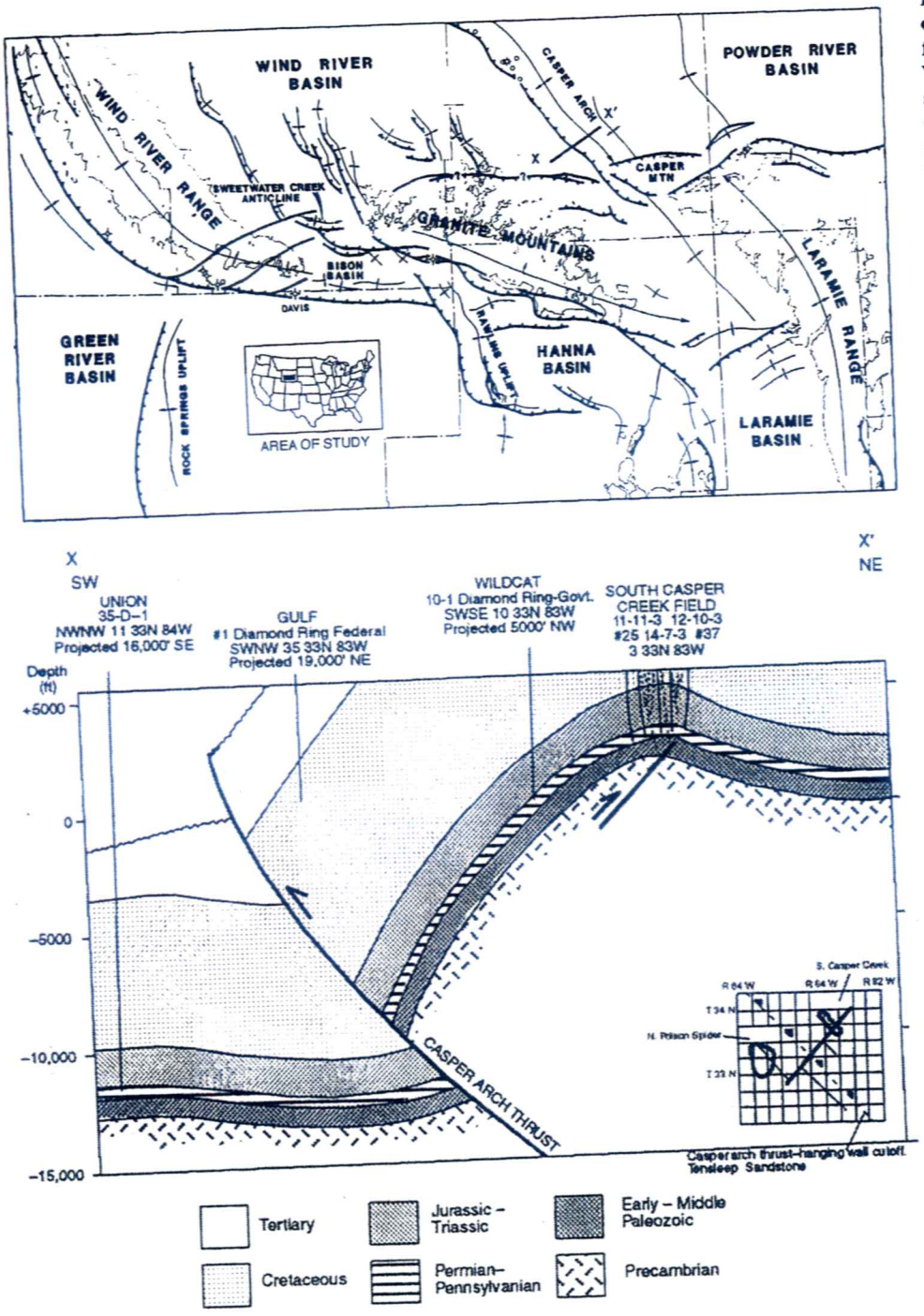

Figure 1—Regional setting of the South Casper Creek field, Natrona County, Wyoming. The field sits at the southern end of the Casper arch, a Laramide (Late Cretaceous–early Tertiary) basement uplift separating the Wind River and Powder River basins. Cross section (XX') shows the field located at the faulted crest of the arch. (Modified from List, 1995.)

geophysical, and reservoir engineering data was performed on the South Dome part of the South Casper Creek field, Natrona County, Wyoming. This study, conducted through the Colorado School of Mines under broad international sponsorship, incorporated information from outcrop, core, well-log analyses, production testing, and both multicomponent vertical seismic profiles (VSP) and multicomponent three-dimensional (3-D) seismic surveys.

Valuable insights gained from this work are summarized here. Relevant information has been derived from a number of publications, including Akhtar (1991), Benson (1991), List (1991, 1995), Stevenson and Mullen (1991), Tanean (1991), and Cole and Mullen (1992).

SOUTH CASPER CREEK FIELD: SETTING AND HISTORY

The South Casper Creek field lies at the southern end of the Casper arch, a foreland basement uplift of Laramide age (Late Cretaceous–early Tertiary) separating the Wind River and Powder River basins in central Wyoming (Figure 1). Seismic data confirm that the arch is bounded to the southwest by a basement thrust (Casper arch thrust) that dips as much as 40° (Skeen and Ray, 1983). The northeast flank of the arch forms a monocline that dips less than 5° beneath the Powder River basin. The South Casper Creek field occupies a double closure (North Dome and South Dome) near the southern end of a northwest-southeast anticlinal trend. This fold trend coincides with the structural crest of the arch in Paleozoic and Mesozoic units (Figure 1). The South Dome part of the field is structurally 100 ft (30 m) higher than the North Dome.

Stratigraphy in the area of the southern Casper arch is shown in Figure 2. The type log of Figure 3 is from the 10-6-3 well in the South Dome part of the field and displays a divisional scheme for the productive, upper Tensleep interval proposed by List (1995), as revised from Stevenson and Mullen (1991). Sand-bearing upper Tensleep units exist below the Nowood anhydrite and Opeche shales of the Goose Egg Formation, a regional equivalent of the Phosphoria Formation. The lower Tensleep consists of nonreservoir marine dolomite and lies above the shallow-marine and evaporitic Amsden Formation.

South Dome, the more productive part of the South Casper Creek field, is structurally an asymmetric, faulted anticline having as much as 220 ft (67 m) of closure (Figure 3). Faults cut the anticline and strike in two directions: northwest, parallel to the fold axis, and east-northeast. Most faults are normal in separation, and have offsets ranging from 10 to 80 ft (12–24 m); however, several reverse faults exist, and at least one fault plane may show change along strike from normal to reverse separation. Intensity of faulting tends to increase toward the hinge area of the fold. Fractures are associated with most of the faults. Fracturing was not identified prior to integrated geological-geophysical-engineering study in the 1990s.

South Casper Creek field was discovered in 1918. Initial discovery was in the Jurassic Sundance sandstone at depths of 1300–1600 ft (395–485 m) (Lawson, 1954). Oil was discovered in the Tensleep Sandstone in 1922, at approximately 2500 ft (758 m) depth. Gross pay was 430 ft (130 m) of highly viscous (13.7° API) oil column, with production dependent upon an active edge-water drive. Development included 27 wells drilled between 1922 and 1950; annual production began declining in the late 1940s, from 210,000 bbl/yr to approximately 140,000 bbl/yr by 1970. A full-field secondary recovery program, involving steam injection, was designed and several pilot steamfloods implemented between 1979 and 1985 (List, 1995). These pilots were based on modeling of a thick, homogeneous reservoir sandstone. Mixed and unpredicted results were obtained. Subsequent improvements to the reservoir model, based on recognized stratigraphic heterogeneities within the Tensleep Sandstone, led to a redesigned steamflood, yet this too yielded poorer than expected results. Further study indicated diagenetic and structural heterogeneities to the reservoir that helped explain these results (Stevenson and Mullen, 1991).

Union Oil of California (UNOCAL), operator of the field until 1996, has estimated 48.65 million bbl

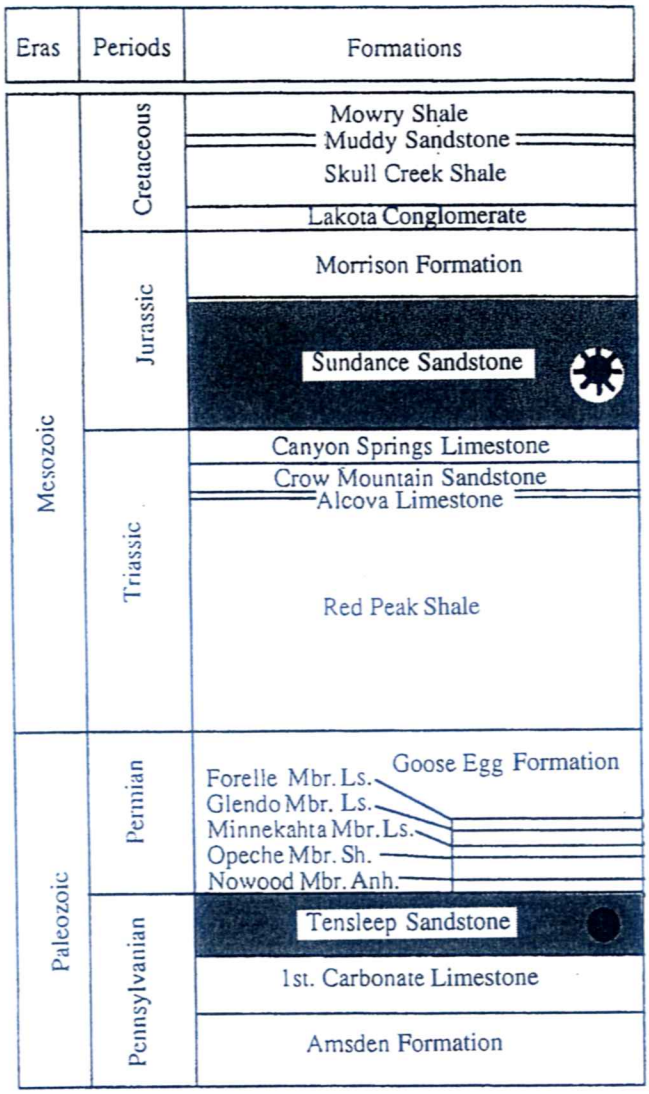

Figure 2—Stratigraphic column, South Casper Creek field.

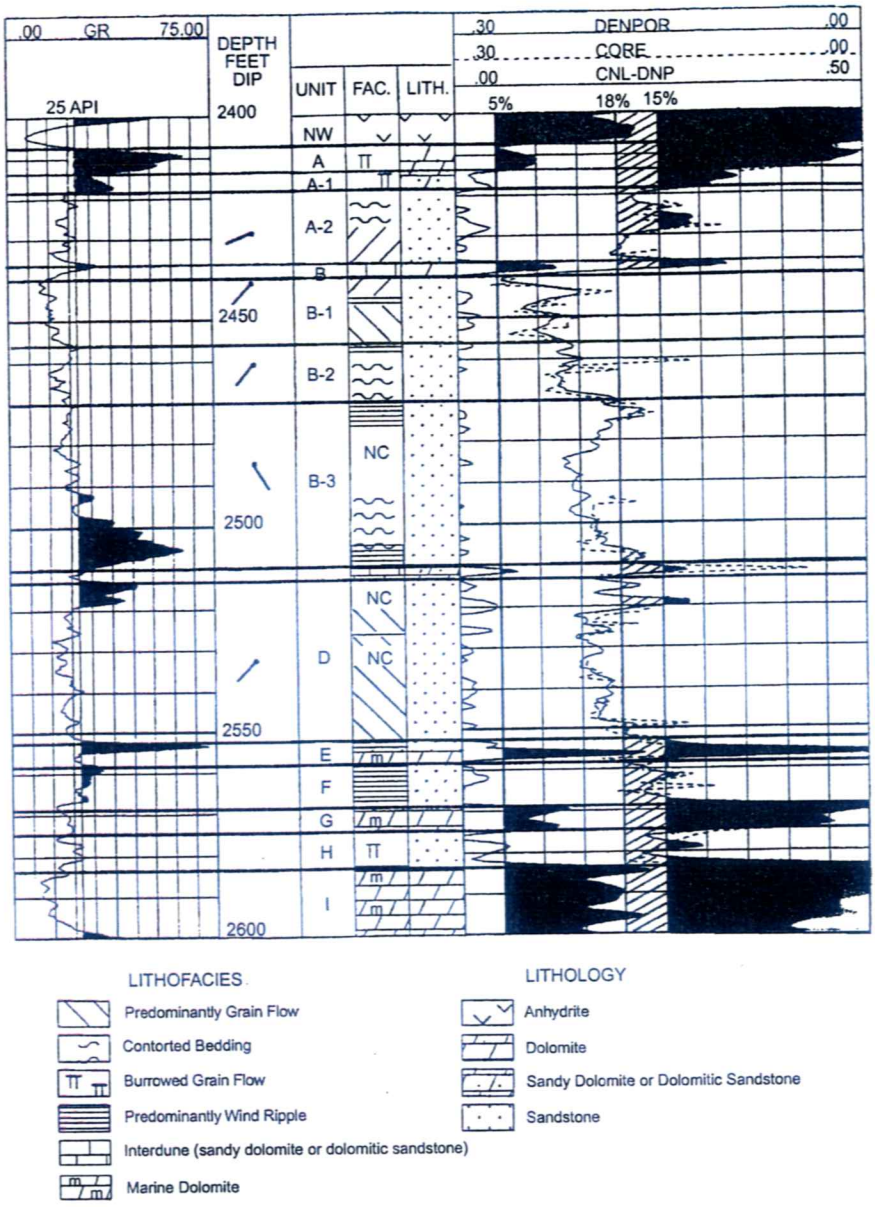

Figure 3—Type log, South Casper Creek field. Data are from the 10-6-3 well. Black areas indicate parts of log above or below cutoff values determined for lithofacies identification (see Table 2). Dip log information is averaged and displayed in depth column. CNL-DNP refers to values derived by subtracting log density porosity from compensated neutron porosity. NW = Nowood; NC = no core. (Courtesy Dave List.)

of original oil in place. As of 1994, when steamflooding was discontinued, approximately 11 million bbl of oil had been produced by primary recovery and 1.5 million bbl by secondary methods. Remaining oil reserves are calculated at 4.3 million bbl (primary) and 9.6 million bbl (secondary).

TENSLEEP SANDSTONE: STRATIGRAPHY, LITHOLOGY, AND DIAGENESIS

The Tensleep Sandstone on the Casper arch conformably overlies the Ranchester Limestone Member of the Amsden Formation and is unconformably overlain by the Nowood anhydrite. The unconformity at the base of the Nowood corresponds to erosion of Upper Pennsylvanian (Missourian, Virgilian) deposits correlative with the Weber Sandstone of southwestern Wyoming and the Upper Minnelusa Formation of the Powder River basin. Removal of this material took place as a result of uplift associated with the Ancestral Rocky Mountain orogenic episode (Mankiewicz and Steidtmann, 1979). Regression is apparent between lower Amsden Formation marine shales, upper Amsden lagoonal dolomites and evaporites, and Tensleep tidal fault, sabkha, and dune deposits.

The Tensleep itself is traditionally divided at South Casper Creek into a lower, dolomitic part

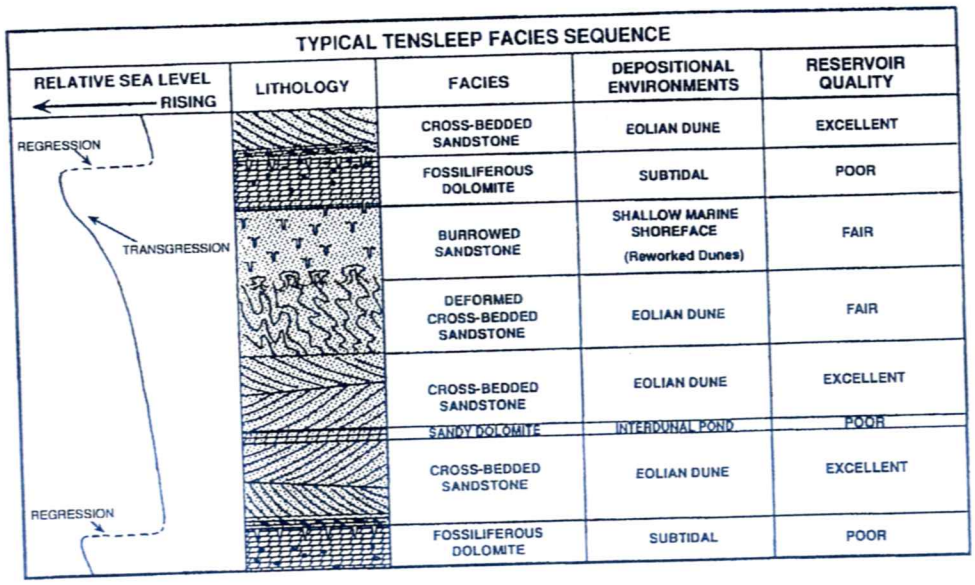

Figure 4—Characteristic facies sequence in the Tensleep Sandstone, South Casper Creek field. Individual facies are shown in relation to sea level changes and general reservoir quality. (Modified from Akhtar, 1991.)

and an upper, sand-rich part. The lower part averages 166 ft thick (50 m), the upper part, 134 ft (41 m) (List, 1995). The most productive reservoir zones exist in the upper part. Recent study has produced a more detailed scheme of division (Figure 3) based on laterally mappable intervals of similar lithology, each bounded by surfaces of erosion or nondeposition. In the upper Tensleep, these intervals are composed of dune deposits, including grain-flow and wind-ripple lithofacies, interbedded with more discontinuous interdune sediments. Bounding surfaces are commonly overlain by thin, low-permeability assemblages of interdune shales, marine dolomites, and, less often, sand sheet deposits.

A typical lithofacies sequence, with an interpreted sea level curve, is shown in Figure 4. This diagram also indicates general reservoir quality for each lithofacies. The best reservoirs are in unburrowed and undeformed grain-flow deposits and, to a lesser extent, poorly cemented wind-ripple subfacies of the dune lithofacies. Average porosities and permeabilities for these subfacies are 24.4% and 1580 md (grain flow), and 18.3%, 293 md (wind ripple). Grain-flow sandstones are medium to coarse grained, well sorted, and represent deposition down the slipface (lee side) of the dune. They show distinctive, high-angle tabular planar and wedge planar cross-bedding. Wind-ripple sandstones are fine to medium grained and moderately sorted, and represent deposition in several possible positions on the dune (both stoss and lee sides). Wind-ripple deposits display low-angle, ripple cross-bedding with much thinner individual laminae than grain-flow deposits, whereas burrowed, clay-bearing, or more highly cemented, wind-ripple deposits have lower reservoir quality.

Analysis of diagenetic properties and history by Akhtar (1991) indicates that porosity development is a result of postdepositional events. Early, near-surface dolomite precipitation from evaporitic brines filled primary pore space and limited mechanical compaction during subsequent burial to about 10,000 ft (3300 m). Selective dissolution of dolomite cement and framework grains took place as a result of later fluid introduction, linked to Late Cretaceous–early Tertiary (Laramide) uplift, fracturing, and dewatering effects. Porosity development is at a maximum on

Table 1. Average Core Permeabilities for Lithologic Units in the Tensleep Sandstone, South Casper Creek Field*

Interval	Average Permeability (md)	
A	0.01	
A-1	68	
A-2	166	
B**	125	(total)
	22.7	(min. range)
B-1	1171	
B-2	845	
B-3	768	
C**	230	(total)
	4.4	(min. range)
D	634	
E	147	
F	270	
G	80	

*Data from List (1995).
**Values given are for total samples and for minimum permeability range.

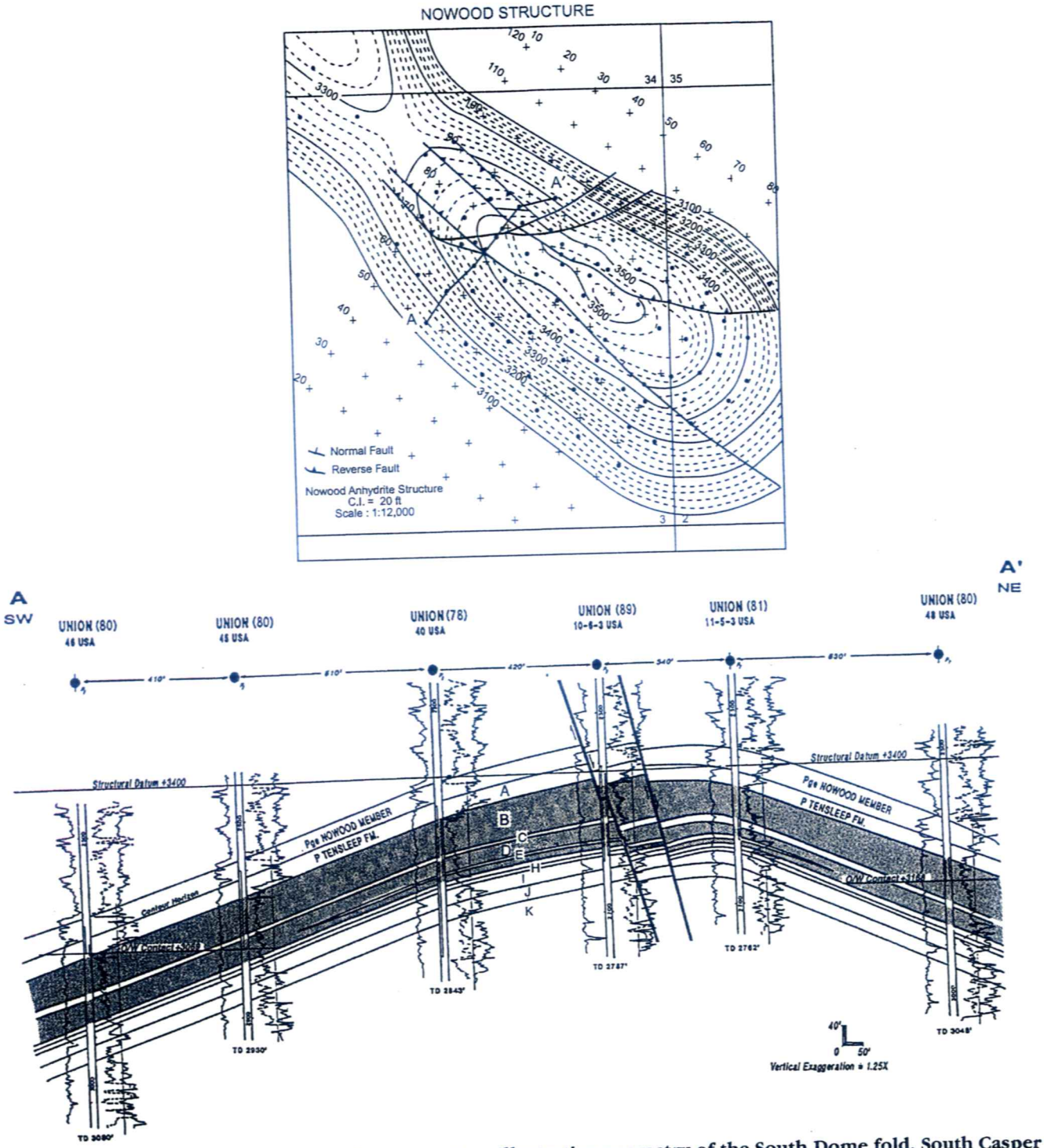

Figure 5—Structure contour map and cross section, illustrating geometry of the South Dome fold, South Casper Creek field. Contours are drawn on top of the Nowood anhydrite. Screened parts of the cross section indicate major reservoir intervals within the Tensleep. Faults introduce significant lateral and vertical heterogeneity in the reservoir interval within the crest of the fold. (Modified from Stevenson and Mullen, 1991; List, 1995.)

structural highs associated with the Casper arch thrust (Faqira, 1991). The degree of dissolution is both facies and structure dependent. Grain-flow intervals, characterized by larger primary pores and pore throats, were selectively leached along the more gently dipping southwest limb of the South Dome structure.

TENSLEEP RESERVOIR UNITS

Reservoir quality studies at South Casper Creek indicate pronounced differences in porosity and permeability between the various lithologic units of the upper Tensleep. Intervals with moderate-to-excellent reservoir character (A-2, B-1, D) tend to be bounded by thin, nonreservoir rock types. This information is summarized in Table 1 and can be briefly described as follows (refer to the log of Figure 3).

Units A, A-1, and A-2: Unit A is a burrowed dolomite, A-1 is a dolomitic sandstone, and A-2 consists of burrowed wind-rippled strata typified by soft-sediment deformation. Units A and A-1 are nonreservoir intervals; unit A-2 has sufficient reservoir quality to be an important productive zone in certain wells.

Units B, B-1, B-2, and B-3: This interval contains the best reservoir rock in the field. Each unit is bounded above and below by a low-permeability zone consisting of wind-ripple sandstone with variable amounts of dolomite cement. The thickest of such nonreservoir zones is unit B, which is associated with a bounding surface at the base of unit A-2. Unit B separates the A-2 moderate-quality reservoir from the "pipeline bed" of unit B-1, a grain-flow deposit interval that comprises the best reservoir interval, with permeabilities typically between 1000 and 3500 md. Unit B-2 consists of similar facies to B-1, but with somewhat more clay and dolomite cement. It is therefore a good reservoir over much of the field.

Unit C: This unit is a wind-ripple, nondune deposit that varies laterally from sandstone to dolomitic sandstone and is associated with a bounding surface at the top of unit D.

Unit D: This unit comprises the second most important reservoir interval, being composed of grain-flow and wind-ripple sandstone as much as 50 ft thick (15 m). Unit D displays a significant decrease in reservoir quality toward its base and top, where it grades into more dolomitic sandstone.

Units E, F, G, and H: Among these intervals, only unit F, a grain-flow deposit with a high percentage of wind-ripple strata, has sufficient porosity and permeability to be locally productive. Units E and G are dolomitic sandstones, and unit H is interpreted as a well-cemented sandstone of mixed eolian and marginal marine origin.

In general, the vertical sequence defined by these units divides the upper Tensleep into a series of wholly or partially segregated reservoir zones. Complexities exist because reservoir and nonreservoir units vary laterally with regard to detailed lithology, degree of cementation, and presence of fractures. In addition, lenticular interdune deposits occur locally within the main reservoir zones (B-1, B-2, and D). The influence of such complexities is evident on profiles representing the distribution of reservoir quality across the field (Tanean, 1991).

Table 2. Log Value Criteria Used to Determine Major Lithofacies Within the Tensleep Formation, South Casper Creek Field*

Lithofacies	Gamma Ray (API Units)	Density (%)	CNL-DNP (pu)**
Mainly Grain Flow	< 25	> 18	< 05
Contorted Bedding	> 25	> 18	< 05
Burrowed Grain Flow or Wind Ripple	> 25	< 18	< 05
Dolomitic Interdune	< 25	< 15	> 05
Marine Dolomite	< 25	< 05	> 10

*Data from List (1995).
**pu = porosity units [neutron porosity minus (–) density porosity].

These profiles show that the thin, nonreservoir zones of units B and C become increasingly less sealing along the northeast side of the structure. At the same time, total thickness of the highest quality reservoir also decreases in this area, due to the dominance of wind-ripple and interdune lithofacies.

STRUCTURE

A structure map and cross section of South Dome field are shown in Figure 5. Two sets of faults are evident. The more prominent set strikes parallel to the fold axis and is concentrated within the fold hinge itself. A secondary fault set is oriented east-west, intersecting the northeast limb of the fold. The largest fault shown, located along the southwestern limb, dips 70° northeast. To the southeast, the fault has normal displacement of as much as 80 ft (21 m); to the northwest, it shows reverse offset of 15–30 ft (4.5–9.0 m) and splits into two structures, one of which strikes east. Two other axial faults dip at 80–83° and show displacement of 10–20 ft (3.3–6.6 m). As shown by abrupt changes in the strike of contours, these structures have a significant amount of rotation associated with them (List, 1995). Axial faults at the Tensleep–Nowood level branch upward, such that as many as five separate structures are evident at the level of the Upper Jurassic Morrison Formation.

East-west faults in the northern part of the field comprise a fault zone up to 300 ft (90 m) wide, with a number of fault blocks dipping an average of 65° to the north. Due to their shallower dip, these faults cut out a significant amount of section (as much as 70 ft [21 m]). Such structural thinning has been identified at various levels in the Tensleep by wells drilled within the fault zone and by interval isopach data (List, 1995; see his figure 52).

Both axial and east-west faults create significant heterogeneity in the Tensleep reservoir. This

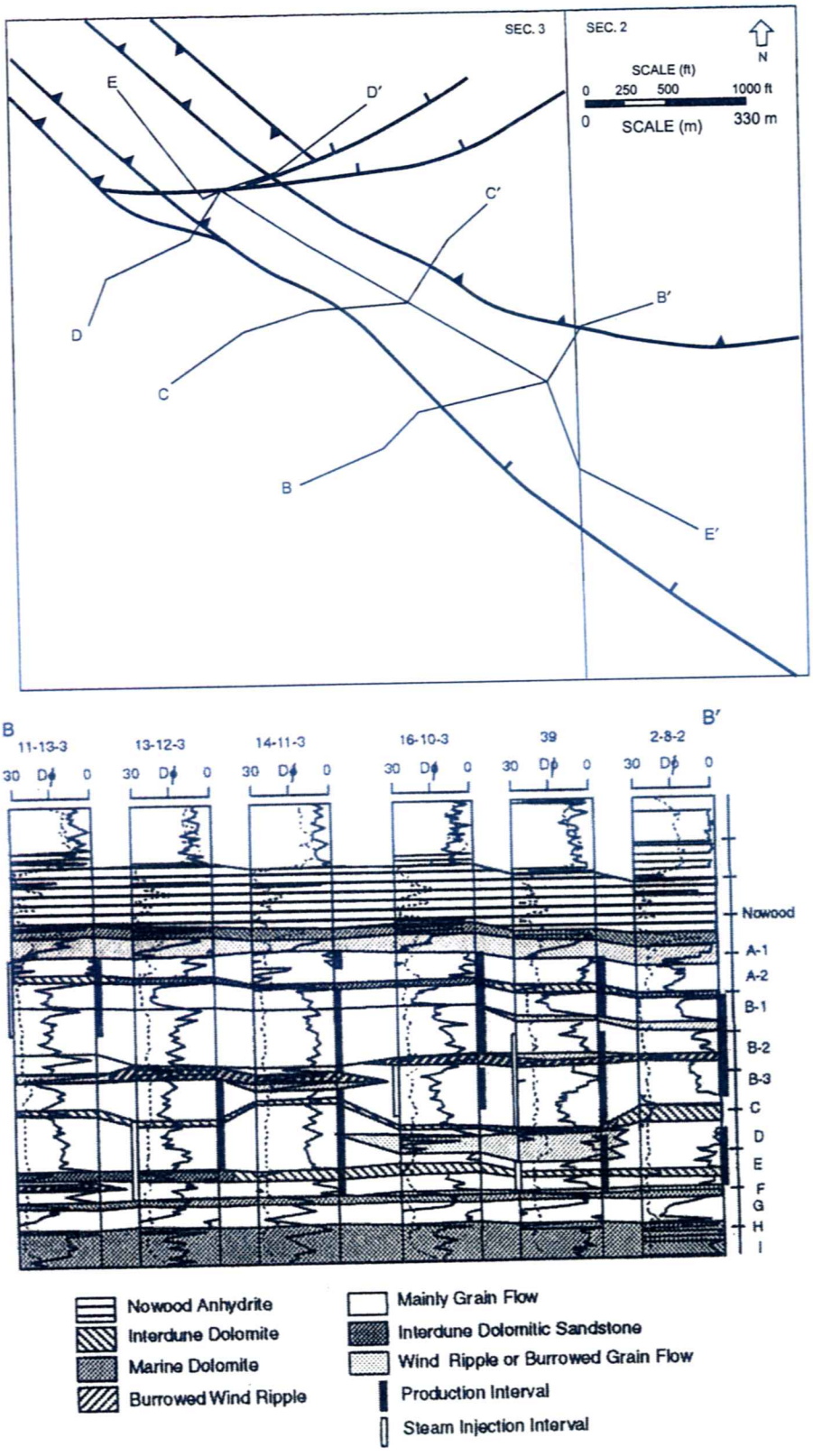

Figure 6—Stratigraphic cross sections through the Tensleep reservoir section, South Dome, South Casper Creek field. Sections BB′, CC′, and DD′ are oriented perpendicular to the axis of the South Dome fold; section EE′ is parallel to the fold axis. Datum is unit G, a marine dolomite. (Courtesy Dave List.)

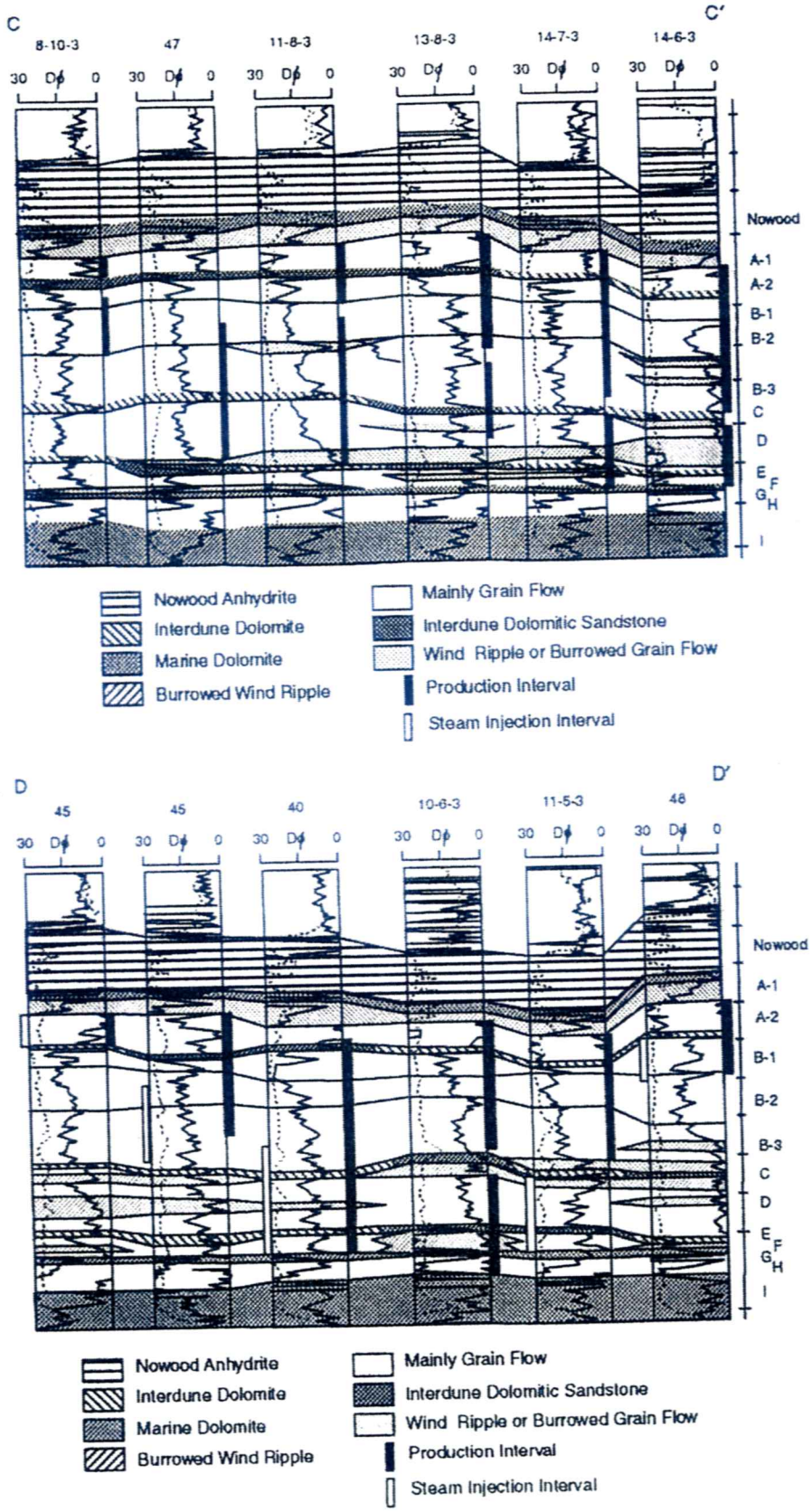

Figure 6—Continued.

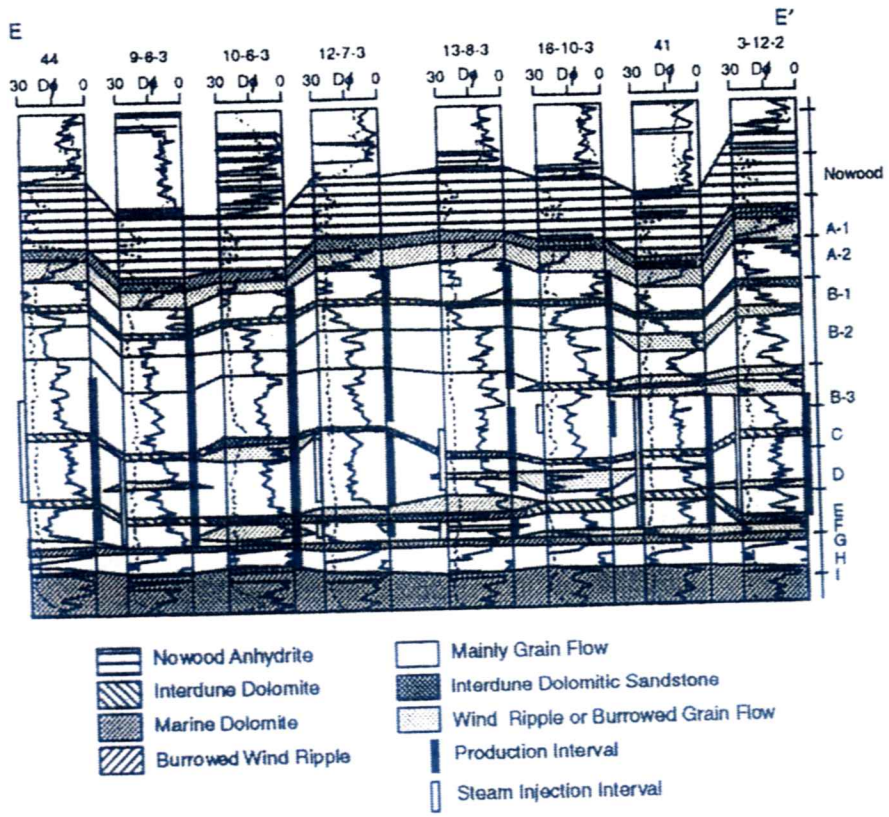

Figure 6—Continued.

is indicated by the generalized cross section on Figure 5. Unit B-1, for example, near the top of zone B on Figure 5, is significantly downdropped in the 10-6-3 well relative to the 40 well located 420 ft (127 m) to the southwest. Offset of thin permeability barriers C and E is also apparent. Drag associated with the northeastern axial fault has resulted in a secondary hinge area at the level of unit C and below.

LOG DATA

Dominant lithofacies can be mapped on the basis of gamma-ray and neutron-density log response (Tanean, 1991; Cole and Mullen, 1992; List, 1995). Criteria employed to distinguish five main lithofacies types on the basis of such data are given in Table 2, in decreasing order of reservoir quality. As shown, highest quality reservoirs (grain-flow deposits) display lower gamma-ray values and higher log-density porosities than do other sandstone lithofacies. On the basis of petrological analysis, the low gamma-ray values have been interpreted as a result of comparatively smaller amounts of clay material (Tanean, 1991).

Application of these criteria to subsurface interpretation is indicated by the stratigraphic cross sections of Figure 6. As shown, all units designed on the type log of Figure 3 can be traced in both dip and strike directions. Notable on the sections of Figure 6 are the thickness variations in most units, as well as pinch-out and local occurrence of low-permeability interdune lithofacies. This information confirms that stratigraphic heterogeneities are typical of the Tensleep reservoir at South Casper Creek.

Formation MicroScanner™ (FMS) logs have shown that the reservoir is also characterized by two other forms of heterogeneity, one depositional and one structural (Figure 7). Primary bounding surfaces, marking contact between different dune lithofacies such as wind-ripple and grain-flow facies, introduce local changes in directional permeability. These surfaces appear on FMS logs as changes in dip amount and direction. These logs have also helped establish the existence of fracturing in certain parts of the field. Fractures are indicated by resistivity events that cross all primary (depositional) events (Figure 7).

FMS logs were run in six wells, located in various parts of the field. A total of 337 fractures interpreted from these logs indicated a dominant strike of N80°E, with two secondary trends, one at N20°–30°E, perpendicular to the anticlinal axis, and another at N20°–30°W. These trends have limited significance, as there are an insufficient number of wells with fracture data to derive conclusions that correlate fracture intensity and orientation with

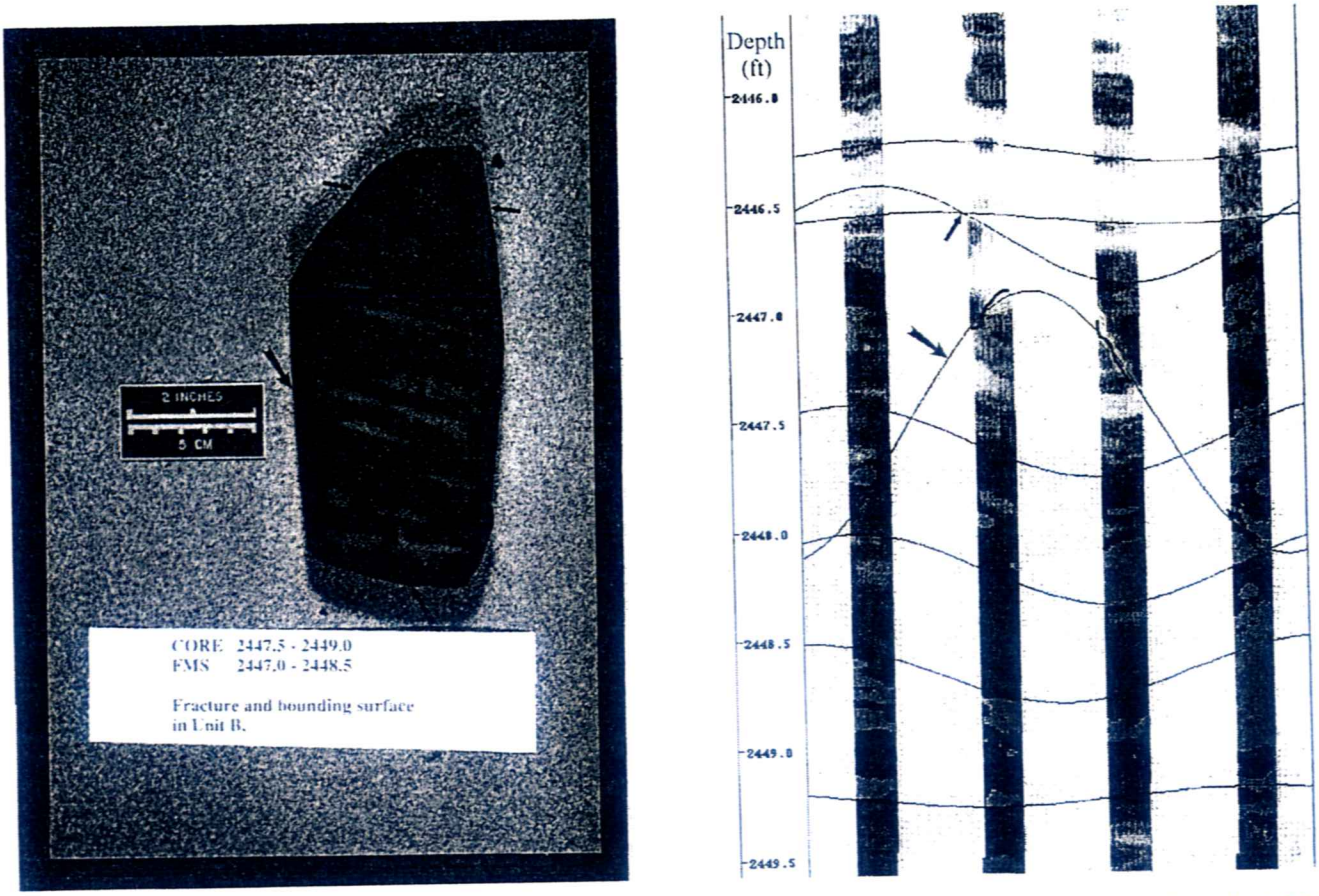

Figure 7—Formation MicroScanner log and core photograph for grain-flow facies (unit B-1, Figure 3), well 10-6-3, showing an example of a dune growth-bounding surface and an open fracture. (Courtesy Dave List.)

position on the fold. Moreover, FMS data are unable to detect vertical fractures and are thus considered limited with regard to mapping fracture occurrence and fracture trends within the field; however, data are adequate to indicate fracturing occurs within both reservoir and nonreservoir intervals. These data are potentially important with regard to variations in vertical fluid conductivity across the field.

SEISMIC DATA

Data from a 3-D seismic survey conducted at South Dome have been crucial to revised interpretations of field structure. This survey has allowed detailed mapping of faults at various levels. As shown by the crossline reflection profiles of Figure 8, the degree of faulting affecting the Tensleep and overlying intervals varies along strike of the South Dome fold, with increased fault intensity toward both the north and south ends of the structure. Upward branching of faults at the Tensleep–Nowood level is also apparent, with considerable breakup of reflections above the level of the Triassic Alcova Limestone. The deepest structures penetrate below the Amsden Formation and either continue to basement or branch off of a subsidiary basement thrust (see cross section, Figure 1).

In general, the pattern of faulting does not display increased graben development in the hinge area, indicative of extension associated with the folding process. Instead, a more complex horst-graben pattern is evident, which may reflect more than one episode of faulting. Asymmetry of the South Dome fold also appears to be a result of faulting.

The profiles of Figure 8, along with the strikeline section of Figure 9, display evidence of attenuated reflections at the Tensleep–Nowood level. Such attenuation may be a result of fracturing in locations immediately adjacent to faults. In general, faulting can be seen to divide the reservoir into a series of variably tilted blocks. Information from production under secondary recovery indicates that some faults are sealing, whereas others are not. Thus, fluid conductivity between the different fault blocks is variable.

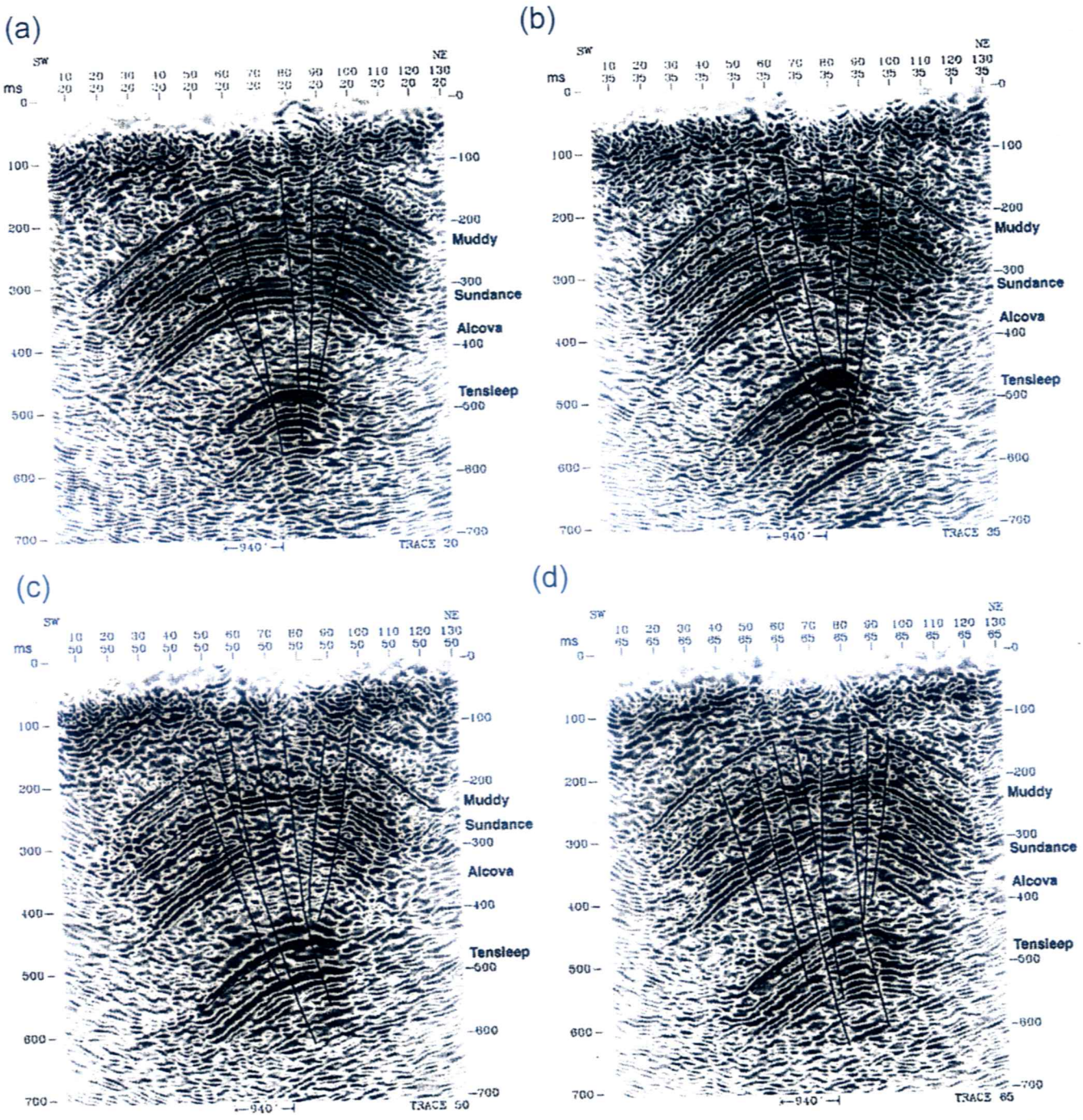

Figure 8—Crossline 3-D seismic profiles oriented northeast-southwest, South Dome part of the South Casper Creek field. Seismic grid shown in Figure 5. See text for discussion. Crossline locations are indicated by the northwest-southeast numbers (Figure 5), e.g., 20, 35, 50, and 65, which are constant for each dip section. Top numbers (10, 20, 30...130) refer to northeast-southwest positions on these lines. Time is two-way traveltime in milliseconds.

PATTERNS OF PRODUCTION AND FLUID FLOW

The various reservoir heterogeneities discussed in preceding paragraphs directly impact patterns of fluid flow at South Casper Creek and help explain the otherwise enigmatic results of production under steamflooding.

Stratigraphic heterogeneities have segregated the upper Tensleep into three main reservoir zones: units

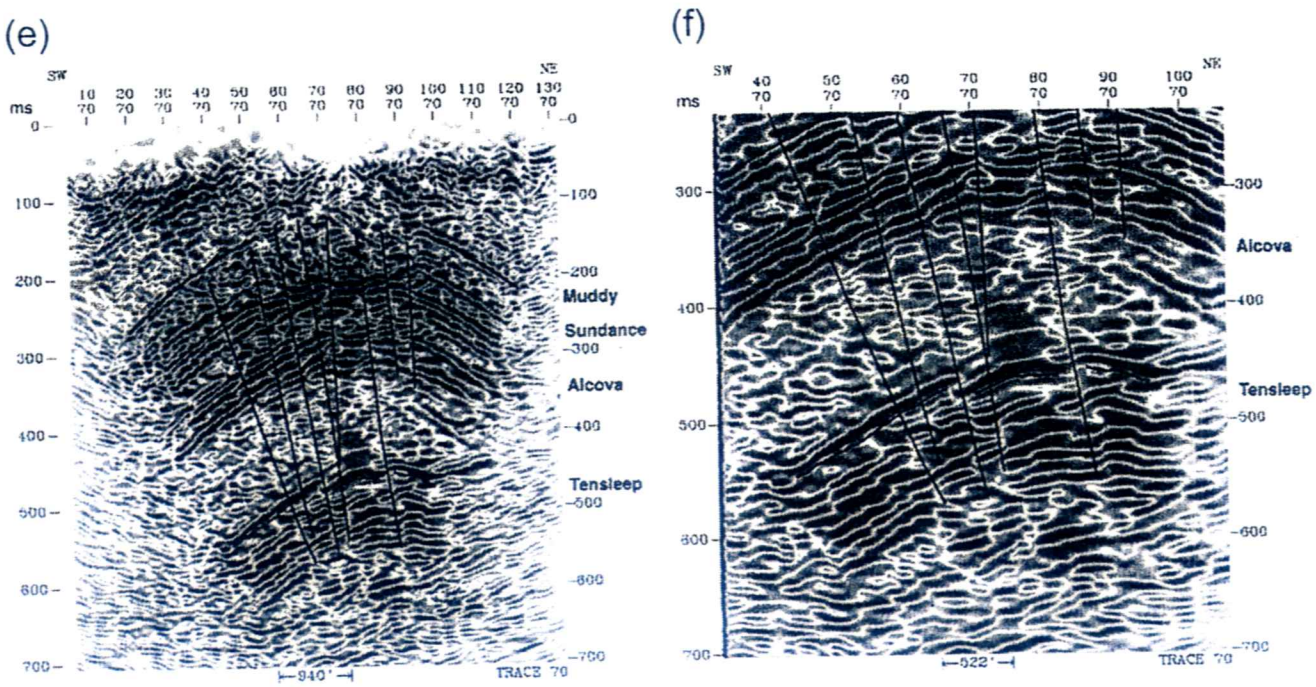

Figure 8—Continued.

A-2, B-1/B-2, and D (see Figure 6). Division between these zones is variable across the field. Figure 10, for example, shows isopach data for the B-1 interval, with superimposed distribution of dolomite (vertical permeability barrier) in the overlying interdunal B interval. Vertical communication between the B-1 and A-2 zones is low over most of the field. Porosity data for the B-1 interval indicate that many areas of excellent reservoir quality are overlain by vertical permeability barriers (Figure 11). Such vertical segregation is important with regard to steam injection intervals and sweep efficiencies.

Mapping of water saturation indicates that water encroachment from five decades of production has preferentially occurred within unit D. Increased water saturations in this unit have effectively transformed an original edge-water drive into a bottom-water drive (List, 1995), leaving overlying reservoir units relatively unswept. Moreover, higher water saturations in unit D are concentrated in the central part of the field (southwest of 55–65%), whereas the northern and southern parts of the South Dome structure display significantly lower values (32–45%). This pattern is partially explained by the influence of east-west faults, which provided zones of conductivity that helped direct encroachment away from the fold axis. Thus, the comparative underproduction of reservoir units A-2, B-1, and B-2 is also confined mainly to the central part of the field.

Structural heterogeneities in the form of fault-associated fractures also affect patterns of production. Wells located near faults typically have had higher rates of production and have responded best and most quickly to steamflooding. This is particularly true for wells sited near the intersection of axial and east-west faults.

Figure 12 shows the pattern of total monthly Tensleep fluid production (oil + water) in 1990, prior to initiation of a major steamflood program. Production rates differ significantly between the northeast and southwest flanks of the fold. Fault-associated fracturing is especially required for good production on the northeast flank, but appears less important to the southwest, where matrix porosity/permeability is considerably higher. Comparison of production rates and reservoir pressure data shows little or no correlation, confirming that factors other than reservoir pressure control production.

Two steamflood pilots illustrate the complex effects of reservoir heterogeneities. Pattern 13-6-3 (injector well), involving nine wells located along the northern crest of the anticline, was first initiated in 1981. Steam was injected into units D and F, whereas adjacent producers were perforated in units B-1 and B-2. Because of the permeability barrier of unit C, results of this pilot were poor. Following evaluation, the pattern was reinitiated in 1988, with the B-1 and B-2 zones the target of both

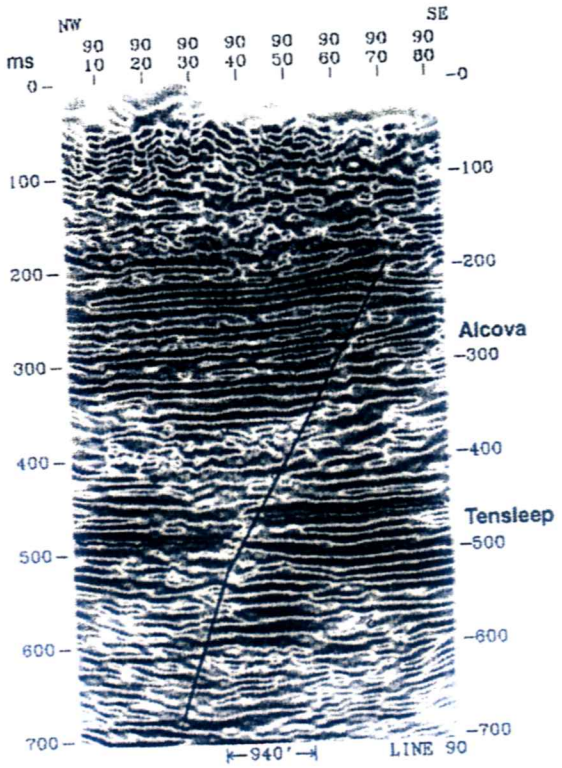

Figure 9—Strike line 3-D seismic profile, South Dome structure, South Casper Creek field. Time is two-way traveltime in milliseconds.

injection and completion. Results of this pilot were generally excellent, showing an average increase of 9600 bbl of oil/month. Patterns of response are shown in Figure 13. Unexpected results included (1) little response at well 25, indicating poor communication with injector, and (2) more rapid response at wells 42 and 12-7 than at well 14-7.

This information suggests the existence of strong directional permeability trends within the B-1/B-2 interval, such that communication between the injector and wells 26, 42, and 12-7 is especially good. Quickest temperature response was observed at well 42, located along the axial fault, which strongly suggests the importance of fracturing to steam migration. Poor communication with well 25, however, is a result of fault displacement juxtaposing the injection zone at the 13-6 well against impermeable Nowood evaporites.

CONCLUSIONS

Reservoir characterization studies, integrated with seismic data and production information, reveal the Tensleep Sandstone at South Casper Creek to be a highly heterogeneous reservoir. Based on information gathered to date, the most important heterogeneity with respect to secondary recovery is fracturing. Fractures are associated with faults in the South Dome fold and are dominantly abundant in areas where two

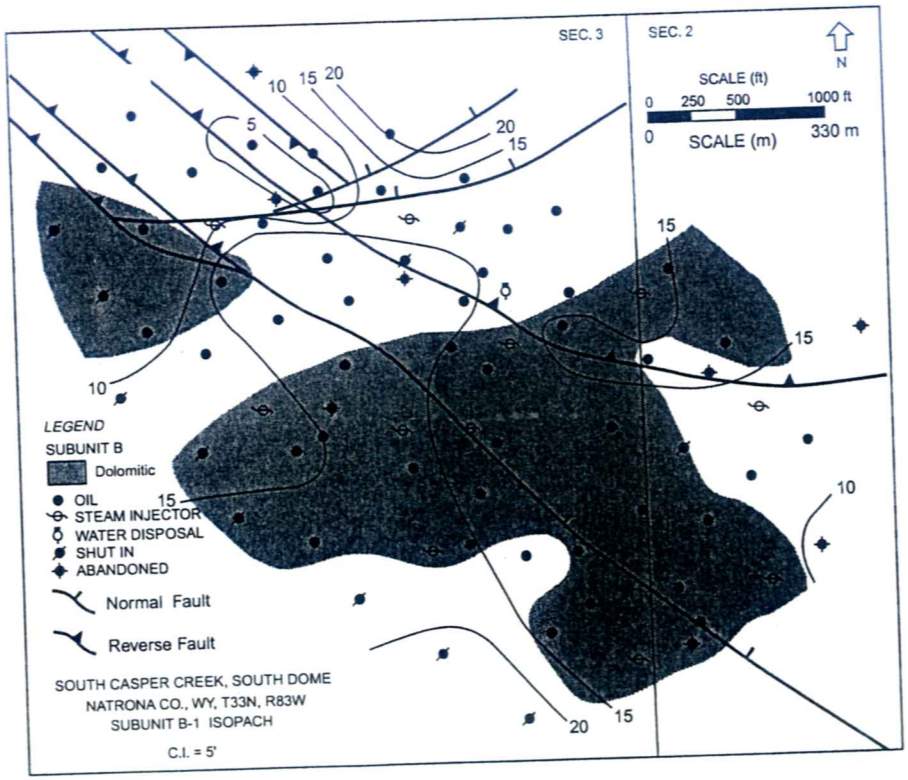

Figure 10—Isopach map, B-1 reservoir subunit, South Casper Creek field. Screened areas indicate dolomitic, low-permeability areas in immediately overlying B subunit. The B-1 subunit has the highest reservoir quality and is typically the most productive in the field. (Modified from List, 1995).

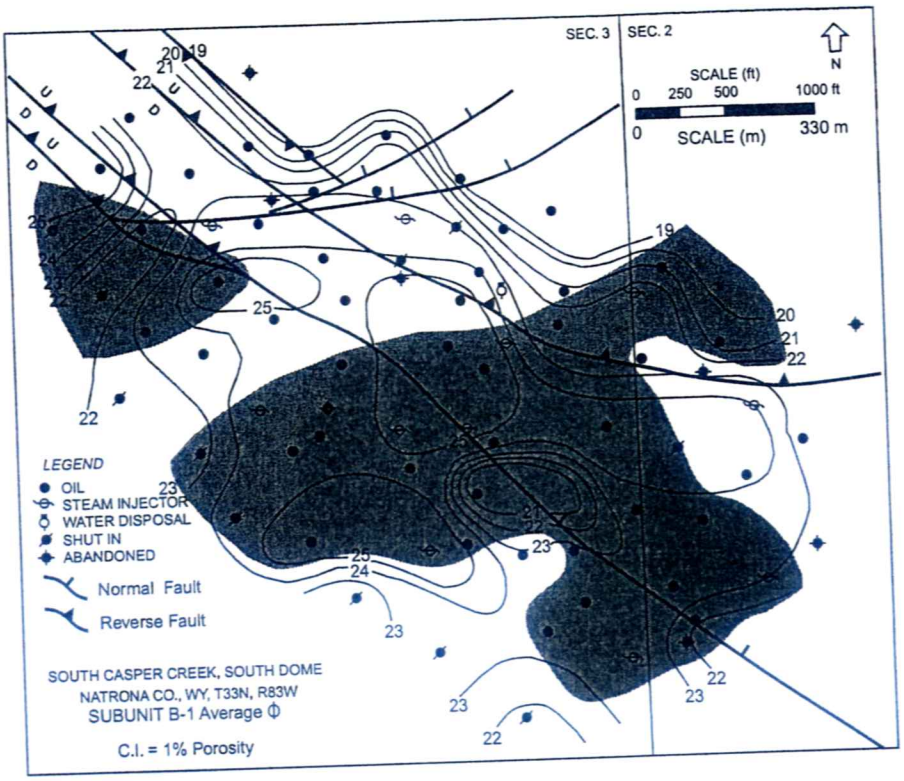

Figure 11—Average net porosity in B-1 subunit. Screened areas indicate dolomitic, low-permeability areas in immediately overlying B subunit. (Modified from List, 1995.)

or more faults intersect. In favorable locations, fracturing is especially present in units F, D, B-3, and A-2, all of which contain zones of dolomitic sandstone, but can exist throughout the upper Tensleep interval.

Several recommendations emerge from study of the Tensleep at South Casper Creek. First, understanding of stratigraphic and diagenetic heterogeneities is needed prior to initiation of secondary

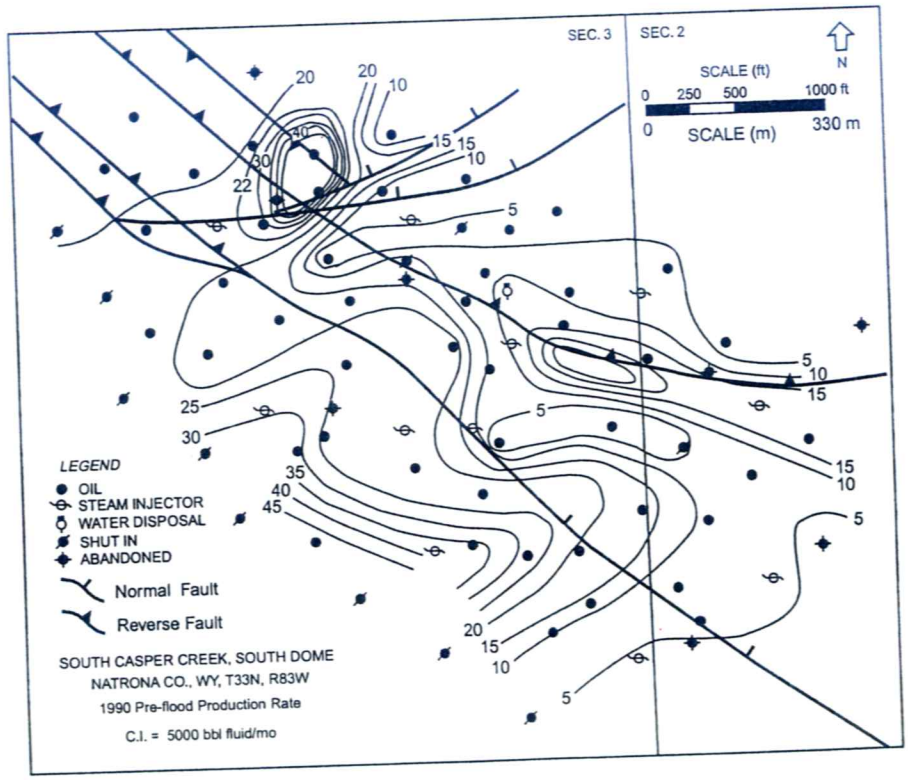

Figure 12—Contour map showing total monthly Tensleep production (oil + water) prior to initiation of a major steamflood program. Contours are in thousand barrels of fluid per month. (Modified from List, 1995.)

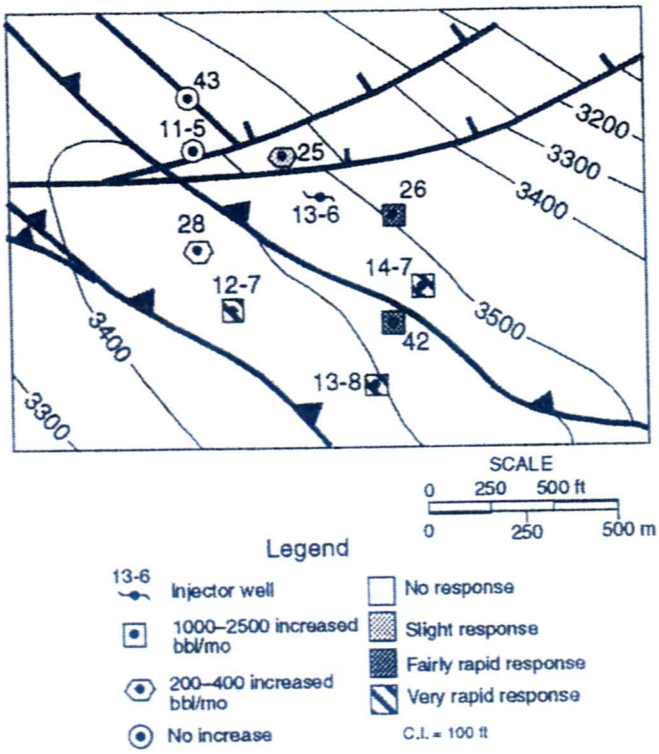

Figure 13—Patterns of well response to steam injection. See text for discussion.

recovery programs. Second, such programs should not be done in areas where the reservoir as a whole has low permeability, where fracturing is absent, or where the reservoir contains an abundance of low-permeability (interdune) layers. Third, given their importance to productivity, fracture patterns should be studied in more detail. At present, only six wells have had fracture identification logs run in them at South Casper Creek. This has proved insufficient to adequately map fracture occurrence and orientation in much of the field.

The results of reservoir characterization at South Casper Creek have implications for production from this interval and its correlatives throughout the Rocky Mountain region, including the Minnelusa, Weber, and Quadrant formations. An increasing number of fields in these reservoirs will be considered for secondary recovery projects in the future. South Casper Creek therefore provides an example of the problems that operators are likely to face in these areas.

REFERENCES CITED

Akhtar, M. K., 1991, Diagenesis of the Pennsylvanian Tensleep Sandstone and its control over reservoir quality, South Casper Creek oilfield, Natrona County, Wyoming: M.S. thesis (T-3955), Colorado School of Mines, Golden, Colorado, 142 p.

Benson, R. D., 1991, Seismic interpretation of South Casper Creek field, Natrona County, Wyoming: Progress Report, Colorado School of Mines, Reservoir Characterization Project, Sponsors Meeting Report (April 11, 1991), 22 p.

Cole, R. D., and C. E. Mullen, 1992, Sedimentologic reservoir characterization of Tensleep Sandstone: Wyoming Geological Association 44th Annual Field Conference Guidebook, p. 121–137.

Faqira, M. I., 1991, An integrated study of porosity distribution in the upper Tensleep Formation, Natrona County, Wyoming: M.S. thesis (T-4085), Colorado School of Mines, Golden, Colorado, 202 p.

Lawson, D. E., 1954, South Casper Creek field: Wyoming Geological Association 9th Annual Field Conference Guidebook, p. 80–83.

List, D. F., 1991, Review of geologic findings in South Casper Creek field: Colorado School of Mines, Reservoir Characterization Project, Sponsors Meeting Report (April 11, 1991), 32 p.

List, D. F., 1995, Tensleep Sandstone heterogeneity and effect on fluid flow, South Casper Creek field, Natrona County, Wyoming: Ph.D. thesis (T-4338), Colorado School of Mines, Golden, Colorado, 294 p.

Mankiewicz, D., and J. R. Steidtmann, 1979, Depositional environments and diagenesis of the Tensleep Sandstone, eastern Big Horn basin, Wyoming, *in* P. A. Scholle and P. R. Schluger, eds., Aspects of diagenesis: SEPM Special Publication 26, p. 319–336.

Morgan, J. T., F. S. Cordiner, and A. R. Livingston, 1978, Tensleep reservoir, Oregon basin field, Wyoming: AAPG Bulletin, v. 62, p. 609–632.

Pedry, J. J., 1975, Tensleep Sandstone stratigraphic-hydrodynamic traps, northeast Bighorn basin, Wyoming: Wyoming Geological Association 27th Annual Field Conference Guidebook, p. 117–127.

Skeen, R. C., and R. R. Ray, 1983, Seismic models and interpretation of the Casper arch thrust: application to Rocky Mountain foreland structure, *in* J. D. Lowell, ed., Rocky Mountain basins and uplifts: Rocky Mountain Association of Geologists, p. 99–124.

Stevenson, V. M., and C. E. Mullen, 1991, Evolution of a successful steamdrive in a geologically complex, steeply dipping reservoir at South Casper Creek field, Wyoming: Society of Petroleum Engineers paper 21528, 12 p.

Tanean, H., 1991, Multiscale reservoir characteristics of the Tensleep Formation, South Casper Creek field, Natrona County, Wyoming: M.S. thesis (T-3827), Colorado School of Mines, Golden, Colorado, 372 p.

ABOUT THE AUTHOR

Scott L. Montgomery

Scott L. Montgomery is a geologist, author, and translator residing in Seattle, Washington. He received his B.A. degree in English from Knox College in 1973 and his M.S. degree in geological sciences from Cornell University in 1978. He is the author of the quarterly monograph series *Petroleum Frontiers*, published by Petroleum Information Corporation, and of books and articles on the history of science. His current research interests include frontier plays and technologies and various topics in the history of geology and astronomy.

APP. 12

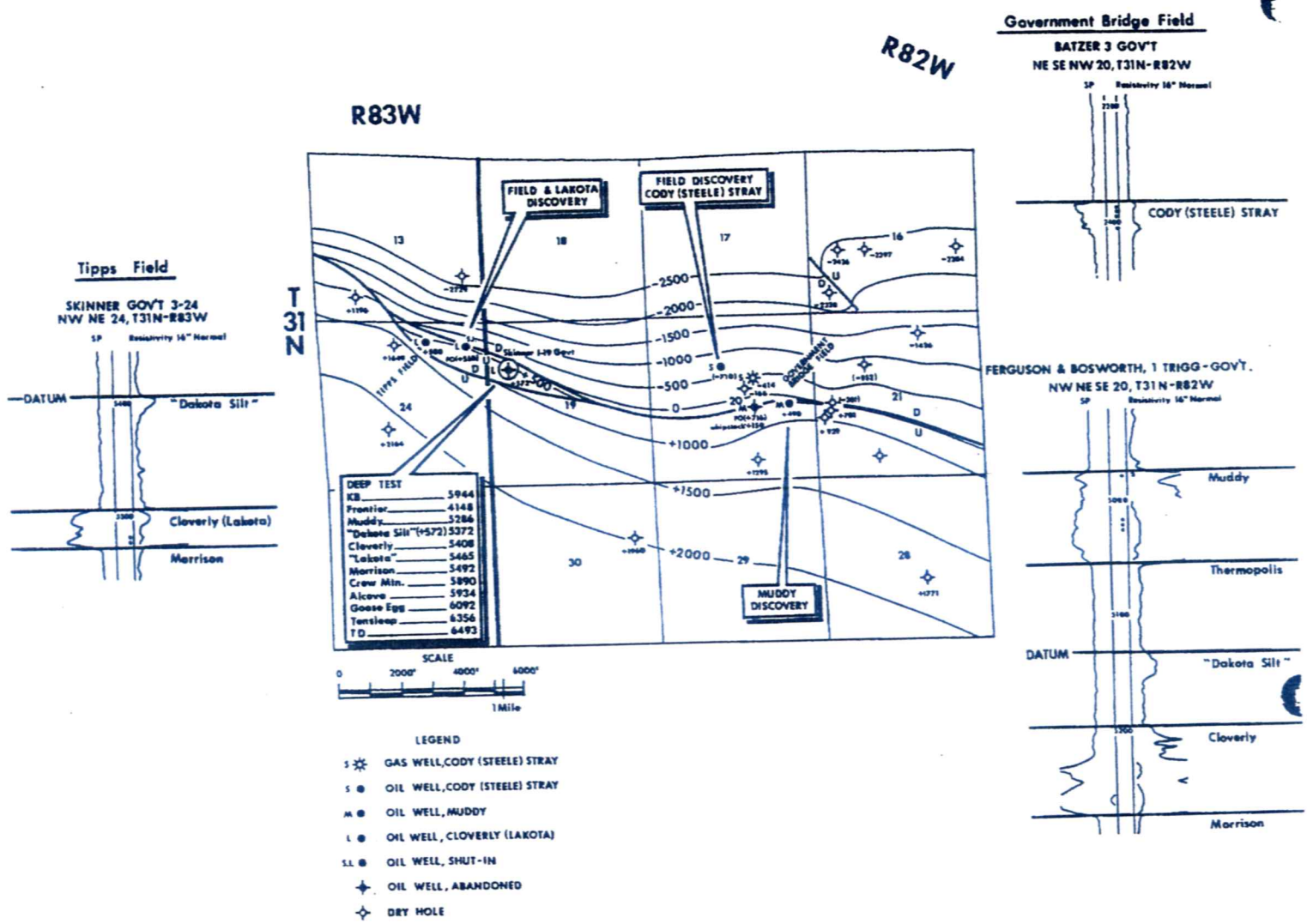

W.G.A.

GOVERNMENT BRIDGE AND TIPPS

NATRONA COUNTY, WYOMING
DATUM – DAKOTA SILT
CONTOUR INTERVAL – 500'

APP. 13

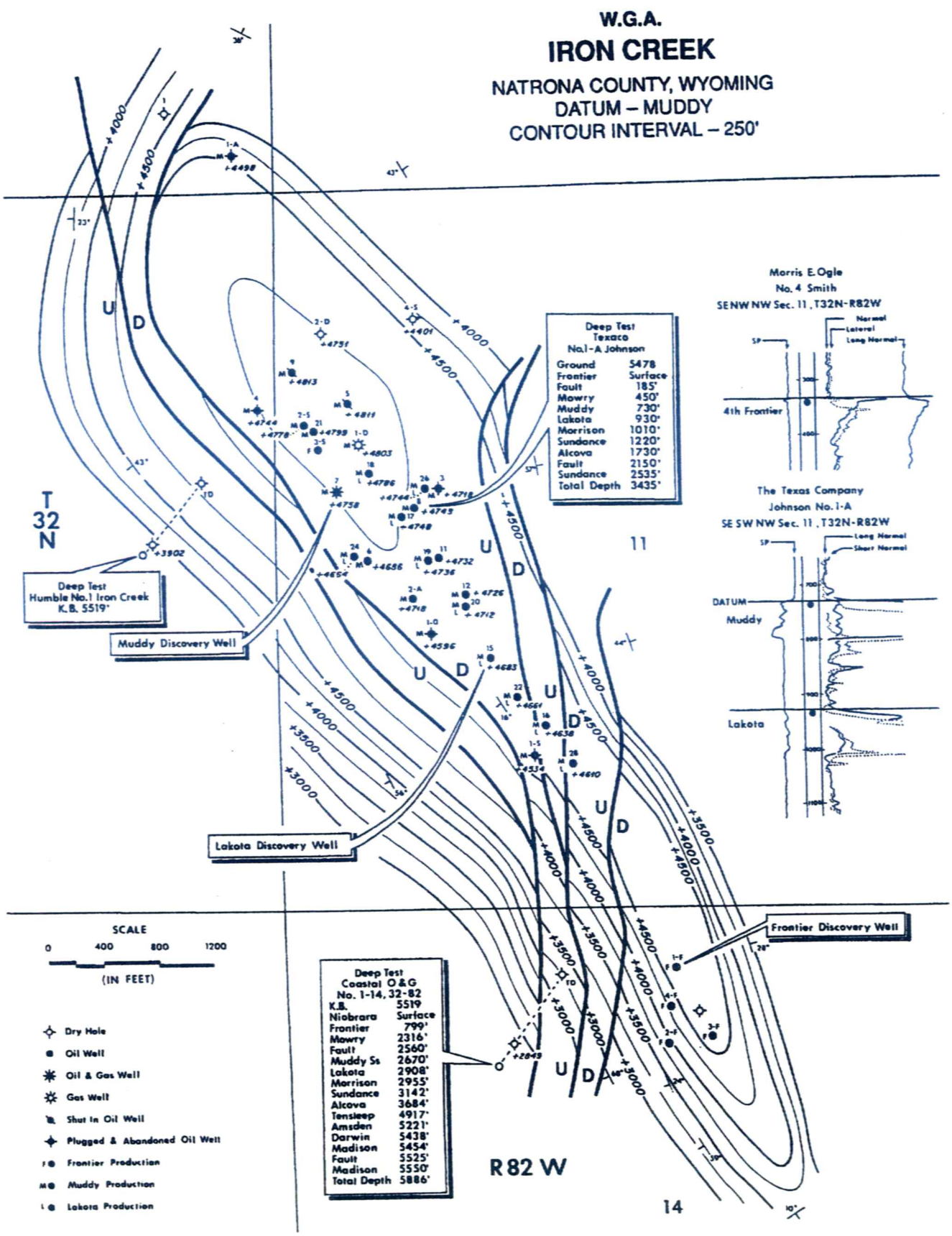
W.G.A.
IRON CREEK
NATRONA COUNTY, WYOMING
DATUM – MUDDY
CONTOUR INTERVAL – 250'
Deep Test
Texaco
No.1-A Johnson
Ground 5478
Frontier Surface
Fault 185'
Mowry 450'
Muddy 730'
Lakota 930'
Morrison 1010'
Sundance 1220'
Alcova 1730'
Fault 2150'
Sundance 2535'
Total Depth 3435'
Morris E. Ogle
No. 4 Smith
SE NW NW Sec. 11, T32N-R82W
Normal
Lateral
Long Normal
SP
4th Frontier
The Texas Company
Johnson No. 1-A
SE SW NW Sec. 11, T32N-R82W
Long Normal
Short Normal
SP
DATUM
Muddy
Lakota
Deep Test
Humble No.1 Iron Creek
K.B. 5519'
Muddy Discovery Well
Lakota Discovery Well
Frontier Discovery Well
T 32 N
R 82 W
11
14
SCALE
0 400 800 1200
(IN FEET)
Dry Hole
Oil Well
Oil & Gas Well
Gas Well
Shut In Oil Well
Plugged & Abandoned Oil Well
F Frontier Production
M Muddy Production
L Lakota Production
Deep Test
Coastal O & G
No. 1-14, 32-82
K.B. 5519
Niobrara Surface
Frontier 799'
Mowry 2316'
Fault 2560'
Muddy Ss 2670'
Lakota 2908'
Morrison 2955'
Sundance 3142'
Alcova 3684'
Tensleep 4917'
Amsden 5221'
Darwin 5438'
Madison 5454'
Fault 5525'
Madison 5550'
Total Depth 5886'

APP. 14

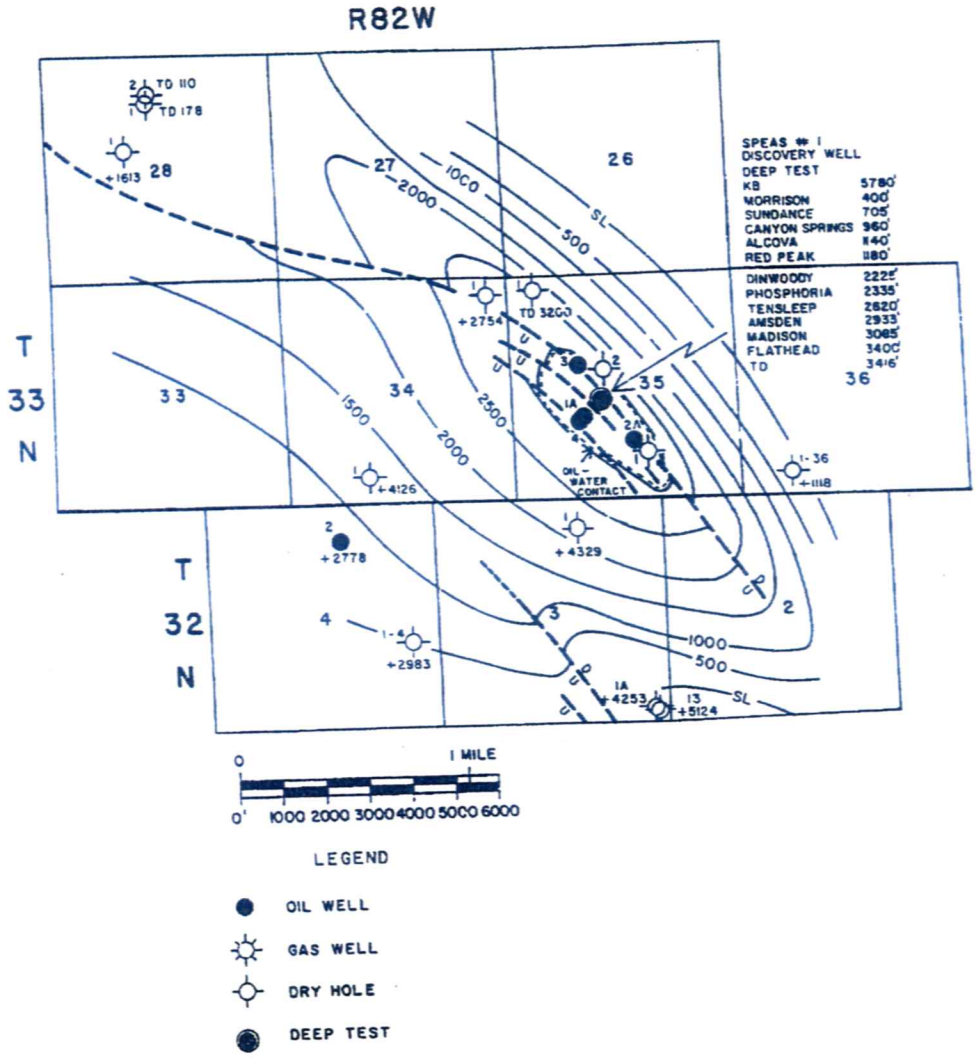

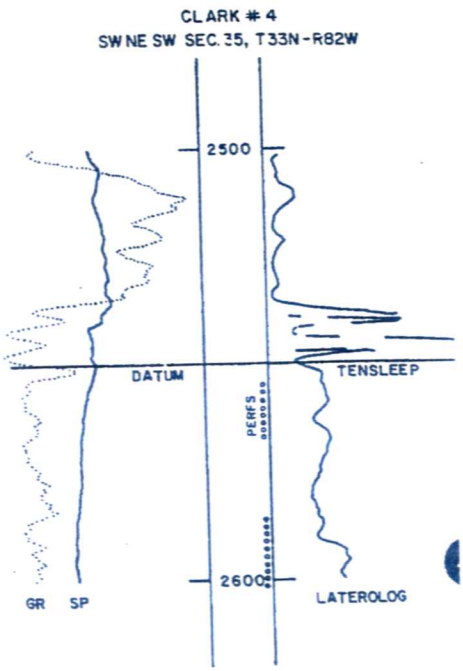

W.G.A.

OIL MOUNTAIN

NATRONA COUNTY, WYOMING
DATUM – TENSLEEP
CONTOUR INTERVAL – 500'

APP. 15

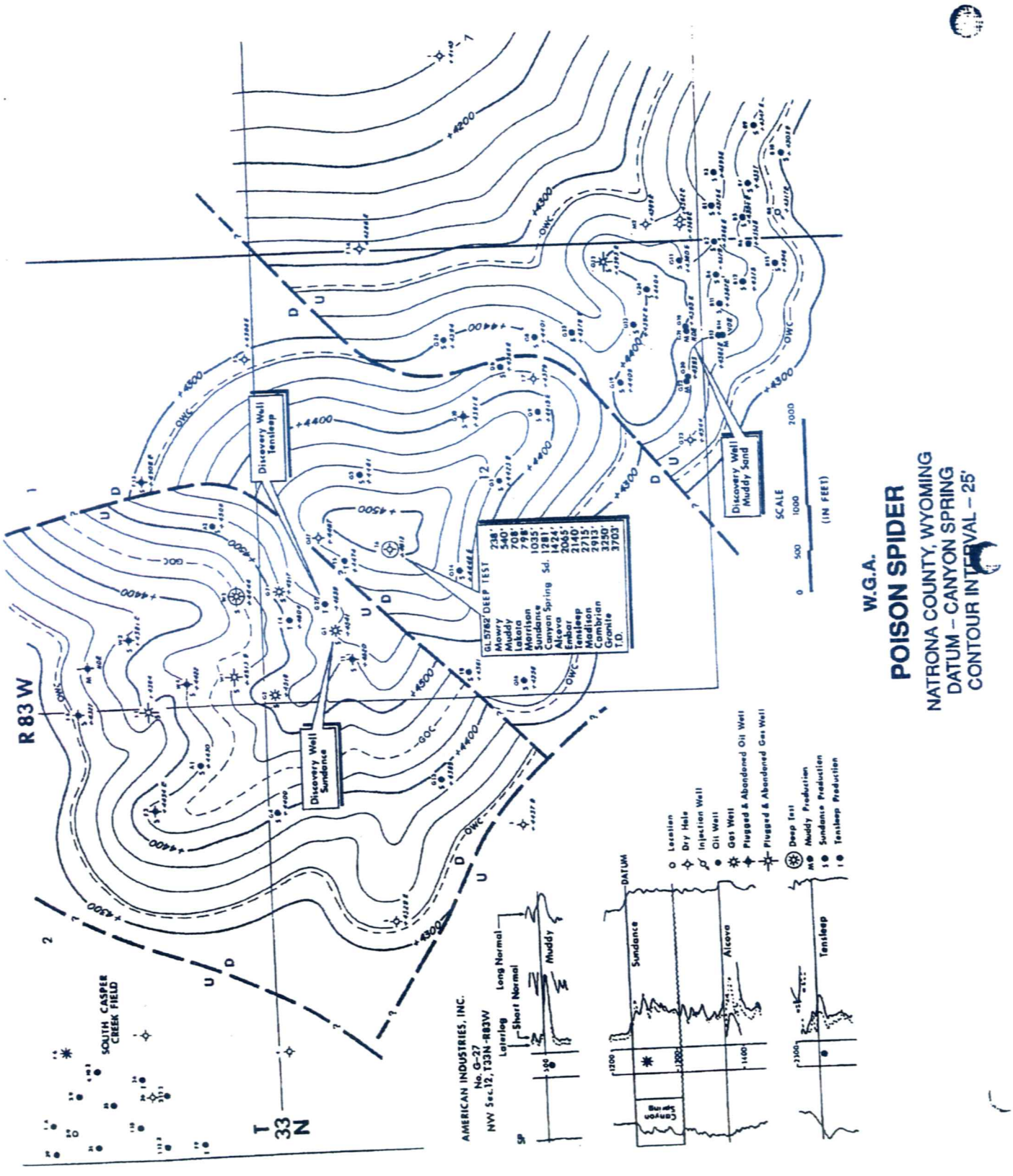
W.G.A.
POISON SPIDER
NATRONA COUNTY, WYOMING
DATUM – CANYON SPRING
CONTOUR INTERVAL – 25'
SCALE
0 500 1000 2000
(IN FEET)
Discovery Well Tensleep
Discovery Well Sundance
Discovery Well Muddy Sand
GL 5782' DEEP TEST
Mowry 238'
Muddy 540'
Lakota 708'
Morrison 798'
Sundance 1035'
Canyon Spring Sd. 1281'
Alcova 1424'
Ember 2065'
Tensleep 2140'
Madison 2715'
Cambrian 3913'
Granite 3250'
T.D. 3703'
GOC
OWC
R 83 W
T 33 N
SOUTH CASPER CREEK FIELD
AMERICAN INDUSTRIES, INC.
No. G-27
NW Sec. 12, T33N-R83W
Laterlog
Long Normal
Short Normal
Muddy
SP
DATUM
Sundance
Alcova
Tensleep
Lacation
Dry Hole
Injection Well
Oil Well
Gas Well
Plugged & Abandoned Oil Well
Plugged & Abandoned Gas Well
Deep Test
Muddy Production
Sundance Production
Tensleep Production

APP. 16

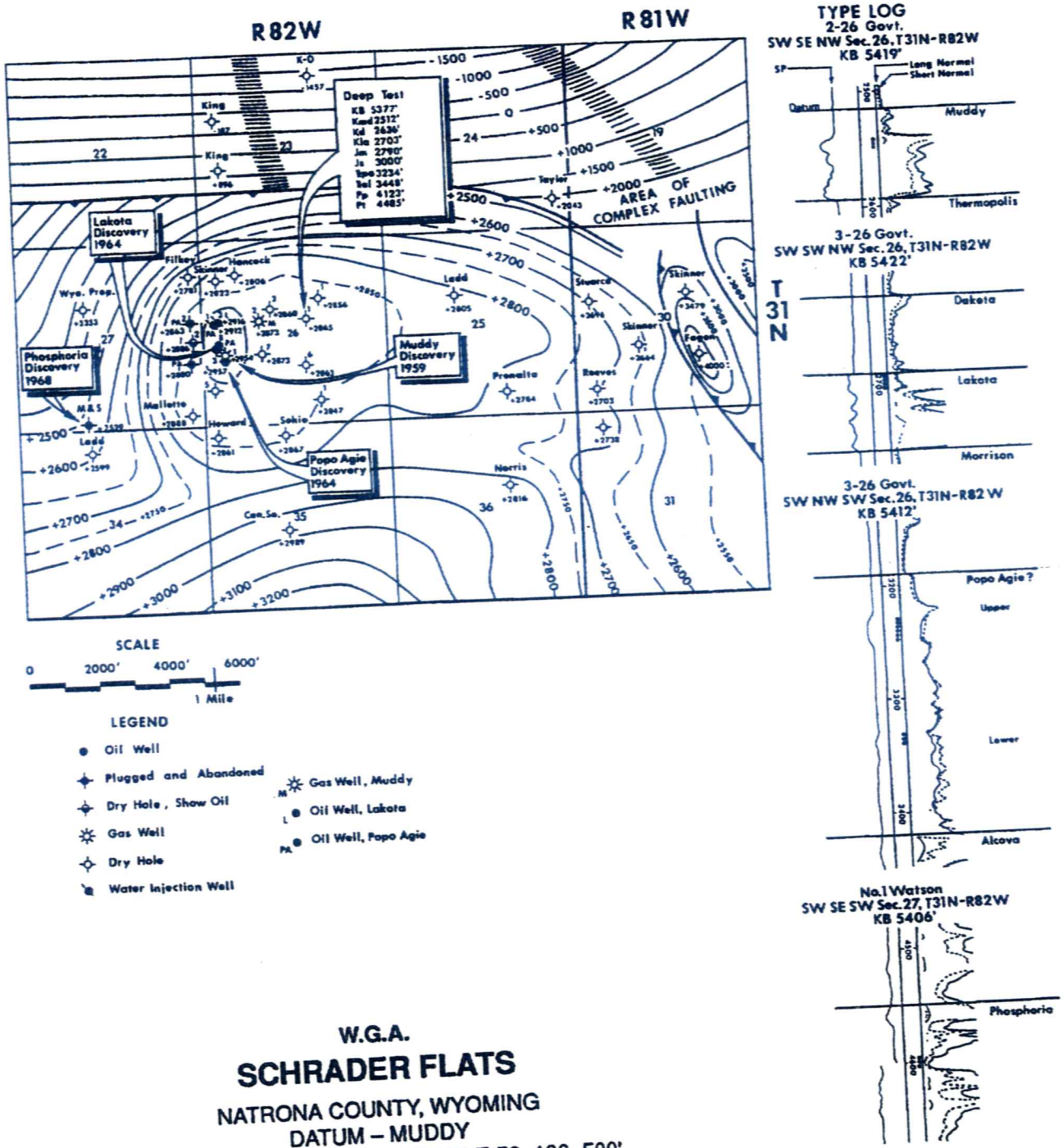

W.G.A.

SCHRADER FLATS

NATRONA COUNTY, WYOMING

DATUM – MUDDY

CONTOUR INTERVAL – VARIABLE 50, 100, 500'

APP. 17

AAPG Annual Meeting
Denver, Colorado
June 3-6, 2001

Bozkurt N Ciftci1, Alexander Aviantara1, Dennis Kerr2, Neil F. Hurley1 (1) Colorado School of Mines, Golden, CO (2) The University of Tulsa, Tulsa, OK

Outcrop based 3-D modeling of the Tensleep Sandstone at Alkali Creek, Bighorn Basin, Wyoming

Bounding surfaces act as permeability barriers or baffles to fluid flow and divide the Tensleep reservoirs into flow compartments at different scales. In order to identify the geometry and volumetric size of these compartments, a 3-D computer model of the Tensleep Sandstone was constructed based on the outcrop exposures. The field data were collected by a precise GPS receiver system at Alkali Creek, Bighorn Basin, Wyoming. The data include coordinates and elevations of 3500 data point that are tied to 0.0-, 1.0-, 0.1- and 2.0-bounding surfaces.

1.0-bounding surfaces display undulatory geometry both in the foreset dip and strike direction. They climb from 0.0-bounding surfaces in the general direction of foreset dip with an angle typically less than 1°. 1.0-bounded compartments are laterally extensive across the study area and display variable thicknesses in the range of 2 to 26 meters. These compartments are further subdivided into smaller 2.0-bounded compartments by 2.0-bounding surfaces. 2.0-bounding surfaces have average spacings of 30m and display variations in their strike orientation forming laterally discontinuous 2.0-bounded compartments.

Wells were simulated by 10-acre, 20-acre, 40-acre and 160-acre templates on the 3-D model. The simulation also includes horizontal wells that are oriented parallel, perpendicular and oblique to foreset dip direction. For each well, the volume of intersected reservoir compartments was calculated. Comparison of these volumes with the ideal drainage volume of wells identified the most efficient drill template for the Tensleep reservoirs. Horizontal wells drilled parallel to foreset dip direction drain the maximum number and volume of reservoir compartments.

APP. 18

AAPG Annual Meeting
Denver, Colorado
June 3-6, 2001

Neil F. Hurley1, Alex Aviantara2, Dennis Kerr2 (1) Colorado School of Mines, Golden, CO (2) The University of Tulsa, Tulsa, OK

Structural and Stratigraphic Compartments Determined from Horizontal Drilling in an Eolian Reservoir, Tensleep Sandstone, Wyoming

The eolian Tensleep Sandstone (Pennslyvanian) is a major oil and gas producer in the Bighorn basin, Wyoming. In 1992, the operator of Byron field drilled a medium-radius lateral hole along a NE trend. The well reached 90 degrees deviation where it encountered the Tensleep Sandstone on the flank of the anticlinal structure. Casing was set at that point. The remainder of the well, which was drilled for roughly 500 ft (150 m) on an uphill slant, stayed in the uppermost Tensleep Sandstone within a 20 ft (6 m) thick stratigraphic section. This part of the borehole was left uncased. The general shape of the borehole is that of a "fishhook," where the structural high is at TD (total depth).

The last 150 ft (45 m) of the borehole was full of oil. This level probably represents the height of the oil-water contact in the fractures. If so, this would put the oil-water contact in the fractures at an elevation several hundred feet above the oil-water contact in the matrix. This suggests an innovative, although untested, method of completing the well. The oil will gravity segregate towards the top (TD) of the fishhook-shaped well. Tubing could be run to a point near TD, and the rate at which the borehole is charged with oil can be determined by using step-rate pump tests. If the rate is economically viable, then the well could be produced with minimal water production. The upside potential for similar horizontal wells could be very high in Bighorn basin fields and in other fractured anticlines.

APP. 19

Morphology of the Casper Mountain uplift and related, subsidiary structures, central Wyoming: Implications for Laramide kinematics, dynamics, and crustal inheritance

Donald S. Stone

ABSTRACT

The general east-west trend of the regional-scale, fault-related Casper Mountain uplift in central Wyoming reflects a preexisting Precambrian fabric along which there was Laramide compressional reactivation. Initial fault displacement on the south-dipping Casper Mountain fault zone probably predates displacement on the intersecting, northwest-trending, northeast-dipping Casper arch thrust that forms the northeastern border of the Wind River basin. Later phase, incremental, Laramide displacements occurred along both fault zones: left-oblique slip on the Casper Mountain fault zone, dip slip on the crosscutting Casper arch thrust. Basement-involved thrust generation of the subsidiary Laramide, northwest-trending Iron Creek and Emigrant Gap anticlines along the north (footwall) side of the Casper Mountain fault zone also occurred during this later phase Laramide deformation.

Perturbation of far-field, northeast-southwest, Laramide maximum horizontal paleostress trajectories (σ_1) to local, nearly fault-normal orientation at Casper Mountain, together with strain partitioning, is proposed to explain the apparent coeval development of divergent hanging-wall and footwall, basement-involved, fault-related structures. This kinematic and dynamic interpretation may be applied conditionally to other east-west–trending Laramide uplifts in the central Rocky Mountain foreland province.

AUTHOR

DONALD S. STONE ~ *6178 South Lakeview Street, Littleton, Colorado, 80120; don@dsstone.com*

Donald S. Stone is an independent geologist and consultant living in Littleton, Colorado. He received his M.A. (1951) from Cornell University, with majors in structural geology and stratigraphy, and began his career as a petroleum geologist with Chevron in California (onshore and offshore). He has spent the last 35 years working the subsurface geology of the Rocky Mountain area with particular emphasis on interpretation of foreland structure.

ACKNOWLEDGEMENTS

Many organizations and individuals supported this investigation with contributions of critical data. I thank Amalgamated Explorations, Inc.; Texaco U.S.A.; Union Pacific Resources; Amerada-Hess; Mobil; and Wold Oil for their contributions. Earth Satellite Corporation provided the image in Figure 2A. Special thanks are due to Murray Dahill, owner of the Iron Creek oil field, who supplied critical data not available anywhere else and served as a guide on two field trips through the Casper Mountain area. Amgad Youres and Bill Muehlberger provided copies of several important papers consulted during the formulation of the concepts developed here. An early draft of this article was reviewed by Murray Dahill, Eric Erslev, Rick Groshong, and Randy Ray, and their critical comments and suggestions were carefully considered in early revisions. Final revision of the manuscript greatly benefited from AAPG reviews by Jon Olson, Jim Lowell, and Peter Hennings.

Manuscript received December 19, 2000; revised manuscript received January 2, 2002; final acceptance January 28, 2002.

INTRODUCTION

Investigative studies of east-west–trending, Precambrian-cored, Laramide uplifts in the central Rocky Mountain foreland province are numerous, but detailed morphological and kinematic interpretations of these structures are scarce. The fault-related, doubly plunging Casper Mountain uplift in east-central Wyoming provides a prototypical model for these so-called anomalous Laramide uplifts.

Casper Mountain is a topographically prominent, east-west–trending Laramide uplift in the central Wyoming foreland (Figure 1). This fault-related uplift is defined by accessible exposures of Phanerozoic strata along forelimb, backlimb, and east and west plunges and by numerous borehole penetrations and critical seismic control around its margins. Consequently, the morphology of the uplift and the related Casper Mountain fault zone can be diagrammed more easily and with more precision than is the case for other east-west–trending Laramide uplifts of the central Rocky Mountain foreland province.

The north face of Casper Mountain lies about 5 mi (8 km) south of Casper, Wyoming, and the highest elevation on the mountain is approximately 8200 ft (~2500 m), about 3000 ft (916 m) above the city. The north flank of the uplift is defined at the surface by steeply dipping footwall and hanging-wall strata vertically rotated into the south-dipping Casper Mountain fault zone. This complex fault zone extends along the entire length of the uplift and into the Wind River basin to the west, but its traces are not continuously exposed (Figure 2). Casper Mountain lies at the southern end of the Casper arch, a northwest-trending, regional platform that separates the Wind River basin on the southwest from the Powder River basin on the northeast (Figure 1). The Casper arch is uplifted along basin-boundary, inward-dipping, northwest-striking, Laramide thrusts that border it along its southwest and northeast sides. In the literature of this region, the Casper Mountain uplift generally has been described as part of the northwest end of the Laramie Range, but it is structurally and topographically separate from the main body of the range.

The morphology of the Casper Mountain uplift, from its orthogonal intersection with the Casper arch thrust (also called the Owl Creek thrust by Montgomery et al. [2001]) on the west to its terminus on the east, is outlined by sedimentary strata throughout most of its approximately 30 mi (~48 km) east-west extent, except for the central core area of about 10 mi^2 (26 km^2) where Phanerozoic rocks have been

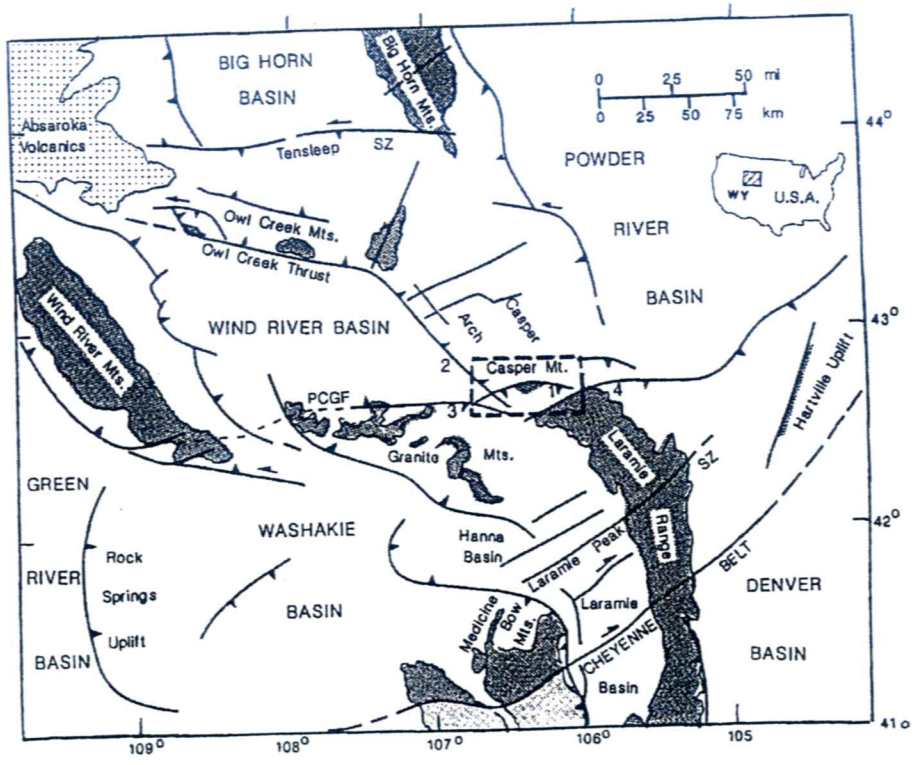

Figure 1. Tectonic index map of part of Wyoming showing heavy dashed outline of the area mapped in this study. Key faults are marked by numbers: 1 = Casper Mountain fault zone; 2 = Casper arch thrust; 3 = North Granite Mountain fault zone; 4 = Muddy Mountain fault zone. The fine dashed line marked as PCGF is the Precambrian geochronologic front described by Peterman and Hildreth (1978), which extends from the southeastern Wind River Range through the Granite Mountains and east along the approximate traces of the North Granite Mountain and Muddy Mountain fault zones (see text for discussion). Precambrian outcrops are shaded.

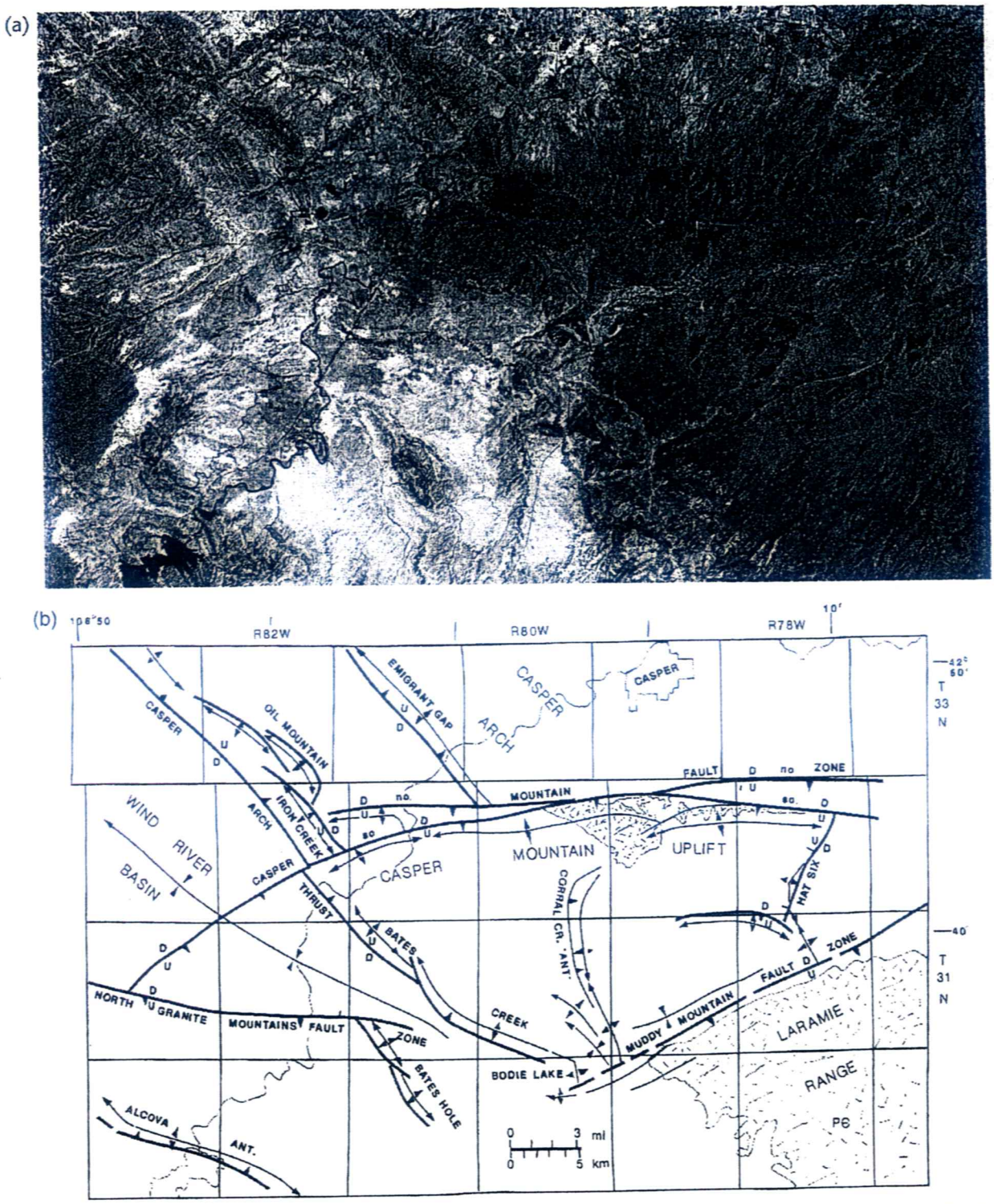

Figure 2. (A) Landsat Thematic Mapper, converted to gray scale, image of the Casper Mountain area (contributed by Earth Satellite Corporation). (B) Tectonic index map of the Casper Mountain area showing named and numbered structural features imaged in part A and discussed in the text.

eroded and Precambrian rocks are exposed. Structural contour maps on the Cretaceous Muddy Sandstone and the Mississippian Madison Limestone that include extrapolation of contours above the eroded Precambrian core of the range, together with a series of structural cross sections, illustrate the three-dimensional morphology of the Casper Mountain area. The Casper Mountain fault/fold trend extends to the west across the Casper arch thrust for another 6 mi (10 km) into the Wind River basin, with a structural elevation drop from the crest of the Casper Mountain uplift to the axis of the Wind River basin of nearly 3 mi (5 km).

The Casper Mountain uplift/Casper Mountain fault zone complex is particularly interesting because of its east-west trend and the abrupt terminations of two prominent, northwest-trending, basement-involved, Laramide, fault-related anticlines against the north (footwall) side of the Casper Mountain fault zone (Figure 2). Interpretation of the morphology and kinematic evolution of the Casper Mountain uplift and related subsidiary structures is considered important because fundamental concepts developed here may well have application to other east-west Laramide uplifts in the Rocky Mountain foreland and, in a general sense, to similar structures elsewhere in the world.

STRATIGRAPHY

The stratigraphic section encountered in boreholes and exposed in the Casper Mountain area totals about 7000 ft (2100 m), from the Devonian through the Upper Cretaceous (Figure 3). In ascending order, Paleozoic rocks begin with the basal Fremont Canyon Sandstone unit, which has been traditionally assigned to the Cambrian (e.g., Gable et al., 1988) but placed in the Devonian by Sando and Sandberg (1987) and Sandberg et al. (1989). (Cambrian, Ordovician, and Silurian rocks are missing by erosion.) Overlying this basal sandstone unit is the Mississippian Madison Limestone (contoured horizon), Pennsylvanian–Permian Casper sandstone (which in deference to oil-field usage is here referred to as Tensleep), and the Permian Goose Egg Formation, a nonmarine red bed equivalent of the marine Phosphoria Formation to the west. Mesozoic rocks in the Casper area are the typical Wyoming clastic sequences from Triassic Chugwater nonmarine red shales and siltstones through Jurassic and Cretaceous marine sandstones and shales.

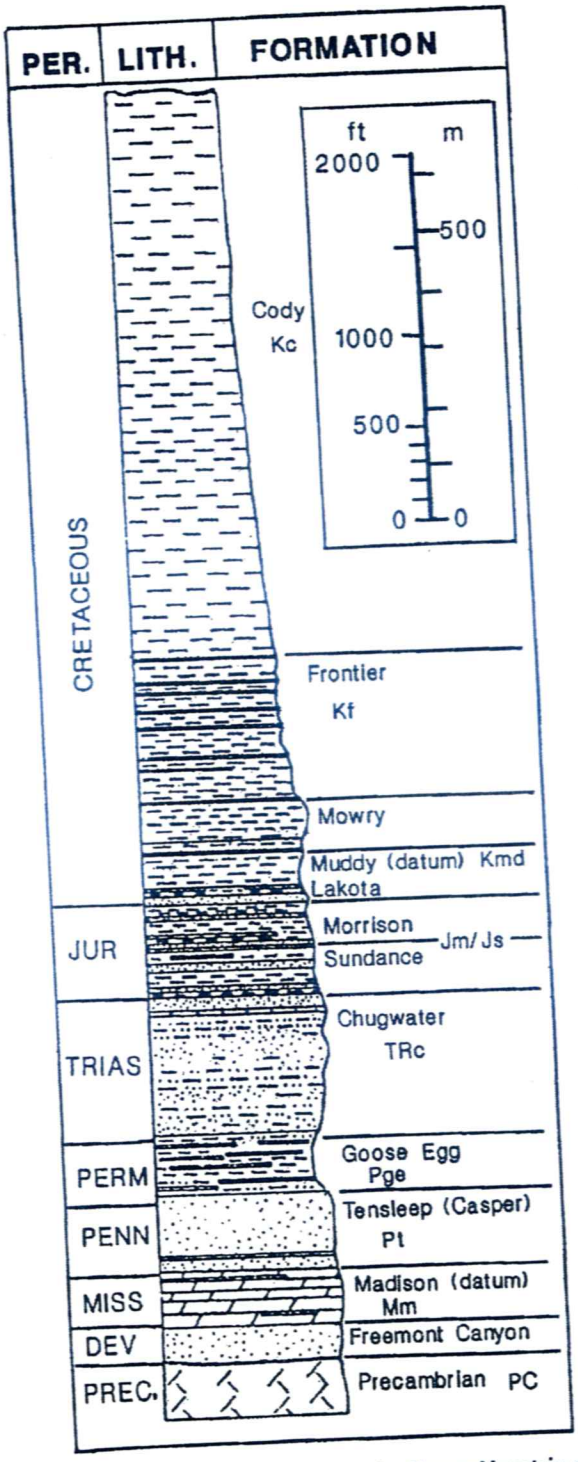

Figure 3. Stratigraphic column in the Casper Mountain area (modified after Burford, 1986b). Formation names with symbols used on structural cross sections and seismic profiles are shown to the right of the lithologic column.

DATABASE AND MAP CONSTRUCTION

Surface Geology

Interpretation of the Casper Mountain area is based on an integration of surface geologic mapping with seismic and borehole control. There are numerous articles on the surface geology of the Casper Mountain area, some of which also include kinematic and dynamic interpretations of the Casper Mountain uplift and related structures (e.g., Hares et al., 1946; Sears, 1948; Sims, 1948; Bergstrom, 1950; Faulkner, 1950; Jenkins, 1950; Sears and Sims, 1954; Stiteler, 1954; Schwarberg, 1959; Wyoming Geological Association, 1965; Crist and Lowry, 1972; Bitter, 1978; Burford et al., 1979; Lageson, 1980; Beck, 1984; Beck and Burford, 1985; Love and Christiansen, 1985; Burford, 1986a, b; Gable et al., 1988; Martinez, 1988; Narr, 1993; Narr and Suppe, 1994; Molzer and Erslev, 1995; Daniels, 1996). All of these articles have been valuable sources in the development of the geologic interpretations presented here.

Borehole Control

There is abundant borehole control along the east and west plunge of the Casper Mountain uplift and in the subsidiary, anticlinal oil-field areas. Although almost all the boreholes shown on the map penetrated the Muddy contour horizon (Figure 4A), only eight wells reached the Madison horizon (well symbols enclosed in triangles in Figure 4B). Wells drilled to test the Tensleep (Casper) Sandstone, a major producer in Wyoming, are much more numerous. Data from Tensleep borehole penetrations were used to establish estimated Madison datums by stratigraphic projection (i.e., the Tensleep–Madison stratigraphic interval is about 500 ft [150 m]) (Figure 3). The primary objective of most of the boreholes, however, was the Cretaceous Muddy Sandstone, which has excellent porosity locally where thick channel deposits are developed. Oil and gas are produced from this reservoir in several small oil fields (e.g., Iron Creek in Figure 4A and cross section AA′ in Figure 5).

Seismic Data

More than 220 line-mi (350 line-km) of 6-, 12-, and 20-fold two-dimensional seismic data (Figure 4) were solicited from oil-industry operators. Seismic profiles are located primarily along the western and eastern plunges of the Casper Mountain uplift. Data quality is generally good, except where collected over nonreflective Precambrian crystalline rocks. Synthetic seismograms from several boreholes around the area were used for reflector identification, and the data were tied to the borehole database and to surface geology. Depth migrations were prepared for all profiles, true dip calculations were made at line intersections, and the data were moved to their indicated lateral offset locations and depths. Note, however, that large lateral velocity changes across the steep-dip and fault-shadow areas required significant adjustments to well ties on most northeast-trending profiles that transect the steeply rotated hanging wall of the Casper arch thrust.

Map Construction

Mapping of both the west and east plunge areas of the Casper Mountain uplift, where most of the borehole and seismic control is concentrated, was first completed at a scale of 1:24,000 then reduced to 1:48,000. Based primarily on surface geologic control, contouring of the remaining areas of the uplift was then completed. Final reductions for Figure 4 were made from these last maps. The entire Casper Mountain complex is contoured, including related subsidiary footwall structures and extrapolated contouring above topography.

Extrapolated contours were produced by projecting stratigraphic thicknesses (Figure 3), corrected for dip, to estimated contour datum elevations above the various formation outcrops. The Wyoming Geological Association's (1965) geologic map of the Casper Mountain area (scale 1:48,000), which includes 100 ft (30 m) overlaid topographic contours (in blue), was the basis for these projections. Also, a series of structural cross sections (Figure 5) were constructed as a check on the compatibility of the contour maps and the internal consistency of the interpretations. These sections also include the extrapolations of Muddy and Madison horizons above topography.

MAJOR FAULTS

Casper Mountain Fault Zone

The Casper Mountain uplift was elevated by movement on the Casper Mountain fault zone. This fault zone is not a single fault surface, as is sometimes implied in the literature, but is composed of several

(A)

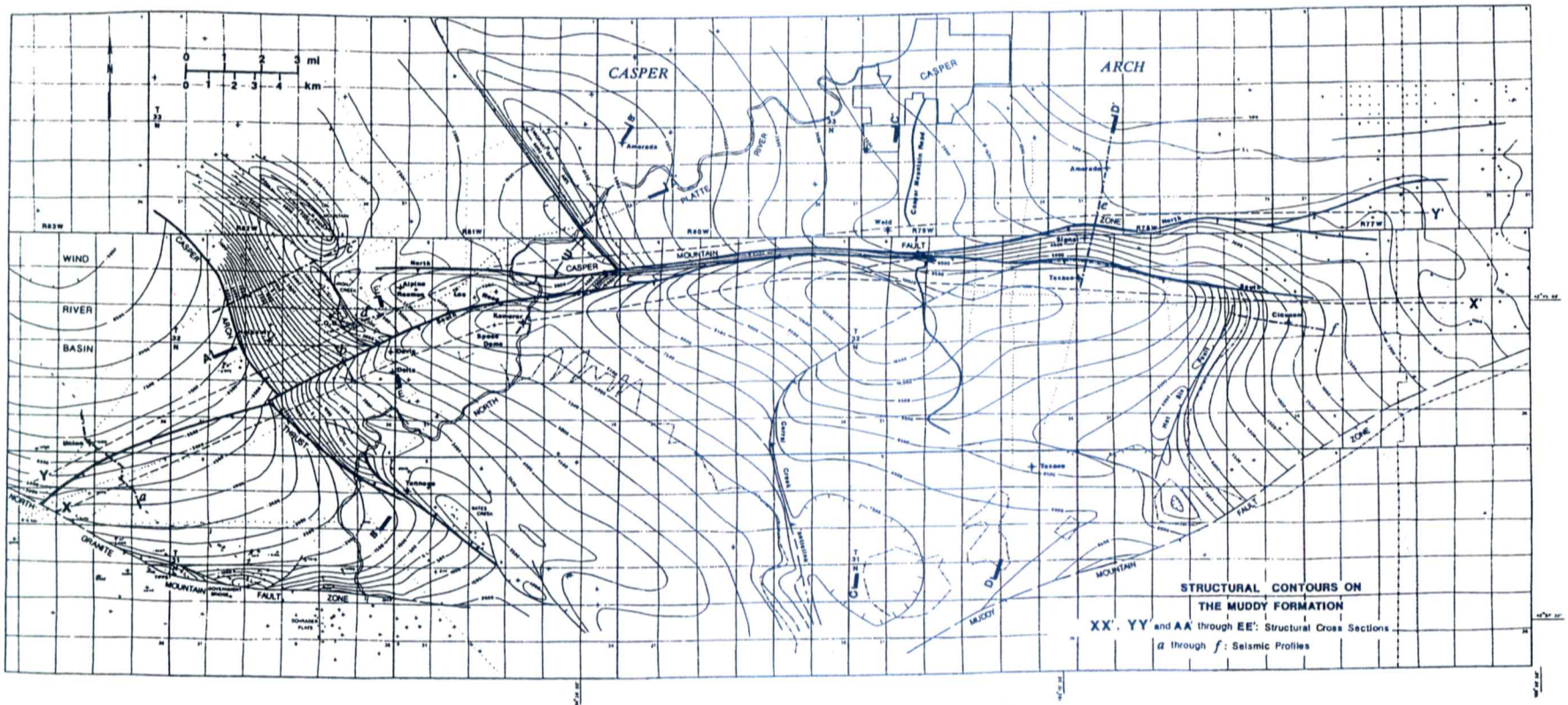

Figure 4 (A) Structural contour map on the Cretaceous Muddy Sandstone. The contour interval is 500 ft (152 m). The Muddy Sandstone outcrop is shown as a heavy dot-dash line. Contours are extrapolated above topography in the area inside the Muddy outcrop. Small black triangles on faults indicate the upthrown side and direction of fault dip. Well locations are shown by standard dry-hole and producing well symbols, with operator names identified on wells shown on structural cross sections and seismic profiles and/or mentioned in the text. Figured seismic profiles are shown as heavy short/long dashes and marked by lower case, italicized letters (*a–f*). All other seismic profiles are shown as fine dotted lines. Structural cross sections are indicated by terminal L marks and capital letters (A–E).

(B)

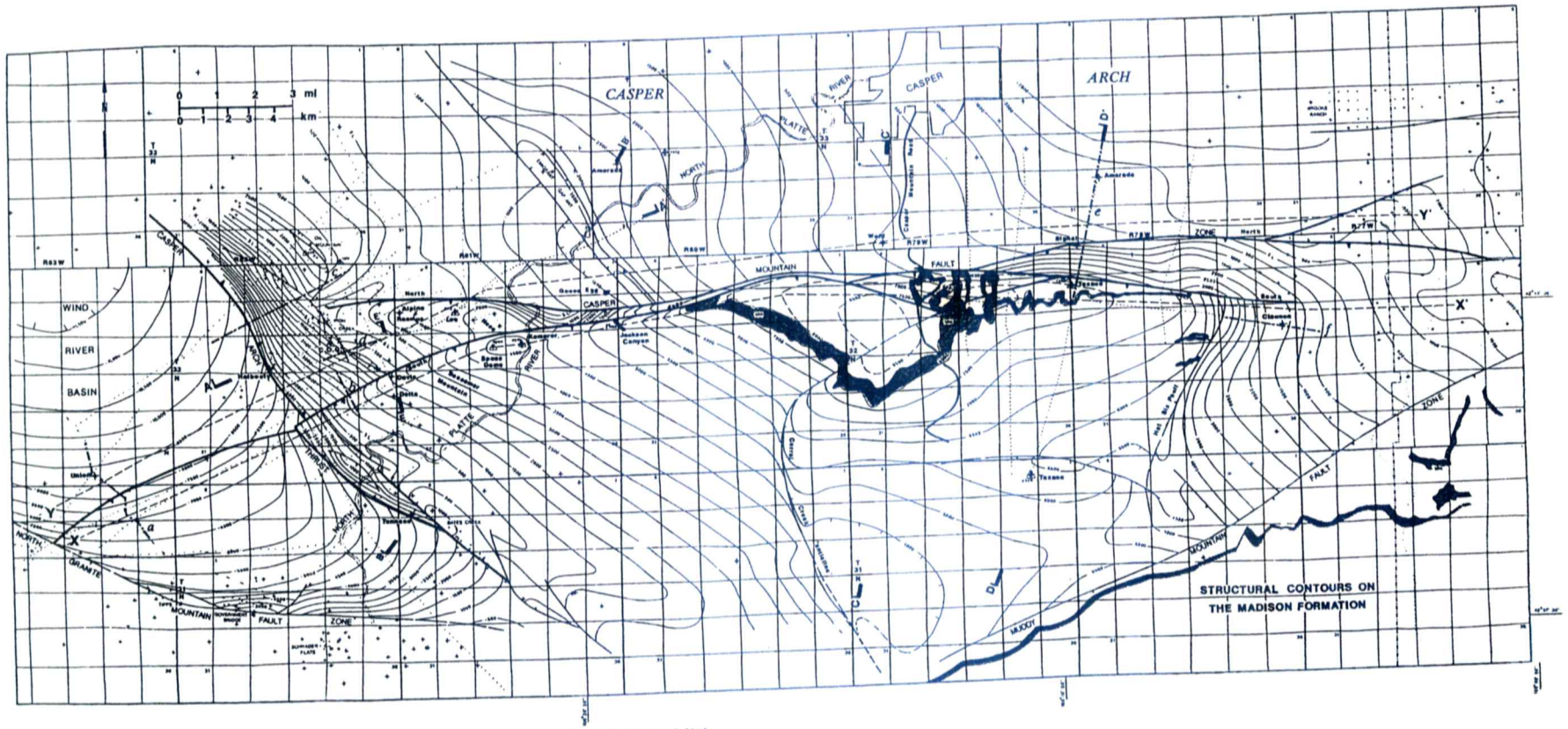

Figure 4 (B) Structural contour map on the Mississippian Madison Limestone. Wells drilled to the Madison datum are enclosed in triangles. The Madison outcrop is shown with shading, and contours are extrapolated above topography in the area inside the Madison outcrop. All notations and parameters are the same as in part A.

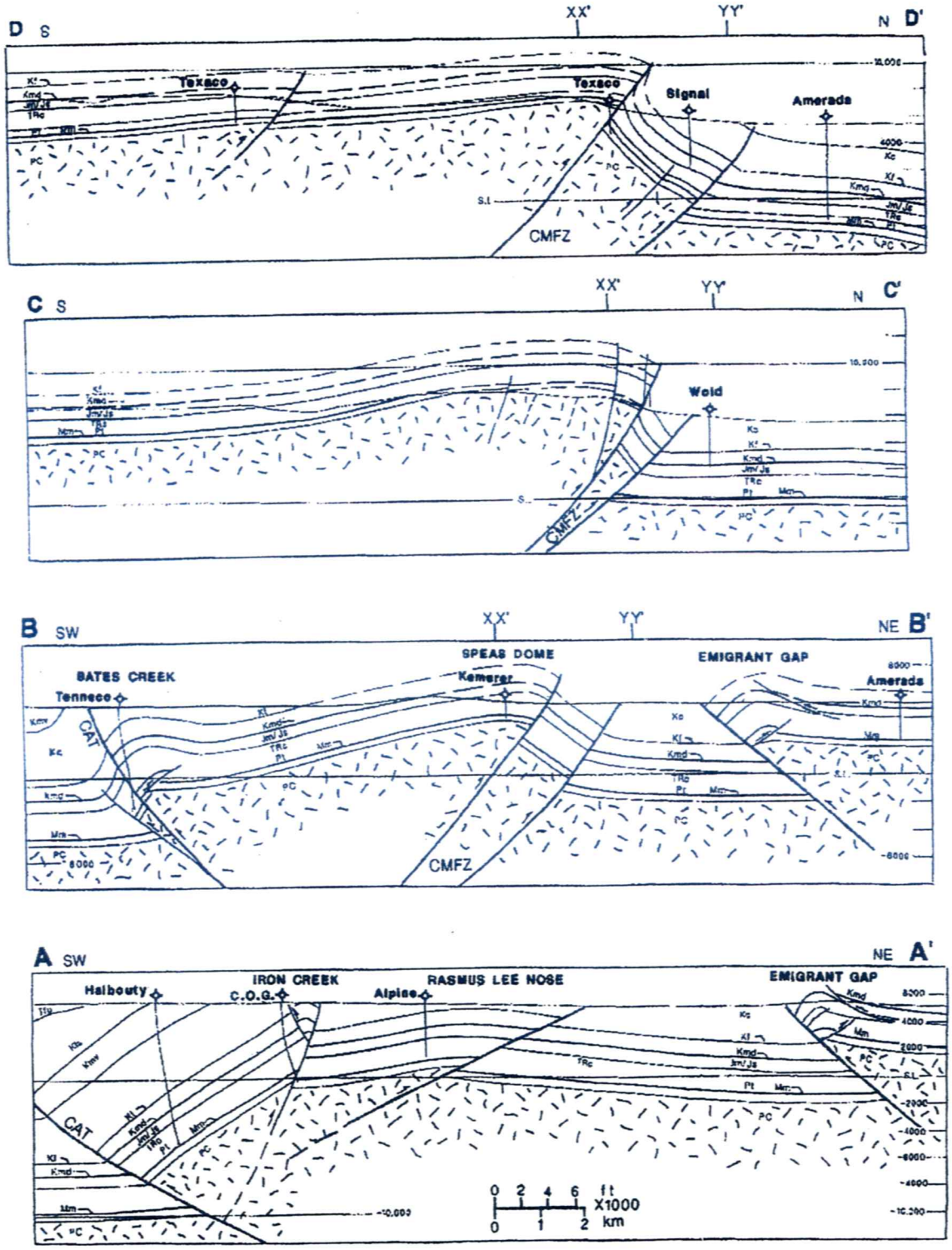

Figure 5. Structural cross sections AA′ through DD′. Formation symbols are identified in Figure 3. Locations are shown in Figure 4. CMFZ = the Casper Mountain fault zone and is placed between the north and south branches. CAT = the Casper arch fault zone. XX′ and YY′ mark intersections with longitudinal cross sections.

branches, segments, splays, and/or slivers (Figures 4, 5). Major displacements occur along two main branches of the fault zone, here described as the north and south branches. The south branch of the Casper Mountain fault zone can be identified at the surface along the central and eastern part of the Casper Mountain uplift, but in the area west of Speas Dome (T32N, R81W in Figures 4, 5), the fault zone is hidden by Quaternary deposits or shallow detachment structures or dies out before reaching the surface.

The north branch of the Casper Mountain fault zone trends nearly due east-west through its entire length and is not visible at the surface except locally at its intersection with the northwest-trending Emigrant Gap anticline near the Goose Egg stage stop (Figure 4B) in the northeast corner of T32N, R81W. West of the Emigrant Gap/Casper Mountain fault zone intersection, the north-branch fault is imaged on several seismic profiles and can be traced to its termination (tip line) in the footwall of the Iron Creek thrust in the NE1/4 of T32N, R82W. In the westward-expanding area between the north and south branches of the Casper Mountain fault zone, there is an approximately 4 mi (6.5 km)–long, west-plunging, low-relief, anticlinal fold, here called the Rasmus Lee nose (Figure 4; cross section AA′ in Figure 5).

The south branch of the Casper Mountain fault zone was penetrated in the Texaco 1 Government-Donely well in the SW1/4 NW1/4, Sec. 7, T32N, R78W, about 325 ft (100 m) south of the interpreted surface trace of the fault (cross section DD′ in Figure 5; Figure 6). Spudded in Precambrian at the surface, the well crossed the fault at about 575 ft (175 m), penetrated the top of the Madison horizon at about 1000 ft (300 m), and drilled into steeply dipping Madison carbonates to a total depth at 1940 ft (590 m). Projection of the surface trace of the fault through the interpreted fault cut in the well indicates a dip of about 50° to the south for this shallow part of the fault plane.

Possible confirmation of this fault-plane dip is supplied by data on a north-south seismic profile about 3 mi (3.8 km) west of the Texaco well (i.e., fine dotted line along the section line 34/35, T33N, R79W in Figure 4). There is an interpreted fault-plane reflection on this profile aligned with the surface trace of the south branch of the Casper Mountain fault zone. Depth migration of this reflection band using a velocity of 18,000 ft/s (5500 m/s) for Precambrian crystalline rocks shows a dip of about 50°. However, the migration velocity could be higher or lower than assumed, and the profile may not be exactly oriented in the true dip

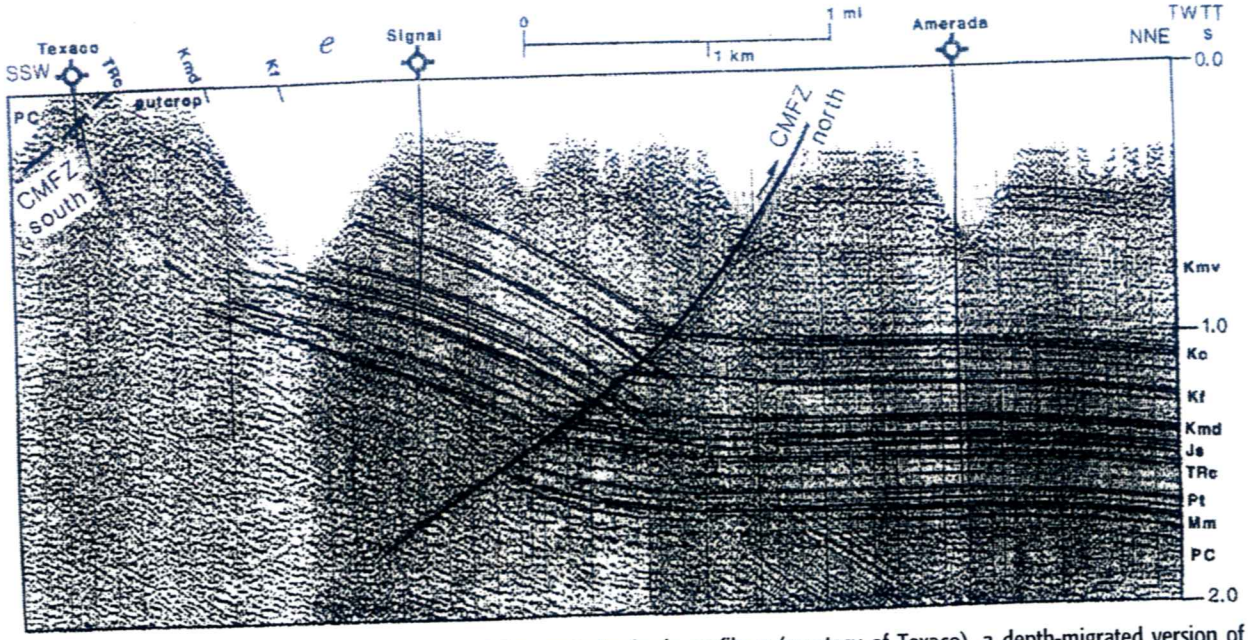

Figure 6. North-northeast–trending, unmigrated, interpreted seismic profile *e* (courtesy of Texaco), a depth-migrated version of which was used as a basis for the construction of part of structural cross section DD′ (Figure 5). The profile images the north-dipping block between the north and south branches of the Casper Mountain fault zone (CMFZ). The scale is approximately equal to 1:1. TWTT = two-way traveltime, in seconds, here and on all subsequent seismic profiles. The location is shown in Figure 4; formation symbols are identified in Figure 3.

direction. Therefore, a range of dips between 40 and 60° for the Casper Mountain fault zone (south branch) fault plane has been used in the cross sections (Figure 5). This range of fault dips for the Casper Mountain fault zone is consistent with the range suggested by hanging-wall and footwall fault cutoffs of depth-migrated reflections along either side of the fault zone on seismic profiles *a* and *b* (Figure 7).

Westward from the NE1/4 of T32N, R81W, vertical separation on the north branch of the Casper Mountain fault zone decreases as the displacement on the south branch locally increases. The ramp area of north- to northeast-striking outcrop between these two branches of the Casper Mountain fault zone is a fault relay (Ramsay and Huber, 1987; Groshong, 1999) where displacement is transferred from the north branch to the south branch of the Casper Mountain fault zone. The north branch is shown on most geologic maps (e.g., Sims, 1948; Wyoming Geological Association, 1965) as dying out westward along the south line of Sec. 2, T32N, R81W, but based on seismic control, the fault can be extended at least another 5 mi (8 km) to the west (Figure 4).

West of Bessemer Mountain in T32N, R81W (cross section BB′ in Figure 4), a straight, west-southwest–trending fault trace, which is shown on geologic maps (Faulkner, 1950; Wyoming Geological Association, 1965) as continuous with the south branch of the Casper Mountain fault zone, cuts the Frontier Formation with minimal vertical separation and dies out westward within Sec. 24, T32N, R82W (Figure 8A). However, this surface fault trace is not the south branch of the Casper Mountain fault zone but the trace of a small-displacement, north-dipping, detached back thrust, relatively up on the north, that overrides and covers the deeper south-branch fault (Figure 8B). In Figure 8C, a seismic profile across the southeastern plunge of the Iron Creek structure illustrates the geometry of the northwestern extension of this fault-bounded, detached pop-up structure. The south branch of the Casper Mountain fault zone is covered from this area southwestward to its intersection with the Casper arch thrust. Seismic control indicates that there is about 2500 to about 4000 ft (760–1200 m) of vertical separation on the Casper Mountain fault zone (on the Muddy and Madison horizons, respectively) within the hanging wall of the Casper arch thrust in Sec. 27/28, T32N, R82W (cross sections AA′, BB′ in Figure 5; Figure 7B).

The south branch of the Casper Mountain fault zone does not terminate at its intersection with the Casper arch thrust in the center of the south half of T32N, R82W (although the fault is blind here) but continues into the footwall of the Casper arch thrust and southwesterly across the southeastern arm of the Wind River basin. The strike of the Wind River basin segment of the Casper Mountain fault zone turns west-southwest through R82W, then more southwesterly into R83W for about 3 mi (5 km) to its nearly orthogonal cutoff at the North Granite Mountains fault zone (Figure 4).

Casper Arch Thrust

The Casper arch thrust is a regional, basement-involved, northwest-trending, northeast-dipping, basin-boundary fault zone. Along the Casper arch thrust, the hanging-wall Casper arch on the northeast is uplifted relative to the Wind River basin (Keefer, 1970; Gries, 1983; Skeen and Ray, 1983; Sprague, 1983; Ray and Berg, 1985; Thompson and Hill, 1986; Morse et al., 1987; Natali et al., 2000a, b). The southeastern tip line at the Muddy horizon (a branch line on the Madison horizon) of the Casper arch thrust is in T31N, R82W, where displacement is relayed to the Bates Creek thrust. The Casper arch thrust extends to the northwest for more than 65 mi (100 km) to its junction with, or transition into, the west-trending Owl Creek thrust in T39N, R89W. Fault dip ranges from perhaps 20 to 45° and is gently listric through the Phanerozoic section (cross sections AA′, BB′ in Figure 5). Maximum vertical separation on basement is at least 25,000 ft (7600 m) near the fault junction with the east-trending Owl Creek thrust but only about 1200 ft (360 m) on the Muddy horizon and about 2400 ft (730 m) on the Madison horizon southwest of Iron Creek in T32N, R82W (Figure 9). The Casper arch thrust is interpreted here to cut and offset the Casper Mountain fault zone (cross sections AA′, BB′ in Figure 5), dividing the Casper Mountain fault zone into the Casper Mountain and Wind River basin segments.

Other Regional Fault Zones

Along the southwest edge of Figure 4, the North Granite Mountain fault zone provides a convenient border for the structural contouring. This east-west zone of faulting extends for about 60 mi (97 km) to the west from its eastern tip in T31N, R81W (Love, 1970; Love and Christiansen, 1985; Schrader Flats, 1989). Significantly, several northwest-trending, Laramide, base-

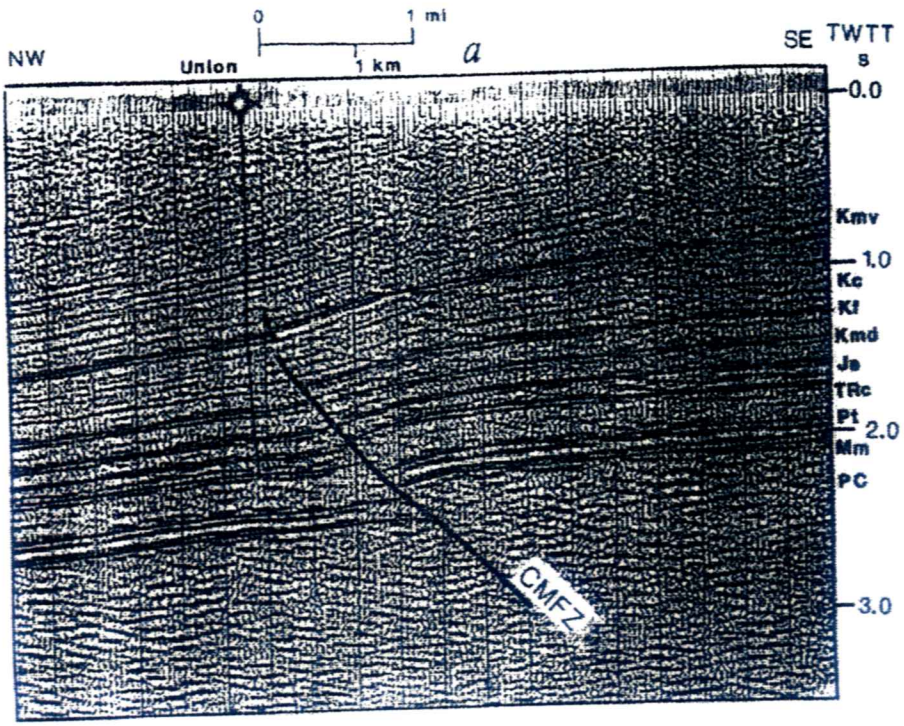

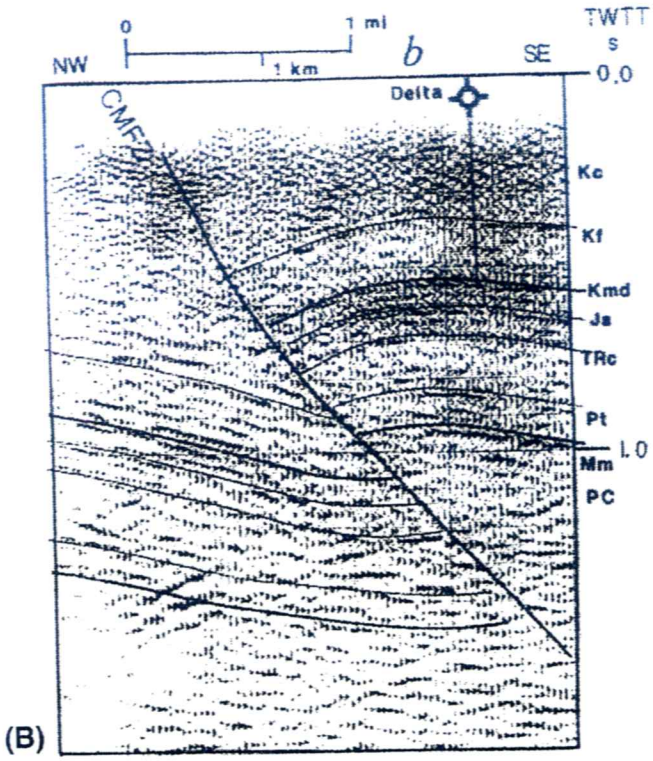

Figure 7. Northwest-southeast, time-migrated, interpreted seismic profiles across the south branch of the Casper Mountain fault zone showing fault dip of approximately 50°. The scales are approximately equal to 1:1. (A) Profile *a* (courtesy of Union Pacific Resources) transects the Wind River basin segment and images a basement-involved, faulted monocline. (B) Profile *b* (courtesy of Amalgamated Explorations Inc.) transects the Casper Mountain segment along the west plunge of the Casper Mountain uplift, just south of Iron Creek, and images a basement-involved, faulted-related anticline. Profile locations are shown in Figure 4; formation symbols are identified in Figure 3.

ment-involved, thrust-generated folds (Stone, 1993a) are abruptly terminated against the north side of the North Granite Mountain fault zone at a high angle in a manner similar to the fault/fold terminations along the north side of the Casper Mountain fault zone at Casper Mountain.

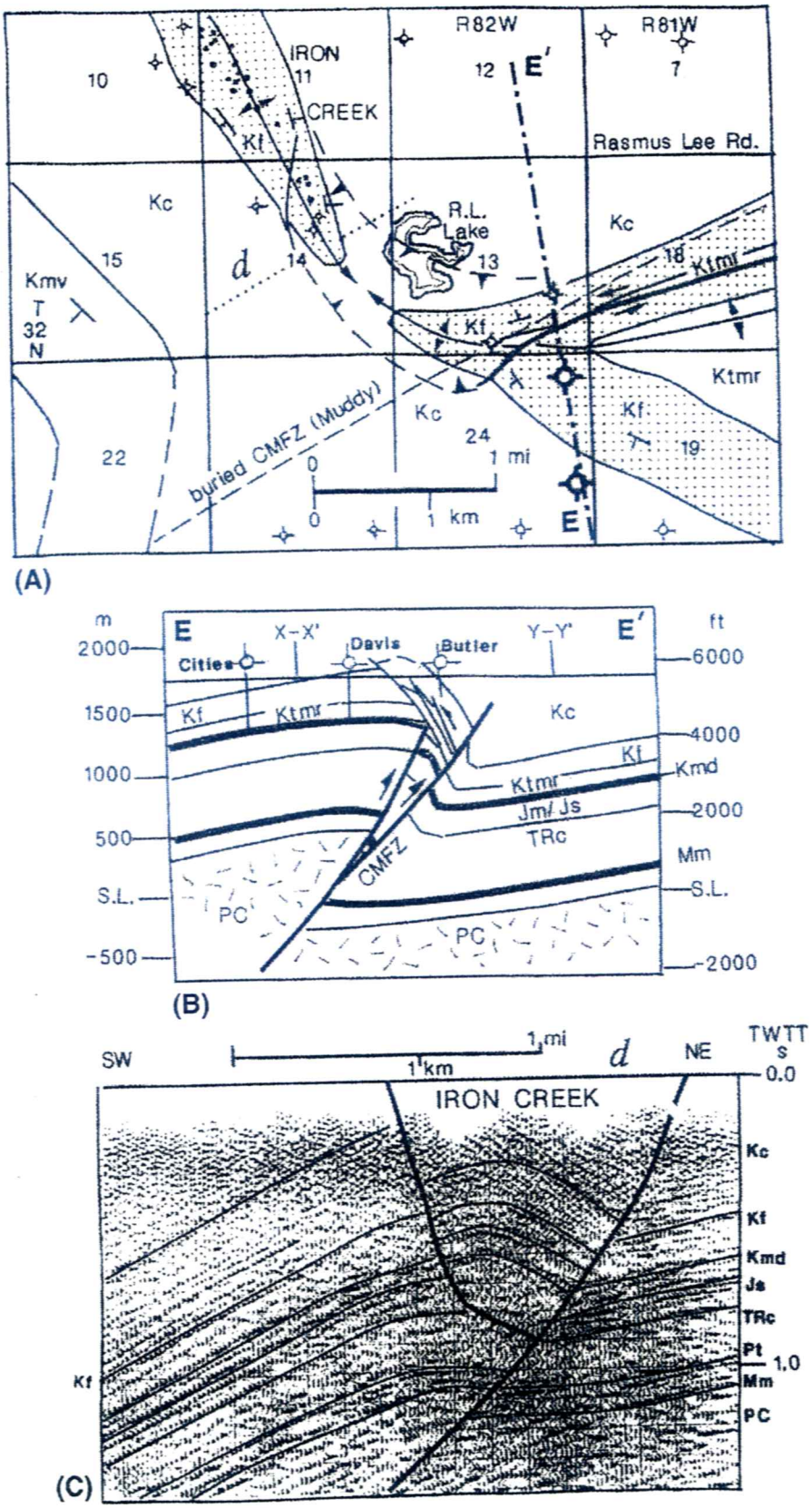

Figure 8. (A) Geologic map showing relationship between the south plunge of the Iron Creek anticline and the west plunge of the Casper Mountain fold axis. The dry-hole symbol below the Kf symbol in Sec. 13 is the Butler well discussed in the text. (B) North-south cross section EE′ in which the anomalous surface fault relationships along the west plunge of the Casper Mountain fold axis are interpreted as the result of shallow antithetic detachment thrusting above the Muddy Sandstone (Kmd). Formation symbols are identified in Figure 3; Ktmr = Thermopolis and Mowry shales (modified from Faulkner, 1950); XX′ and YY′ mark intersections of longitudinal cross sections in Figure 12. (C) Northeast-southwest, time-migrated, interpreted seismic profile *d* (courtesy of Amalgamated Explorations Inc.) across the southeast plunge of Iron Creek illustrating the geometry of the thrust-bordered, central pop-up structure. The scale is approximately equal to 1:1. The section and profile locations are indicated in Figure 4; formation symbols are identified in Figure 3.

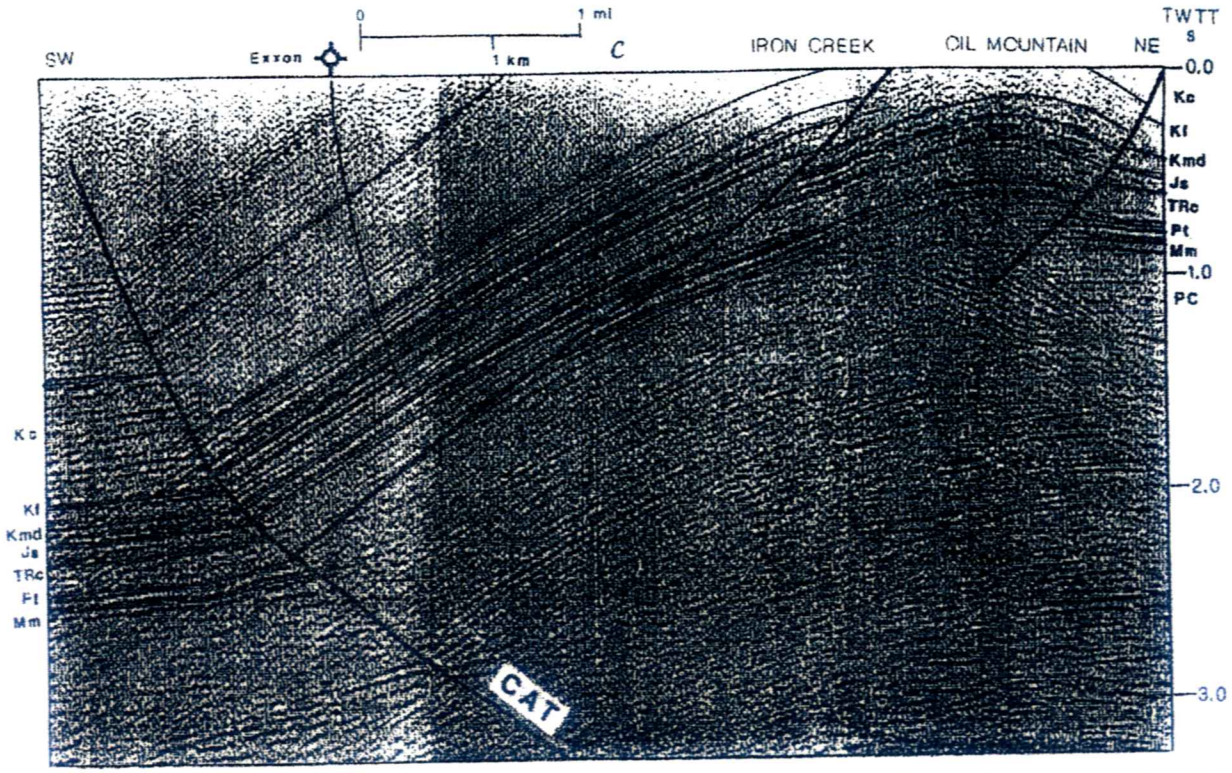

Figure 9. Northeast-southwest, unmigrated, interpreted seismic profile *c* (courtesy of Texaco) across the Casper arch thrust, the northwest plunge of the Iron Creek structure, and the southeast plunge of the Oil Mountain structure. The scale is approximately equal to 1:1. After depth migration, the southwest dip into the Casper arch thrust (CAT) is steepened, the overlap of hanging-wall and footwall data is eliminated, deep Paleozoic footwall (velocity pulled-up) data are pushed down, the CAT fault dip is increased, and fault displacement and listricity are reduced (cf. Figure 5). Also, dip on the Iron Creek and Oil Mountain thrusts is increased. The location is shown in Figure 4; formation symbols are identified in Figure 3.

The northeast-trending Muddy Mountain fault zone (Sears, 1948; Bergstrom, 1950; Schwarberg, 1959), also called the Corral Creek fault zone (Jenkins, 1950; Brown, 1975; Daniels, 1996) and shown on the Wyoming state geologic map (Love and Christiansen, 1985), forms the southeastern limit of the present structural contouring (Figure 4). The abrupt, high-angle, southward termination of the Corral Creek and Bodie north-northwest–trending, basement-involved, fault-related structures against the Muddy Mountain fault zone (Figure 2) also is analogous to the structural geometry along the north sides of the Casper Mountain and North Granite Mountain fault zones.

The Geochronologic Front

Peterman and Hildreth (1978) described an important east-west–trending Precambrian discontinuity, the geochronologic front (Chamberlain et al., 1993), that approximately follows a line joining the Muddy Mountain and the North Granite Mountain fault zones and extending west across the Granite Mountains to the southeastern end of the Wind River Range (PCGF in Figure 1). This geochronologic discontinuity separates Archean whole-rock and mineral radiometric ages of 2300 m.y. or older on the north from reset Proterozoic K-Ar and Rb-Sr ages of between 1400 and 1600 m.y. to the south. Peterman and Hildreth (1978) interpret the steep age gradients along this zone as the result of major vertical tectonics during the Proterozoic, when the southern block was uplifted several kilometers and cooled through the 300°C isotherm. Note that the Precambrian–Devonian unconformity (Figure 3) in this area spans at least 1.5 b.y., during which pre-Laramide tectonic movements (e.g., faulting and uplift) could have occurred along this east-west discontinuity. These observations are considered relevant to evaluation of the structural genesis of the Casper Mountain area.

CASPER MOUNTAIN UPLIFT

Central Precambrian Core

The Phanerozoic sedimentary cover has been eroded from the central part of the Casper Mountain uplift, exposing the Precambrian rocks in its core. Here there is considerable variety in Precambrian rock types, including gneiss, amphibolite, quartzite, serpentinite, metamorphosed ultramafic rocks, granite, pegmatite, and diabase. These rocks are part of the Wyoming (Archean) province. A radiometric age determination by Hills et al. (1968), using microcline and muscovite from pegmatite in the central part of the mountain, is reported as 2.5 ± 0.06 Ga.

Most important to this study, however, is the well-established easterly trending structural fabric within the Precambrian core of Casper Mountain. Foliations, lineations, small faults and folds, dikes, and some joint sets (Condie, 1969; Burford et al., 1979; Gable et al., 1988; Houston, 1993, sheet 1) within the Precambrian core all trend east to east-northeast. Also, several of the east-northeast–trending Precambrian faults in the core of the uplift have been traced into the Paleozoic outcrop, where small offsets indicate fault reactivation probably coeval with Laramide development of the Casper Mountain uplift/Casper Mountain fault zone (Gable et al., 1988). This pervasive east to east-northeast Precambrian fabric on Casper Mountain has been attributed to regional, high-grade, ductile Precambrian deformation (Gable et al., 1988) and is considered here to have controlled the trend of the Casper Mountain uplift during subsequent Laramide compressional deformation (also see Sears and Sims, 1954; Brown, 1975; Gable et al., 1988).

East Plunge

From the crest of the Casper Mountain uplift in the northwest corner of T32N, R79W, there is about 7000 ft (~2100 m) of east plunge that extends to the tips of the north and south branches (including a small, northeast-trending termination splay) of the Casper Mountain fault zone (Figure 4). The steepest area of east plunge occurs in Sec. 13, 14, and 15, T32N, R78W, where the north-northeast–trending Hat Six fault (Sears, 1948; Bergstrom, 1950; Burford, 1986b), a probable west-dipping reverse fault, cuts across the Casper Mountain fold axis and probably terminates on the north against the south branch of the Casper Mountain fault zone at the Precambrian level (Figure 4). East-trending seismic profile *f* (Figure 10), beginning just east of the Hat Six fault, images the terminal east plunge of the Casper Mountain uplift.

Of particular interest in the Casper Mountain uplift east-plunge area is the north-dipping fault block between the north and south branches of the Casper Mountain fault zone. This part of the north branch fault, not previously recognized in the literature, is evident on several north-south seismic profiles (e.g., profile *e* of Figure 6). The present interpretation is also constrained by limited surface geologic control and data from several boreholes drilled within the fault-bounded, north-dipping panel (cross section DD′ in Figure 5). Here the north branch fault separates low-dipping footwall beds from the steeply north-dipping hanging-wall beds in the block between the two Casper Mountain fault zone branches. Eastward attenuation of the displacement on the north and south branch faults in this area accompanies the easterly plunge-out of the Casper Mountain uplift.

West Plunge

The Casper Mountain uplift plunges more than 13,000 ft (3900 m) from its crest in the northwest corner of T32N, R79W through R80W and R81W and into the east half of R82W, where the structure is transected by the Casper arch thrust. The west dip along the Casper Mountain uplift plunge axis ranges from about 10° just west of Speas Dome (Figure 4) to greater than 30° near the Casper arch thrust, and there are more structural complexities in this area of west plunge than along the east plunge of the uplift. Seismic control images several southwest-dipping detachment thrusts, antithetic to the Casper arch thrust, that cut the Muddy horizon (Figure 4A); at least one of these displaces the Madison horizon (Figure 4B). Also, along the west plunge of the Casper Mountain uplift, there appears to be a small, east-dipping synthetic thrust at the Paleozoic–Precambrian level, which is northwest of, and nearly on trend with, the Bates Creek thrust.

Bates Creek is a fault-related, northwest-trending, anticlinal structure in the hanging wall of both the Casper Mountain fault zone and the Casper arch thrust (Figure 4); it provides a structural trap for a small oil accumulation in the Frontier Formation (Twiford, 1989). This basement-involved, thrust-generated fold (Stone, 1993a) trends northwest across T31N, R81W and dies out at the northern township line. The structure has a southwesterly vergence, and the causal thrust, which forms a branch line with the southeast-

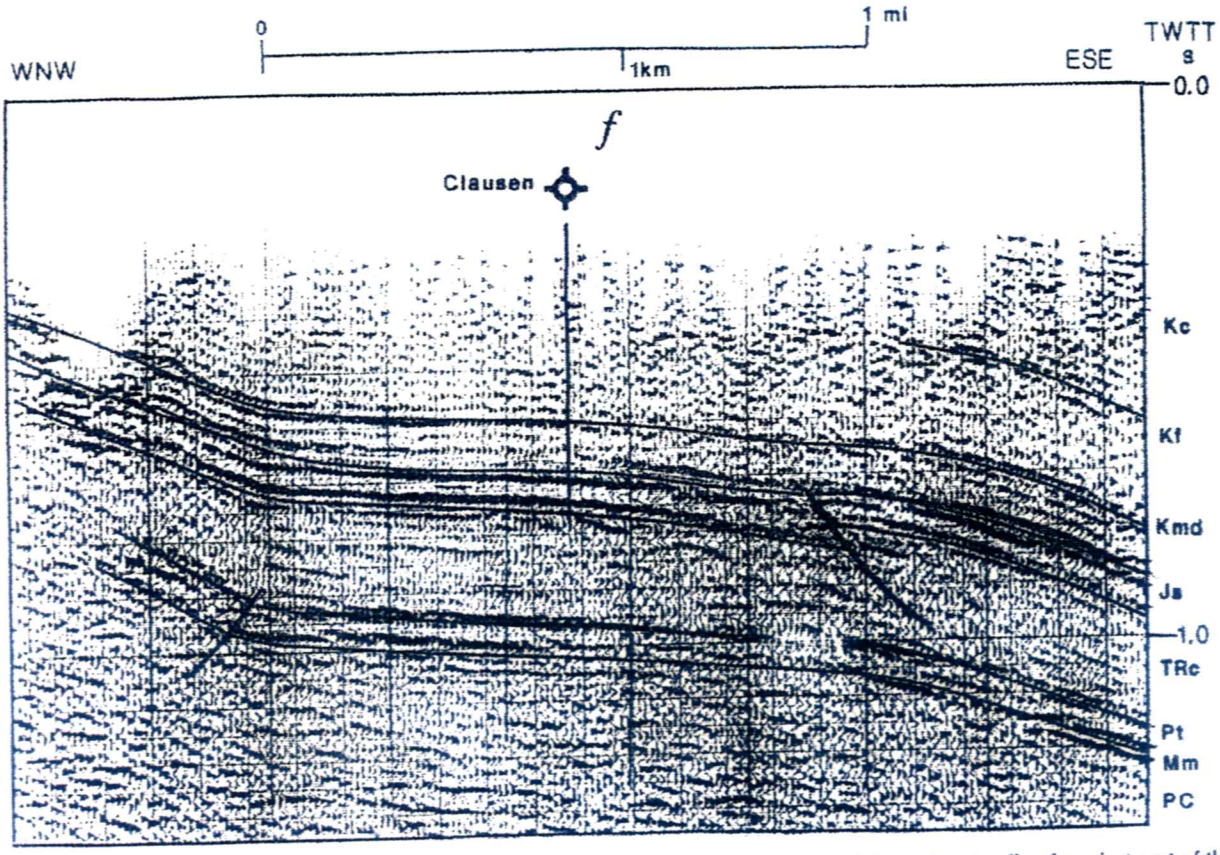

Figure 10. East-northeast–trending, unmigrated, interpreted seismic profile *f* (courtesy of Texaco), extending from just east of the Muddy Sandstone outcrop and Hat Six fault trace for about 2 mi (3.2 km) along the terminal east plunge of the Casper Mountain uplift. The scale is approximately equal to 1:1. The location is shown in Figure 4; formation symbols are identified in Figure 3.

erly attenuating Casper arch thrust at Paleozoic depths, has a vertical separation of from 3000 to 4000 ft (900 to 1200 m) on the mapped horizons.

In the western, footwall block of the Casper arch thrust, vertical separation along the Wind River basin segment of the Casper Mountain fault zone decreases to less than 1000 ft (<300 m) on the Madison horizon and less than 500 ft (<150 m) on the Muddy horizon near its cutoff line with the North Granite Mountain fault zone. The southwesterly plunging antiformal geometry of the hanging-wall Casper Mountain uplift, typical of the Casper Mountain segment, is no longer apparent. There is northwestward rotation of hanging-wall strata into the fault zone along the Wind River basin segment (Figure 7A), but the structure is monoclinal, with consistent northwest dip in both the hanging wall and footwall. Also, there is a gentle, northwest-southeast–trending, synformal cross trend—the Wind River basin axis—that is evident in both the hanging wall and footwall of the fault (Figure 4).

SUBSIDIARY FOOTWALL STRUCTURES

General

In the footwall of the Casper Mountain fault zone, there are three northwest-trending subsidiary structures that terminate to the south against the east-west Casper Mountain fault zone; these are the Emigrant Gap anticline, the Rasmus Lee nose, and the Iron Creek anticline.

Emigrant Gap Anticline

The southeastern termination of the Emigrant Gap anticline against the Casper Mountain fault zone (Figure 4) may be viewed along Highway 220 near the Goose Egg stage stop in the northwest corner of T32N, R80W (cf. Sears and Sims, 1954; Stiteler, 1954; Beck and Burford, 1985; Burford, 1986a). Burford (1986a) thought the Emigrant Gap anticline was

rootless, but seismic data show clearly that the structure is a typical, Laramide, basement-involved, thrust-generated fold (Stone, 1993a) with a southwesterly vergence (see the seismic profile in Thompson and Hill [1986] or Hennings et al. [2000]).

The Emigrant Gap anticline trends northwest and extends for at least 20 mi (32 km) from its southeastern termination at the Casper Mountain fault zone. A small central closure in T33N, R81W has been repeatedly tested to the Pennsylvanian Tensleep objective without success. Based on seismic control, vertical separation on the causal thrust is about 3000 ft (900 m) on Precambrian basement (Figure 4; cross sections AA′, BB′ in Figure 5). Small-displacement, low-angle, longitudinal, synthetic and antithetic detachment thrusts also have been mapped at the surface (Beck and Burford, 1985), cutting Mesozoic strata along both limbs of the anticline near the Emigrant Gap/Casper Mountain fault zone intersection; there may be a small back thrust cutting the Madison horizon and possibly detached above basement (cross sections AA′, BB′ in Figure 5).

The axial trace of the Emigrant Gap anticline forms an angle of about 60° with the traces of the north and south branches of the Casper Mountain fault zone near the SW1/4, Sec. 6, T32N, R80W (Figures 2A, 4A). Just to the west of this fault/fold intersection is the ramp area of displacement relay from the north branch to the south branch of the Casper Mountain fault zone. Although the Emigrant Gap anticlinal trend does not continue into the hanging wall of the Casper Mountain fault zone, the Emigrant Gap and Casper Mountain structures involve the same Mesozoic strata in contractional deformation, implying essentially concurrent Laramide development.

Rasmus Lee Nose

About 4 mi (6.4 km) west of the Emigrant Gap intersection with the Casper Mountain fault zone, between the north and south branches of the Casper Mountain fault zone, is a west-plunging, fault-related fold named the Rasmus Lee nose (after Rasmus Lee Lake and Rasmus Lee Road). Seismic and borehole data control the mapping of this structure (Figure 4), as there is little surface evidence of its presence. The Rasmus Lee nose and related north branch of the Casper Mountain fault zone trend west through Sec. 9, 8, and 7, T32N, R81W and into Sec. 12 and 13, T32N, R82W, so that the north-branch fault forms a tip line in the footwall of the Iron Creek thrust.

The Rasmus Lee fold axis appears to turn toward the southeast in Sec. 9, T32N, R81W and terminate against the south branch of the Casper Mountain fault zone. In the hanging wall of the south branch of the Casper Mountain fault zone, directly opposite the footwall cutoff of the southeast-trending Rasmus Lee fold axis, is a small structural closure along the west-plunging Casper Mountain fold axis mapped in the Goose Egg outcrop and called the Speas (or Goose Egg) Dome (Figure 4; cross section BB′ in Figure 5). Two wells were drilled on this dome to a shallow Madison Formation objective (penetrated at 650 and 800 ft [200 and 240 m], respectively), without commercial success.

It may be significant that the subtle change in trend of the Rasmus Lee fold axis from east to southeast in the footwall of the Casper Mountain fault zone south branch occurs directly opposite Speas Dome in the hanging wall. This relationship suggests that late-stage cross folding along the south end of the Rasmus Lee nose affected the Casper Mountain footwall and hanging wall together and without significant lateral offset along the Casper Mountain fault zone.

Iron Creek Anticline

Like the Emigrant Gap anticline, the Iron Creek anticline is a Laramide, basement-involved, thrust-generated fold trending northwest (Figures 2, 4). However, the structure is asymmetric to the northeast, directionally apposing the southwest-vergent Emigrant Gap anticline. The Iron Creek anticline has an approximately 2 mi (3.2 km)–long, southwest-dipping (~30–45°) backlimb, rotated into its cutoff at the Casper arch thrust, and a short, steeply dipping (locally overturned) forelimb (cross section AA′ in Figure 5). As the structure is antithetic to the Casper arch thrust, it is considered a back thrust that probably developed as an adjustment mechanism required by the so-called space problem created during rotational movement of the Casper arch hanging wall through a listric thrust surface (cf. Stone, 1993a, figure 24). Structural closure at Iron Creek provides a trap for a small oil field with production from Cretaceous Frontier, Muddy, and Lakota sandstones (Dahill, 1989).

The Iron Creek anticline, like the Emigrant Gap anticline, does not have a northwest-trending counterpart in the hanging-wall block of the Casper Mountain fault zone. Instead, the southeast-plunging Iron Creek fold axis exposed in the sandstone outcrops of the Frontier Formation (Sec. 14, T32N, R82W) bends

easterly from the southeastern plunge of Iron Creek, through a half-mile–wide (0.8 m–wide), covered, low saddle area along the west side of Rasmus Lee Lake to join smoothly with the Frontier outcrop of the west plunge of the Casper Mountain fold trend in Sec. 13, T32N, R82W (Figure 8A). Apparently, no significant intervening fault separates the adjacent, folded Frontier outcrops along the crest line. However, seismic control (Figure 7B) shows that there is about 2000 ft (600 m) of vertical separation along this part of the south branch of the Casper Mountain fault zone at depth (Figure 4), hidden beneath the Frontier outcrop.

Based on seismic control, the Muddy datum is carried around this bend in a fault-bordered pop-up structure extending from the southeast plunge of Iron Creek and dragged laterally into the south branch of the Casper Mountain fault zone (Figure 8). The southwest-striking fault trace cutting the north-dipping Frontier Formation outcrop along the west plunge of the Casper Mountain fold axis is interpreted here as a shallow, internally complex, antithetic thrust block, detached above the Muddy horizon and hiding the deeper structure (Figure 8B). The Butler well, SE1/4 SE1/4 SW1/4, Sec. 13, was drilled to a depth of 1220 ft (372 m) in this thrust block and encountered the top of the Mowry Shale three times because of thrust repetition. The north side of this surface fault is upthrown, with Mowry and Thermopolis formations on the north against Frontier on the south. Faulkner (1950) suggested a component of left slip on the fault with displacement arrows.

Structural relationships in this area are important because they indicate a close kinematic and temporal interaction between the northwest-southeast–trending Iron Creek and the east-west–trending Casper Mountain fold axes, both of which were generated by Laramide compressional deformation.

CASPER ARCH THRUST /CASPER MOUNTAIN FAULT ZONE INTERSECTION

About 3 mi (5 km) southwest of the Iron Creek/Casper Mountain fault zone intersection (in Sec. 27 and 28, T32N, R82W), the Casper Mountain fault zone (south branch) and Casper arch thrust intersect at nearly right angles (Figures 2B, 4). Several northeast-trending, fault-parallel seismic profiles along either side of the Casper Mountain fault zone in this area were available for this study, but these data do not provide enough control to accurately resolve the details of the structure at this complex fault intersection. Nevertheless, the fault intersection shown on the two structural contour maps (Figure 4) has been contoured to conform to the interpretation that the Casper arch thrust is the younger fault and cuts and offsets the Casper Mountain fault zone. The rationale for this interpretation is as follows.

The Casper Mountain fault zone does not terminate at the Casper arch thrust, as shown on some regional maps (e.g., Keefer, 1970; Gries, 1983; Blackstone, 1993; Hennings et al., 2000), but extends into and across the southeastern arm of the Wind River basin. This conclusion is based primarily on the clear fault evidence seen on the northwest-trending seismic profile *a* (Figure 7A) and constraints on fault strike by other seismic profiles in this area (Figure 4). Note that here the Casper Mountain fault zone is blind, that is, the fault emerges from basement and dies out upward within the Cretaceous section. Vertical separation on the Madison horizon along this segment of the fault zone decreases from about 2000 ft (600 m) in the immediate Casper arch thrust footwall area to about 750 ft (230 m) near its intersection with the North Granite Mountain fault zone (Figure 4B). On the Muddy horizon, corresponding vertical separations are about 1000 ft (300 m) and only a few hundred feet (<100 m), respectively (Figure 4A).

Note that the structure associated with the Wind River basin segment of the Casper Mountain fault zone can be described as a north-dipping, faulted monocline, which is significantly different from the Casper Mountain segment of the Casper Mountain fault zone in the hanging wall of the Casper arch thrust. Geometric comparison of these two fault segments suggests that early Laramide movements along the entire length of the Casper Mountain fault zone, before development of the Casper arch thrust, may have been like that displayed along the Wind River basin segment and that the major uplift and fault-related folding on the Casper Mountain segment represent a later phase of Laramide uplift that accompanied later incremental displacement on the Casper arch thrust. Clearly, fault slip along the Casper arch thrust, basinward rotation of the Casper arch hanging wall, and generation of the Iron Creek and Oil Mountain antithetic structures are kinematically and temporally related contractional events (cf. Figure 9).

A three-dimensional sketch of the Casper Mountain fault zone/Casper arch thrust intersection at the Paleozoic level (Figure 11) illustrates the present interpretation. In Figure 11, the Casper arch thrust (the

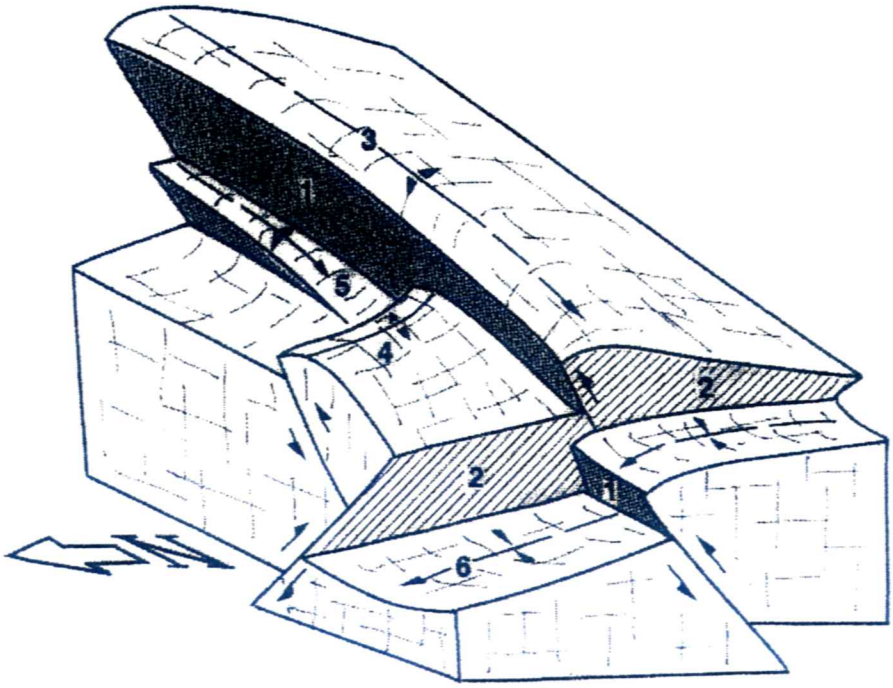

Figure 11. Three-dimensional sketch of the intersection of the Casper Mountain fault zone (south branch) with the Casper arch thrust showing the Casper arch thrust as the younger fault offsetting the Casper Mountain fault zone. 1 = Casper Mountain fault zone; 2 = Casper arch thrust; 3 = Casper Mountain uplift; 4 = Iron Creek anticline and back thrust; 5 = Rasmus Lee nose; 6 = Wind River basin axis.

younger of the two faults) cuts and offsets the Casper Mountain fault zone. Consequently, the easterly offset of the trace of the Casper arch thrust at the fault intersection shown on the Muddy and Madison structural contour maps (Figure 4) results from the structurally deeper intersection of these contour horizons with the easterly dipping Casper arch thrust plane in the footwall block of the Casper Mountain fault zone. In contrast, only a (postulated) small lateral offset of the Casper Mountain fault zone at the Casper arch thrust is shown on the two contour maps, although there is a considerable vertical offset of the Casper Mountain fault zone by the Casper arch thrust. This is because this fault intersection is essentially orthogonal, and slip on the Casper arch thrust is assumed to be in the (southwesterly) dip direction, so that differences in structural elevation would not change the placement of the Casper Mountain fault trace on a structural contour map.

KINEMATIC GENESIS

General

As a Laramide feature, the Casper Mountain uplift has been considered anomalous because it trends east-west within a foreland province dominated by northwest-trending Laramide structures. Regional horizontal compressive stress (σ_1) in the central Rocky Mountain foreland during the Laramide orogeny must have been generally oriented northeast-southwest, normal to the dominant northwest-southeast fault/fold trend. Why then did the Casper Mountain uplift and the causal Casper Mountain fault zone develop with an east-west trend and at a significant angle to the dominant northwest-trending anticlines on the Casper arch (Figure 2)?

According to Sears and Sims (1954, p. 31), "limited evidence indicates that the Casper Mountain anticline was formed along an east-west fault of pre-Cambrian [sic] age." There is no substantive reason to challenge this surmise 46 years later. The documentation of a pervasive east to east-northeast grain in Precambrian exposures, not only in the core of Casper Mountain but also in most other exposed Precambrian rock masses in southeastern Wyoming (Condie, 1969; Gable et al., 1988; Houston, 1993), adds strength to this concept. It seems unlikely that a major, east-west–trending, basement-involved, fault-related contractional structure of the size and importance of the Casper Mountain uplift would be initially generated (neoformed) in a homogeneous crust under northeast-southwest–directed Laramide compression. Therefore, it is proposed here that a preexisting mechanical anisotropy (e.g., shear zone?) at Casper Mountain provided a root zone of weakness along

which there was fault reactivation under Laramide compression. The Casper Mountain uplift developed in association with progressive growth of the Casper Mountain fault zone, which nucleated in basement and propagated upward into the Phanerozoic cover rocks. According to this interpretation, the east-west Casper Mountain uplift/Casper Mountain fault zone and the northwest-trending Emigrant Gap, Oil Mountain/Iron Creek, and other Laramide, basement-involved, thrust-generated folds on the Casper arch are regarded as essentially coeval Laramide compressional structures. This concept is in agreement with the statement of Dickinson et al. (1988, p. 1036) that in the central Rocky Mountain region, "the intricate geometry of Laramide uplifts and basins with diverse structural trends probably developed jointly within a complex but generally synchronous strain field imposed across a region of varied crustal architecture."

East-West Shortening along the Casper Mountain Fault Zone

To check on the differential, east-west shortening along either side of the Casper Mountain fault zone, fault-parallel, longitudinal structural cross sections XX′ and YY′ were constructed (see Figure 4 for locations) and are superimposed in Figure 12. This figure illustrates the contrast between the geometry of the structure along the footwall and along the hanging wall of the Casper Mountain fault zone and allows a rough measurement of relative fault-parallel shortening. Note that the vertical separation shown between the Muddy/Madison horizons in the hanging-wall section XX′ and in the footwall section YY′ is not entirely attributable to slip on the Casper Mountain fault zone, as the elevation drop across the zone is distributed through the north and south branches and the vertically rotated, north-dipping panel between them (cross sections BB′, CC′, DD′ in Figure 5).

East-west shortening in the northern, footwall block of the Casper Mountain fault zone occurs on comparatively smaller scale, basement-involved, thrust-generated folds oriented obliquely to the regionally throughgoing fault zone. In the southern, hanging-wall block, however, shortening occurs over a single broad arch or vaulted slab over which there is only minor internal deformation expressed in the form of numerous, small-displacement, mostly northeast-trending faults (too small to show in Figure 4) (see Gable et al., 1988). Shortening measured between the southwestern cutoff at the North Granite Mountain fault zone and the eastern tip line of the Casper Mountain fault zone along the two 39 mi (62.5 km)–long, longitudinal cross sections is about 8400 ft (~2560 m) or 4.1% in the footwall and about 5600 ft (~1700 m) or 2.7% in the hanging wall. Thus, the shortening differential of about 2800 ft (~850 m) is only about 1.4%. This difference in shortening is interpreted as reflecting a small component of strike slip along the Casper Mountain fault zone. Although there are no true piercing points available for measurement, it is assumed here that strike slip would have been sinistral under regional northeast-southwest Laramide transpression (Stone, 1969; Molzer and Erslev, 1995). A sinistral sense of lateral slip is reflected in the angle of intersection of the Emigrant Gap anticline with the Casper Mountain fault zone (Figure 4) and also at the Iron Creek/Casper Mountain fault zone intersection where the southeasterly plunging Iron Creek fold axis in the Frontier Formation outcrop curves smoothly into the

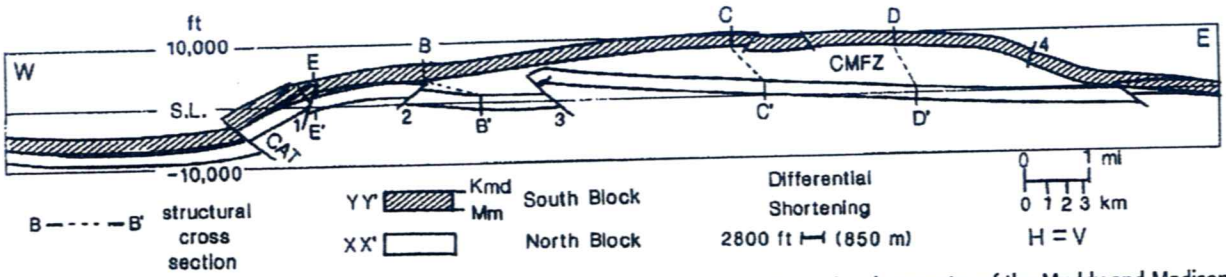

Figure 12. Near-parallel, longitudinal structural cross sections showing the two-dimensional geometry of the Muddy and Madison horizons along the hanging wall (XX′) and footwall (YY′) of the Casper Mountain fault zone. The figure illustrates the difference in east-west deformational geometry along either side of the fault zone and provides a basis for comparison of relative fault-parallel shortening. Connected vertical lines with capital letters mark intersections with the structural cross sections of Figures 5 and 8B. Numbered faults: 1 = Iron Creek thrust; 2 = Rasmus Lee fault; 3 = Emigrant Gap thrust; 4 = Hat Six fault. Section locations are shown on Figure 4; formation symbols are identified in Figure 3.

west-plunging axis of the Casper Mountain uplift (Figure 8A). A sinistral slip component on the Casper Mountain fault zone is also suggested by the sense of the basculation along the zone. Along the Casper Mountain fault zone, from Emigrant Gap to Iron Creek, there is greater local east-west contraction in the footwall block than in the hanging-wall block, whereas along the east plunge of the Casper Mountain uplift, there is greater local east-west contraction in the hanging-wall block than in the adjacent footwall block (Figures 4, 10). This fault geometry is consistent with some sinistral slip. However, along the west plunge of the Casper Mountain uplift west of Iron creek, seismic control indicates that the magnitude of westerly dip along the hanging-wall and footwall sides of the Casper Mountain fault zone (south branch) is approximately the same, that is, there is no basculation (differential shortening); therefore, any lateral slip component along this part of the Casper Mountain fault zone must be very small. Similarly, there appears to be little or no sinistral slip component along the Wind River segment of the Casper Mountain fault zone.

In the north-south direction (normal to the Casper Mountain fault zone), shortening near the middle of the Casper Mountain segment of the fault zone (cross section CC′ in Figure 5) is about 4700 ft (1430 m), measured across a section length of 12.5 mi (20 km). The restored section length is 13.4 mi (21.5 km), and the north-south shortening is about 6.6%. However, percentage shortening here is not comparable with that along XX′ and YY′, as section lengths are not the same. Comparison of the measured differential shortening along XX′/YY′ with the measured shortening in the north-south fault-dip direction suggests that net slip on the Casper Mountain fault zone is left-oblique, with the dip-slip component exceeding the strike-slip component by a factor of about 1.7. Proposals for much larger sinistral slips along the Casper Mountain fault zone by Daniels (1996) are based on the use of invalid piercing points.

Incremental Displacement on the Casper Mountain Fault Zone?

In Figure 12, the broadly arched, longitudinal geometry of the Casper Mountain uplift, its locally steep east plunge in the Hat Six area (Figures 4, 10), and its steep west plunge (expressed as strong southwesterly rotation into the Casper arch thrust) contrast with the low-relief folding and blind, smaller displacement faulting along the Wind River basin segment of the Casper Mountain fault zone. This difference in the geometry, fold intensity, and magnitude of slip along the Casper Mountain fault zone, from hanging wall to footwall of the Casper arch thrust, is interpreted as an indication that the Casper Mountain and Wind River basin segments of the Casper Mountain fault zone had disparate developmental histories. The data suggest that there was an early phase of incremental fault slip, characterized by the geometry of the Wind River basin segment (before basinward tilting), but which occurred along the entire length of the Casper Mountain fault zone. This early deformational episode produced only part of the total fault displacement now recorded along the Casper Mountain segment of the fault zone. Then a later phase of Laramide arching occurred concurrently with slip on the Casper arch thrust, involving only the Casper Mountain segment, that is, limited to the hanging wall of the Casper arch thrust. Because southwestward rotation into the Casper arch thrust is apparently the same along (immediate) hanging-wall and footwall blocks of the Casper Mountain fault zone, however, the implication is that both blocks moved together in response to dip slip on the Casper arch thrust, and the Casper arch thrust was not offset by the Casper Mountain fault zone. This concept is consistent with a relatively small strike-slip component on the Casper Mountain fault zone, concentrated along the Iron Creek–Emigrant Gap part of the zone.

DYNAMIC INTERPRETATION

Background

Two contrasting notions about Laramide dynamics have evolved from efforts to rationalize the nature of the horizontal stresses that produced the contrasting trends of contractual fault-related structures in the central Rocky Mountain foreland. The challenge is to develop an explanation for the apparent simultaneous, side-by-side formation of independent structures of northwest-southeast and east-west trend. Gries (1983) proposed a sequential counterclockwise rotation of the regional horizontal stress field from northeast-southwest to north-south during a late stage of Laramide contraction. In the model presented here, however, temporal control is not required, as the northwest-southeast–trending structures originated as plain-strain (dip-slip) features under fault-normal, Laramide maximum horizontal stress (σ_1), whereas the east-west uplifts developed coevally by oblique-slip reactivation

along existing anisotropies in the Precambrian basement (cf. Beckwith, 1941; Hoppin et al., 1965; Stone, 1969, 1986, 1993b; Brown, 1975, 1987, 1988; Dickinson et al., 1988; Blundell and Marrs, 1991; Molzer and Erslev, 1995; Schmidt et al., 1996; Marshak et al., 2000).

Beck and Burford (1985) concluded that Laramide σ_1 at the Emigrant Gap anticline was northeast-southwest and horizontal and at Casper Mountain, north-south and horizontal, followed in both cases by rotation to vertical. These conclusions were based primarily on dynamic interpretation of Laramide joint sets, small fault offsets, and the trend of small secondary folds. Using the iterative method of Angelier (1984, 1989), Varga (1993) analyzed 28 minor faults and their striae within the Precambrian exposures on Casper Mountain and derived a σ_1 direction of 348°. (They interpreted this finding as Laramide, but might it be Precambrian[?].) Mozler and Erslev (1995) analyzed fault orientation, conjugate fault geometry, and slickenline data for 254 minor faults in the Fremont Canyon Sandstone and Madison Limestone outcrops in the central area of Casper Mountain. They concluded that Laramide σ_1 was applied in single-stage, northeast-southwest horizontal compression (ranging from N18°E to N68°E) and proposed that slip on the Casper Mountain fault zone was reverse left-oblique; they did not suggest a slip magnitude.

Paleostress Interpretation

Based on stress measurements in deep boreholes, it has been reported that the direction of maximum horizontal stress around the dextral San Andreas fault zone in central California is currently nearly normal to the fault zone (Mount and Suppe, 1987; Zoback et al., 1987). Since this revelation, there has been a significant change in ideas about stress distribution around regional-scale faults. It has been observed that regional stress fields may be locally perturbed toward orthogonal to some fault zones and other macrostructures, particularly around those structures with crustal ancestry.

For example, based on statistical analysis of tectonic stylolite teeth in the Big Bend region of Texas, Erdlac (1994) showed that Laramide σ_1 stress trajectories were locally rotated counterclockwise through an angle of about 31° (from a mean of N58°E) to become nearly normal to the west-northwest–trending Terlingua uplift. He concluded that this curvature of stress trajectories results "from contemporaneously developed structures which locally altered the shape of the field" (Erdlac, 1994, p. 165). Applying this fundamental concept to the current problem, it is hypothesized here that a perturbation of Laramide σ_1 paleostress trajectories occurred around the reactivated Casper Mountain fault zone and related east-west–trending anticlinal uplift, so that σ_1 was diverted locally from a mean northeast-southwest far-field orientation to near north-south (Figure 13). This concept is consistent with the conclusion that lateral slip along the Casper Mountain fault zone was minimal, because without fault-normal reorientation the acute (ψ) angle between the applied northeast-southwest regional σ_1 horizontal stress and the east-west Casper Mountain fault zone would be expected to produce a relatively greater component of sinistral slip than of dip slip (expressed as important differential longitudinal shortening).

Possible confirmation of this hypothesis may be drawn from the study of joints. It has been shown that extension joints grow perpendicular to a minimum principal stress (σ_3) and parallel to the maximum principal stress (e.g., Engelder and Geiser, 1980; Dyer, 1988; Lorenz et al., 1991) and therefore may be used as paleostress markers in those cases where the time of joint formation relative to that of related structures is well established. For example, from a study of joints in Lias of Great Britain, Rawnsley et al. (1992) concluded that propagating joints curve to follow the direction of stress-field trajectories and can reflect perturbation or regional stress fields around faults.

At Casper Mountain, the proposed local reorientation of Laramide σ_1 stress trajectories around the Casper Mountain fault zone is consistent with the orientation of the prominent joint systems I (horizontal) and II (vertical) identified in the Precambrian core of Casper Mountain by Gable et al. (1988) and interpreted to be of Laramide origin (Figure 14). Both systems crosscut rotated joint system III, interpreted by Gable et al. (1988) as probably of Precambrian origin. Joint sets normal to the axes of fault-related folds at Emigrant Gap (Beck and Burford, 1985) and Iron Creek/Oil Mountain (set J_2 of Hennings et al. [2000]) are also consistent with the illustrated fault-normal orientation of the stress trajectories around these fault/fold structures (Figure 13).

Strain Partitioning

There is a growing awareness that compressive structures of different orientations may develop together through a mechanism referred to as strain partitioning

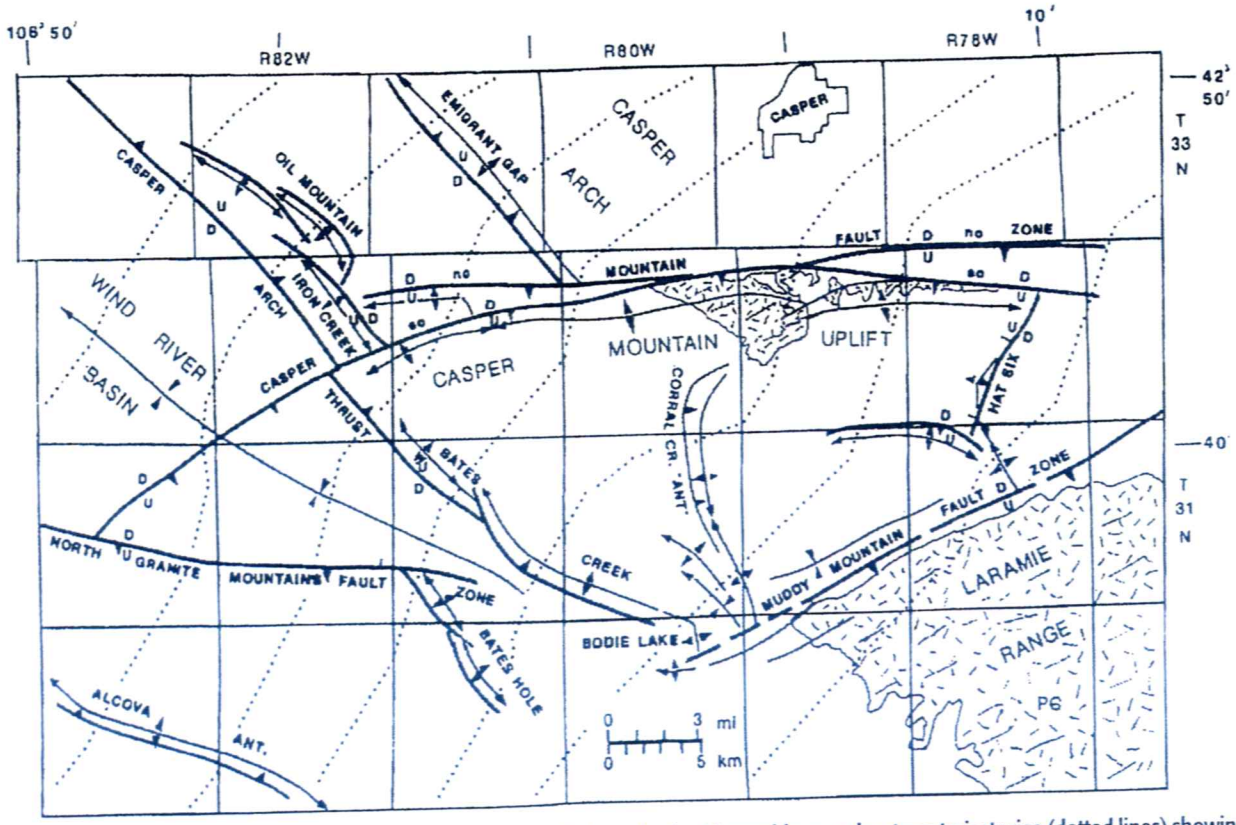

Figure 13. Tectonic map of the Casper Mountain area with hypothesized Laramide σ_1 paleostress trajectories (dotted lines) showing local perturbation to near fault-normal orientations around the Casper Mountain fault zone.

(e.g., Lettis and Hanson, 1991; Varga, 1993; Tikoff and Teyssier, 1994; McNulty et al., 1998; Miller, 1998; Tavarnelli and Holdsworth, 1999). According to this concept, complex strain patterns around regional faults may be explained by partitioning of deformation into fault-normal and fault-parallel shortening, simultaneously expressed as thrust and strike-slip or oblique-slip faults and related folds. Moreover, Tavarnelli and Holdsworth (1999) have pointed out that reactivation of preexisting structural anisotropy can be important in the partitioning process. This idea is relevant to this discussion because the east-west–trending Casper Mountain uplift/Casper Mountain fault zone and northwest-trending Emigrant Gap, Iron Creek, and Casper arch thrust structures appear to have developed together in Laramide contraction, influenced importantly by the reactivation of a preexisting Precambrian zone of weakness at Casper Mountain. A comparable evolutionary sequence has been proposed for the east-west–trending Uinta Mountain uplift, where well-defined, Proterozoic, rift-boundary, extensional faults have been reactivated and inverted to become mountain-flank (basin-boundary) left-oblique-slip thrusts under Laramide contraction (Bryant, 1985; Stone, 1993b). Marshak et al. (2000) have applied a similar inversion hypothesis to the entire Rocky Mountain–Colorado Plateau province.

SUMMARY AND CONCLUSION

Casper Mountain is a major east-west–trending, basement-cored, fault-related, doubly plunging, Laramide anticlinal uplift. The morphology of the whole Casper Mountain complex and subsidiary structures displayed in the structural contour maps (Figure 4) and the series of structural cross sections (Figure 5) provides a basis for evaluation of the development of the fault zone and the related uplift and places constraints on concepts of its kinematic and dynamic genesis.

The east-west trend of Casper Mountain is attributed to the influence of the preexisting fabric in the Archean core of the range. I propose that the Casper Mountain fault zone and related Casper Mountain up-

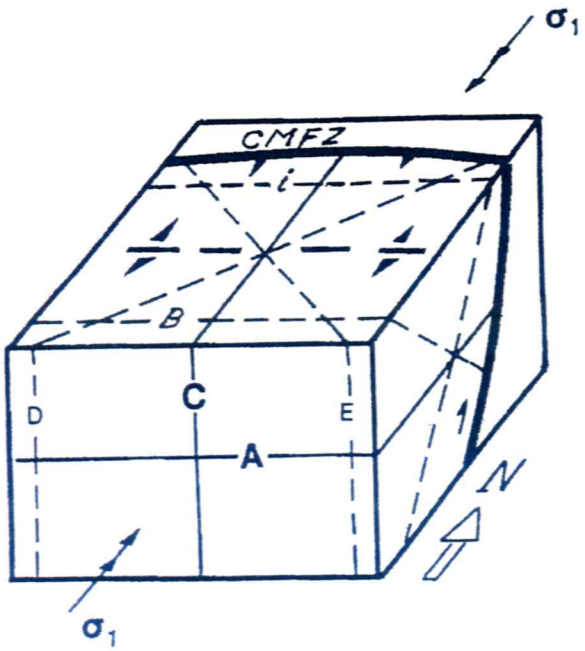

Figure 14. Block diagram of interpreted Laramide joint sets in system I (horizontal) and II (vertical) identified in the Precambrian outcrop at Casper Mountain by Gable et al. (1988). System I includes the complimentary sets B and i, bisected by extensional set A. System II includes the complimentary sets D and E, bisected by the extensional set C. Both sets crosscut joint system III (not shown), interpreted as a rotated Precambrian system (Gable et al., 1988). The north-south orientation of systems I and II is consistent with the proposed, locally perturbed, Laramide axis of maximum principal stress σ_1 (horizontal) at Casper Mountain. Note that the minimum principal stress axis, σ_3, would be perpendicular to σ_1 and horizontal for system I but vertical for system II. CMFZ = Casper Mountain fault zone.

lift developed along an existing Precambrian structure that was reactivated under Laramide contraction. This concept probably also can be applied to other east-west mountain ranges in the Rocky Mountain foreland province (e.g., Uinta Mountains, Owl Creek Mountains, Granite Mountains). An existing basement anisotropy localized perturbation of far-field northeast-southwest, Laramide maximum horizontal stress (σ_1) into nearly fault-normal application along the length of the Casper Mountain fault zone. (Note: Questions about the strength of fault zones in the case of locally reoriented stress are still being debated. Although the San Andreas fault in central California has long been interpreted as a weak [low-heat, frictionless] fault zone [Brune et al., 1969; Lachenbruch and Sass, 1980, 1992], this concept is rejected by Miller [1988] and Scholz [2000].)

Measurement of differential, fault-parallel shortening along either side of the Casper Mountain fault zone suggests that slip on the zone was left-oblique, with the dip-slip component nearly twice the strike-slip component. In the footwall of the Casper Mountain fault zone (Casper Mountain segment), shortening parallel to fault strike occurred primarily on northwest-trending, basement-involved, thrust-generated folds (i.e., the Emigrant Gap and Iron Creek anticlines), whereas in the hanging wall, the east-west–trending Casper Mountain block was shortened longitudinally as a single, broad arch. Along the Wind River basin segment of the Casper Mountain fault zone, the geometry of the structure suggests that there was little or no differential shortening along fault strike.

Consequently, I propose that early Laramide displacement on an unsegmented Casper Mountain fault zone preceded initiation of Casper arch thrusting. The Iron Creek and Emigrant Gap anticlines developed somewhat later, coevally with the rise of the Casper arch above the Casper arch thrust. As the Casper arch thrust cut and segregated the Casper Mountain fault zone, there was regional southwesterly rotation of the Casper arch hanging wall toward the Wind River basin (accompanied by antithetic thrusting along the Iron Creek/Oil Mountain trend) and incremental movement on the Casper Mountain segment of the Casper Mountain fault zone. This scenario is consistent with the proposed perturbation of Laramide stress trajectories around the Casper Mountain fault zone and the concept of strain partitioning.

REFERENCES CITED

Angelier, J., 1984, Tectonic analysis of fault slip data: Journal of Geophysical Research, v. 89, p. 5835–5848.

Angelier, J., 1989, From orientation to magnitudes in paleostress determinations using fault slip data: Journal of Structural Geology, v. 11, p. 37–50.

Beck, W. C., 1984, Joint analysis of the Casper Mountain/Emigrant Gap anticline juncture, Natrona County, Wyoming: Master's thesis, University of Akron, Akron, Ohio, 101 p.

Beck, W. C., and A. E. Burford, 1985, Stress analysis of the Casper Mountain–Emigrant Gap anticline juncture, Natrona County, Wyoming, *in* G. E. Nelson, ed., The Cretaceous geology of Wyoming: Wyoming Geological Association Guidebook, 36th annual field conference, p. 59–65.

Beckwith, R. H., 1941, Structure of the Elk Mountain district, Carbon County, Wyoming: Geological Society of America Bulletin, v. 52, p. 1445–1486.

Bergstrom, J. R., 1950, Geology of the east portion of Casper Mountain and vicinity: Master's thesis, University of Wyoming, Laramie, Wyoming, 55 p.

Bitter, R. K., 1978, Geologic map of the Casper Mountain area, *in*

P. Knittel, ed., A field guide to the Casper Mountain area: Wyoming Geological Survey Reprint 45, p. 6a–6b.

Blackstone Jr., D. L., 1993, Precambrian basement map of Wyoming (MS 43), *in* A. W. Snoke, J. R. Steidtmann, and S. M. Roberts, eds., Geology of Wyoming: Geological Survey of Wyoming Memoir 5, scale 1:1,000,000, 1 sheet (in separate case).

Blundell, J. S., and R. W. Marrs, 1991, Precambrian control of Laramide faulting, Sheep Ridge anticline, western Owl Creek Mountains, Wyoming, *in* H. R. Lang, O. A. Chadwick, and E. D. Paylor II, eds., Joint publication of the Rocky Mountain Association of Geologists and NASA, solid earth science branch: The Mountain Geologist, v. 28, p. 83–89.

Brown, W. G., 1975, Casper Mountain area (Wyoming)—structural model of Laramide deformation (abs.): AAPG Bulletin, v. 59, p. 906.

Brown, W. G., 1987, Structural style of the Laramide orogeny, Wyoming foreland: Ph.D. thesis, Geophysical Institute, University of Alaska-Fairbanks, Alaska, 343 p.

Brown, W. G., 1988, Deformation style of Laramide uplifts in the Wyoming foreland, *in* C. J. Schmidt and W. J. Perry Jr., eds., Interaction of the Rocky Mountain foreland and the Cordilleran thrust belt: Geological Society of America Memoir 171, p. 1–25.

Brune, J. N., T. L. Henyey, and R. F. Roy, 1969, Heat flow, stress, and rate of slip along the San Andreas fault, California: Journal of Geophysical Research, v. 74, p. 3821–3827.

Bryant, B., 1985, Structural ancestry of the Uinta Mountains, *in* M. D. Picard, ed., Geology and energy resources, Uinta basin, Utah: Utah Geological Association Publication 12, p. 115–120.

Burford, A. E., 1986a, Structural aspects of the juncture of Emigrant Gap anticline and Casper Mountain anticline: Wyoming Geological Association Earth Science Bulletin, v. 19, part 2, p. 119.

Burford, A. E., 1986b, Structure and stratigraphy of the east plunge of Casper Mountain, Natrona County, Wyoming: Wyoming Geological Association Earth Science Bulletin, v. 19, part 2, p. 125–129.

Burford, A. E., R. G. Corbett, P. C. Franks, L. M. Friberg, R. C. Lorson, F. A. Marsek, R. F. Nanna, J. C. Schumacher, and R. E. Wymer, 1979, Precambrian complex of Casper Mountain, Wyoming—a preliminary paper: The Wyoming Geological Association Earth Science Bulletin, v. 12, p. 58–69.

Chamberlain, K. R., C. P. Suresh, B. R. Frost, and G. L. Snyder, 1993, Thick-skinned deformation of the Archean Wyoming province during Proterozoic arc-continent collision: Geology, v. 21, p. 995–998.

Condie, K. C, 1969, Petrology and geochemistry of the Laramide batholith and related metamorphic rocks of Precambrian age, eastern Wyoming: Geological Society of America Bulletin, v. 80, p. 57–82.

Crist, M. A., and M. E. Lowrey, 1972, Ground-water resources of Natrona County, Wyoming: U.S. Geological Survey Water-Supply Paper 1897, 92 p.

Dahill, M. P., 1989, Iron Creek, *in* D. F. Cardinal, T. Miller, W. W. Stewart, and J. F. Trotter, eds., Wyoming oil and gas symposium Bighorn and Wind River basins: Casper, Wyoming, Wyoming Geological Association, p. 244–248.

Daniels, J. L., 1996, Kinematic interaction of Haygood anticline and the Casper Mountain thrust: Master's thesis, University of Texas at Arlington, Texas, 94 p.

Dickinson, W. R., M. A. Klute, M. J. Hayes, S. U. Janecke, E. R. Lundin, M. A. McKittrick, and M. D. Olivares, 1988, Paleogeographic and paleotectonic setting of Laramide sedimentary basins in central Rocky Mountain region: Geological Society of America Bulletin, v. 100, p. 1023–1039.

Dyer, R., 1988, Using joint interactions to estimate paleostress ratios: Journal of Structural Geology, v. 10, p. 985–699.

Engelder, T., and P. Geiser, 1980, On the use of regional joint sets as trajectories of paleostress fields during development of the Appalachian Plateau, New York: Journal of Geophysical Research, v. 85, p. 6319–6341.

Erdlac Jr., R. J., 1994, Laramide paleostess trajectories from stylolites in the Big Bend region, *in* T. M. Laroche and J. J. Viveiros, eds., Structure and tectonics of the Big Bend and southern Permian basin, Texas: West Texas Geological Society Field Trip Guidebook, p. 165–187.

Faulkner, G. L., 1950, Geology of the Bessemer Mountain–Oil Mountain area, Natrona County, Wyoming: Master's thesis, University of Wyoming, Laramie, Wyoming, 63 p.

Gable, D. J., A. E. Burford, and R. G. Corbett, 1988, The Precambrian geology of Casper Mountain, Natrona County, Wyoming: U.S. Geological Survey Professional Paper 1460, 50 p.

Gries, R., 1983, North-south compression of Rocky Mountain foreland structures, *in* J. D. Lowell, ed., Rocky Mountain foreland basins and uplifts: Denver, Colorado, Rocky Mountain Association of Geologists, p. 9–32.

Groshong Jr., R. H., 1999, 3-D structural geology: New York, Springer-Verlag, 324 p.

Hares, J. C., M. W. Ball, S. St. Clair, J. B. Reeside, K. C. Heald, and A. C. Collins, 1946 (rpt. 1955), Geologic map of the southeastern part of the Wind River basin and adjacent areas in central Wyoming: U.S. Geological Survey Preliminary Oil and Gas Investigations Map 51, scale 1:126,720, 1 sheet.

Hennings, P. H., J. E. Olson, and L. B. Thompson, 2000, Combining outcrop data and three-dimensional structural models to characterize fractured reservoirs: an example from Wyoming: AAPG Bulletin, v. 84, p. 830–849.

Hills, F. A., P. W. Gast, R. S. Houston, and R. G. Swainbank, 1968, Precambrian geochronology of the Medicine Bow Mountains, southeastern Wyoming: Geological Society of America Bulletin, v. 79, p. 1757–1784.

Hoppin, R. A., J. C. Palmquist, and L. O. Williams, 1965, Control by Precambrian structure on the location of the Tensleep–Beaver Creek faults, Bighorn Mountains, Wyoming: Journal of Geology, v. 73, p. 189–195.

Houston, R. S., 1993, Late Archean and Early Proterozoic geology of southeastern Wyoming, *in* A. W. Snoke, J. R. Steidtmann, and S. M. Roberts, eds., Geology of Wyoming: Geological Survey of Wyoming Memoir 5, v. 1, p. 79–116.

Jenkins, C. E., 1950, Geology of the Bates Creek–Corral Creek area, Natrona County, Wyoming: Master's thesis, University of Wyoming, Laramie, Wyoming, 80 p.

Keefer, W. R., 1970, Structural geology of the Wind River basin, Wyoming: U.S. Geological Survey Professional Paper 495-D, 35 p.

Lachenbruch, A., and J. Sass, 1980, Heat flow and energetics of the San Andreas fault zone: Journal of Geophysical Research, v. 85, p. 6185–6222.

Lachenbruch, A., and J. Sass, 1992, Heat flow from Cajon Pass, fault strength, and tectonic implications: Journal of Geophysical Research, v. 97, p. 4995–5015.

Lageson, D. R., 1980, Geology, *in* Natrona County, Wyoming: The Geological Survey of Wyoming, County Resource Series 6, 8 sheets.

Lettis, W. R., and K. L. Hanson, 1991, Crustal strain partitioning: implications for seismic-hazard assessment in western California: Geology, v. 19, p. 559–562.

Lorenz, J. C., L. W. Teufel, and N. R. Warpinski, 1991, Regional fractures I: a mechanism for the formation of regional fractures at depth in flat-lying reservoirs: AAPG Bulletin, v. 75, p. 1714–1737.

Love, J. D., 1970, Cenozoic geology of the Granite Mountains area, central Wyoming: U.S. Geological Survey Professional Paper 495-C, 154 p.

Love, J. D., and A. C. Christiansen, 1985, Geologic map of Wyoming: U.S. Geological Survey, scale 1:500,000, 1 sheet.
Marshak, S., K. Karlstrom, and J. M. Timmons, 2000, Inversion of Proterozoic extensional faults: an explanation for the pattern of Laramide and Ancestral Rockies intracratonic deformation, United States: Geology, v. 28, p. 735–738.
Martinez, R. D., 1988, Tectonic synthesis of the Hat Six area, east end of Casper Mountain, Natrona County, Wyoming: Master's thesis, University of Akron, Akron, Ohio, 67 p.
McNulty, B. A., D. L. Farber, G. S. Wallace, R. Lopez, and O. Palacios, 1998, Role of plate kinematics and plate-slip vector partitioning in continental magmatic arcs: evidence from the Cordillera Blanca, Peru: Geology, v. 26, p. 827–830.
Miller, D. D., 1998, Distributed shear, rotation, and partitioned strain along the San Andreas fault, central California: Geology, v. 26, p. 867–870.
Molzer, P. C., and E. A. Erslev, 1995, Oblique convergence during northeast-southwest Laramide compression along the east-west Owl Creek and Casper Mountain arches, central Wyoming: AAPG Bulletin, v. 79, p. 1377–1394.
Montgomery, S. C., F. Barrett, K. Vickery, S. Natali, R. Roux, and P. Dea, 2001, Cave Gulch field, Natrona County, Wyoming: large gas discovery in the Rocky Mountain foreland, Wind River basin: AAPG Bulletin, v. 85, p. 1543–1564.
Morse, V. C., J. H. Joohnson, J. L. Crittenden, and T. D. Anderson, 1987, Techniques for seismic delineation of complex structure: a case history: Geophysics, v. 52, p. 802–809.
Mount, V. S., and J. Suppe, 1987, State of stress near the San Andreas fault: implications for wrench tectonics: Geology, v. 15, p. 1143–1146.
Narr, W., 1993, Deformation of basement-involved, compressive structures, *in* C. J. Schmidt, R. B. Chase, and E. A, Erslev, eds., Laramide deformation in the Rocky Mountain foreland of the western United States: Geological Society of America Special Paper 280, p. 107–124.
Narr, W., and J. Suppe, 1994, Kinematics of basement-involved compressive structures: American Journal of Science, v. 294, p. 802–860.
Natali, S., R. Roux, P. Dea, and F. Barrett, 2000a, Cave Gulch 3-D survey, Wind River basin, Wyoming: The Mountain Geologist, v. 37, p. 3–13.
Natali, S., R. Roux, P. Dee, and F. Barrett, 2000b, Cave Gulch 3-D survey, Wind River basin, Wyoming: a major gas discovery developed using poststack depth migration: The Leading Edge, v. 19, p. 1286–1294.
Peterman, Z. E., and R. A. Hildreth, 1978, Reconnaissance geology and geochronology of the Precambrian of the Granite Mountains, Wyoming: U.S. Geological Survey Professional Paper 1055, 22 p.
Ramsay, J. G., and M. I. Huber, 1987, The techniques of modern structural geology, v. 2: folds and fractures: London, Academic Press, 462 p.
Rawnsley, K. D., T. Rives, J. P. Petit, S. R. Hencher, and A. C. Lumsden, 1992, Joint development in perturbed stress fields near faults: Journal of Structural Geology, v. 14, p. 939–951.
Ray, R. R., and C. R. Berg, 1985, Seismic interpretation of the Casper Arch thrust, Tepee Flats field, Wyoming, *in* R. Gries and R. C. Dyer, eds., Seismic exploration of the Rocky Mountain region: Rocky Mountain Association of Geologists and Denver Geophysical Society, p. 51–58.
Sandberg, C. A, F. G. Poole, and J. G. Johnson, 1989, Upper Devonian of western United States, *in* N. J. McMillan, A. F. Embry, and D. J. Glass, eds., Devonian of the World, v. I: regional synthesis: Canadian Society of Petroleum Geologists Memoir 14, p. 183–220.
Sando, W. J., and C. A. Sandberg, 1987, New interpretations of Paleozoic stratigraphy and history in the northern Laramie Range and vicinity, southeastern Wyoming: U.S. Geological Survey Professional Paper 1450, 39 p.
Schmidt, C. J., D. S. Stone, and J. M. O'Neill, 1996, Influence of the lower Proterozoic boundary of the Wyoming province on trends and kinematics of Laramide deformation (abs.): Geological Society of America Abstracts with Programs, v. 28, no. 7, p. A-447.
Scholz, C. H., 2000, Evidence for a strong San Andreas fault: Geology, v. 28, p. 163–166.
Schrader Flats, 1989, *in* D. F. Cardinal, T. Miller, W. W. Stewart, and J. F. Trotter, eds., Wyoming oil and gas symposium, Bighorn and Wind River basins: Casper, Wyoming, Wyoming Geological Association, p. 436–438.
Schwarberg Jr., T. M., 1959, The geology of Muddy Mountain southeastern Natrona County, Wyoming: Master's thesis, University of Wyoming, Laramie, Wyoming, 103 p.
Sears Jr., W. A., 1948, Geology of the Deer Creek–Smith Creek area, Converse and Natrona Counties, Wyoming: Master's thesis, University of Wyoming, Laramie, Wyoming, 56 p.
Sears, W. A., and F. C. Sims, 1954, Structural geology of the Casper Mountain area: Wyoming Geological Association Ninth Annual Field Conference Guidebook, Casper Area, p. 27–31.
Sims, F. C., 1948, Geology of the west end of the Laramie Range, Natrona County, Wyoming: Master's thesis, University of Wyoming, Laramie, Wyoming, 52 p.
Skeen, R. C., and R. R. Ray, 1983, Seismic models and interpretation of the Casper Arch thrust: application to Rocky Mountain foreland structure, *in* J. D. Lowell, ed., Rocky Mountain foreland basins and uplifts: Denver, Colorado, Rocky Mountain Association of Geologists, p. 99–124.
Sprague, E. L., 1983, Geology of the Tepee Flats–Bullfrog fields, Natrona County, Wyoming, *in* J. D. Lowell, ed., Rocky Mountain foreland basins and uplifts: Denver, Colorado, Rocky Mountain Association of Geologists, p. 339–343.
Stiteler, C. C., 1954, Emigrant Gap anticline: Wyoming Geological Association Ninth Annual Field Conference Guidebook, Casper Area, p.58–63.
Stone, D. S., 1969, Wrench faulting and Rocky Mountain tectonics: The Mountain Geologist, v. 6, p. 67–79.
Stone, D. S., 1986, Seismic and borehole evidence for important pre-Laramide faulting along the Axial arch in northwest Colorado, *in* D. S. Stone, ed., New interpretations of northwest Colorado geology: Denver, Colorado, Rocky Mountain Association of Geologists, p. 19–36.
Stone, D. S., 1993a, Basement-involved thrust-generated folds as seismically imaged in the subsurface of the central Rocky Mountain foreland, *in* C. J. Schmidt, R. B. Chase, and E. A. Erslev, eds., Laramide basement deformation in the central Rocky Mountains of the western United States: Geological Society of America Special Paper 280, p. 271–318.
Stone, D. S., 1993b, Tectonic evolution of the Uinta Mountains: palinspastic restoration of a structural cross section along longitude 109° 15′, Utah: Utah Geological Survey Special Publication 93-8, 19 p., 3 plates.
Tavarnelli, E., and R. E. Holdsworth, 1999, How long do structures take to form in transpression zones?: a cautionary tale from California: Geology, v. 27, p. 1063–1066.
Thompson, G. A., and J. L. Hill, 1986, The deep crust in convergent and divergent terranes: Laramide uplifts and basin-range rifts, *in* M. Barazangi and L. Brown, eds., Reflection seismology: the continental crust: American Geophysical Union Geodynamics Series, v. 14, p. 243–256.
Tikoff, B., and C. Teyssier, 1994, Strain modeling of displacement-field partitioning in transpressional orogens: Journal of Structural Geology, v. 16, p. 1575–1588.
Twiford, F., 1989, Bates Creek, *in* D. F. Cardinal, T. Miller, W. W. Stewart, and J. F. Trotter, eds., Wyoming oil and gas

symposium Bighorn and Wind River basins: Casper, Wyoming, Wyoming Geological Association, p. 44–45.
Varga, R. J., 1993, Rocky Mountain foreland uplifts: products of a rotating stress field or strain partitioning?: Geology, v. 21, p. 1115–1118.
Wyoming Geological Association, 1965, Geologic map of Casper Mountain: scale 1 in = 4000 ft, with 100-ft topographic contours, 1 sheet.
Zoback, M. D., et al., 1987, New evidence on the state of stress of the San Andreas fault system: Science, v. 238, p. 1105–1111.